Guide with scenarios, exemplary load profiles and recommendations for parametrization

HydroFlex

HydroFlex

Increasing the value of hydropower through increased flexibility

Deliverable D2.4: Guide with scenarios, exemplary load profiles and recommendations for parametrization

Work package	WP 2 Definition of scenarios and reference cases
Task	Task 2.4: Guide describing demands for flexible hydropower
Lead beneficiary	RWTH Aachen University
Authors	Peter Wirtz, Maik Schönefeld, Marius Siemonsmeier, Johannes Hüllenkremer, Alexander Heckmann, Andrea Schönbauer, Albert Moser
Due date of deliverable	28.02.2022
Actual Submission date	28.02.2022
Type of deliverable	Report
Dissemination level	Public

This project has received funding from the European Union's Horizon 2020 research and innovation programme under grant agreement No 764011.

Executive Summary

In the context of climate change and the climate policy goals of the European Union, the European power system is undergoing a structural transformation to a CO_2-neutral system. Generation plants based on renewable energy sources (RES) are increasingly replacing conventional thermal generation plants. The high volatility and difficult predictability of RES pose a challenge and will lead to an increased need for flexibility. Storage hydropower plants can provide flexibility both by adjusting generation and by shifting generation over time. Furthermore, pumped-storage hydropower plants are able to provide flexibility for the power system on the consumer side. Another form of flexibility, as inertia and primary control reserve, is needed in case of disturbances in grid operation to maintain frequency stability.

The methodology contains three parts in order to identify the demand for flexibility both before physical fulfillment and in grid operation: A European power market simulation, grid operation simulations and time domain simulations to investigate frequency stability.

The results of the market simulations show that the large generation from photovoltaic (PV) systems in Central Europe and Great Britain in the future scenarios influences the hydropower plant operation in the Nordics. During the day, electricity in the Nordics is mainly imported to meet the demand in the Nordics itself, especially in the summer months, while at night the Nordics export electrical energy. The number of power changes of the hydropower plants in the Nordics is therefore in most cases not more than two per day. The flexibility demand in the Nordics is only slightly higher due to this described behavior in comparison to the present operation from the spot market perspective. In a comparison of flexible and inflexible hydropower plants it is noticeable that the more flexible plants have a multiple of start/stop cycles compared to the less flexible plants, which run one to two start/stop cycles per day in the summer months. One investigation showed that a partly flexibilization of the hydropower plant park can reduce the operational violations of the less flexible plants by more than 60 %. In addition, the number of start/stop cycles of the less flexible plants is lower in the case of partial flexibilization. With regard to slowing down the aging process of a power plant park, both the reduction in operational violations and the reduction in the start/stop cycles of the less flexible plants have a positive effect. In a scenario with an increased expansion of wind turbines, a relation between an increased flexibility demand and an expansion of wind turbines in the same bidding zone could be found but has only a minor impact on the flexibility demand of neighboring bidding zones.

Frequency stability investigations were carried out for today's power plant park and for a scenario where the nuclear power plants are substituted by RES. In order to create worst case scenarios, all RES power plants do not provide any ancillary services. The investigations on different types and locations of faults show that the deviation of the frequency from the nominal frequency and rate of change of frequency is slightly higher for the second scenario. Frequency stability within the Nordic power system is guaranteed for all load and fault situations in both scenarios considered. There is no need for additional flexibility for grid operation under the given assumptions and for the models used.

Table of Contents

Abbreviations

AC	Alternating current
DC	Direct current
DKE	East Denmark
DKW	West Denmark
ENTSO-E	European Association of Transmission System Operators for Electricity
EU	European Union
GW	Gigawatt
HVDC	High Voltage Direct Current
IAEW	Institute for High Voltage Equipment and Grids, Digitalization and Energy Economics
IGBT	Insulated Gate Bipolar Transistor
IRES	Intermittent Renewable Energy Sources
LCC	Line-commutated Converter
MDT	Minimum Downtime
NGC	Net Generation Capacity
MOT	Minimum Operating Time
MW	Megawatt
NTC	Net Transfer Capacities
PID	Proportional-Integral-Derivative
PSS	Power System Stabilizer
PV	Photovoltaic
RES	Renewable Energy Sources
SEXS	Simplified Excitation System
TRM	Transmission Reliability Margin
TSO	Transmission System Operator
TTC	Total Transfer Capacity
TW	Terawatt
TWh	Terawatt hour
VSC	Voltage Source Converter
WP	Work Package

1 Introduction

1.1 Background and motivation

In the context of climate change and the climate policy goals of the European Union (EU), the European power system is undergoing a structural transformation to a CO_2-neutral power generation. At the EU summit in December 2020 it was decided to reduce greenhouse gas emissions in the EU by at least 55 % net by 2030 compared to 1990 (European Council 2020).

Accordingly, generation plants based on renewable energy sources (RES) are increasingly replacing conventional thermal generation plants such as lignite and coal-fired power plants. The high volatility and difficult predictability of RES – especially wind turbines and photovoltaic (PV) systems – pose a challenge for the design of the power system. In addition, some European countries are planning to move away from nuclear power such as Germany by 2022 and Belgium by 2025 and replace the resulting loss of electricity generation with generation from RES. It is expected that this expansion will lead to an increased need for flexibility within the European power system due to the supply dependence of these generation plants. Furthermore, the increasing power feed-in via converters and the lack of synchronous coupling on the one hand, as well as the reduction of rotating masses in the grid on the other hand, change the dynamic behaviour of the grid. The stabilizing influence of the rotating masses on the grid frequency as a momentary reserve is lost, as RES that are connected to the grid via converters do not intrinsically contribute to power system stability (Forschungsverbund erneuerbare Energien 2014).

In addition to conventional generation plants, there are other options providing flexibility. These include options for demand-side flexibility, such as demand-side management, sector-coupling units, such as power-to-gas units, and energy storage. Hydraulic storage power plants represent one option for energy storage. As one of the few RES that can be variably controlled over a large operating range with very low losses, it is of future importance (Saarinen 2015). This mature technology, which has been in use for many decades, is particularly widespread in the Alpine region and in the Nordics. All flexibility options will help to provide flexibility in the future. However, due to very diverse characteristics, they have different areas of deployment. In order to evaluate the complex interaction of these technologies for the future, simulations of the power system are necessary.

The provision of flexibility in the European power system differs according to the time interval before physical fulfillment from future markets years ahead to spot markets minutes ahead to frequency reserve or system inertia right after fault occurences in real-time operation. One focus of this guide is flexibility provision on spot markets. Spot markets' main task is coordinating the efficient allocation of generation and consumption, taking into account security of supply and other technical restrictions. The structural transformation of the power system from fossil-fueled to renewable generation is posing challenges to this task. Flexibility options such as hydro storage power plants are becoming increasingly important in this context. In order to investigate future flexibility provision of hydropower, market simulations are conducted.

However, hydropower's increasing importance applies not only before physical fulfillment, but also in real-time operation. The Nordic transmission system operators (TSOs) have identified three main drivers and their effects on the dynamic behaviour of the power system (Nordic Transmission System Operators: Svenska kraftnät, Statnett, Fingrid and Energinet.dk 2016). These include frequency quality, which is directly related to the availability of rotating masses and system flexibility, increased feed-in via converters due to the addition of wind turbines, and a potential threat to power system stability due to the reduction of rotating masses synchronised with the grid frequency. Hydropower plants, as synchronously coupled power plants based on renewable energy sources, represent a great opportunity to face these challenges. Thus, the second focus of this guide are time domain simulations to investigate future system stability.

1.2 Objectives and structure

In a joint effort of 16 research and industry partners from five European countries, the HydroFlex project 'Increasing the value of Hydropower through increased Flexibility' explores the role of hydropower as a flexibility option. HydroFlex is a research and innovation action funded under the EU Horizon 2020 programme "H2020-EU3.3.2 – Low-cost, low-carbon energy supply" (funding code: 764011). It addresses the technology-specific challenge "Hydropower: Increasing flexibility of hydropower" of the work programme topic "LCE-07-2016-2017 – Developing the next generation technologies of renewable electricity and heating/cooling", which focuses on the need to develop new technologies, generators and turbine designs to increase the flexibility of hydropower plants while mitigating environmental impacts. The project is divided into seven work packages. Figure 1 depicts the tasks of work package two (WP2), which this report originates from.

Figure 1: Tasks of work package 2.

The main objective of WP2 is to identify and describe the demands hydropower plants will be confronted with in future power systems. The focus will be on identifying dynamic loads such as those resulting from providing high ramping rates and frequent start-stop cycles. In order to achieve this main objective, market simulations to analyze the time interval before physical fulfilment and stability simulations to analyze real-time operation are performed in Task 2.3. Due to an already existing, extensive hydropower plant park, the focus will be on the Nordic countries Norway and Sweden. Within the scope of the Hydroflex project, a very flexible turbine will be developed, which will be applied in some power plants in the Nordic countries. These power plants are also called Reference Sites in the following. For this reason, the effects of such a flexibilization will be investigated in detail based on the simulations mentioned above. This

guide, which is Task 2.4 of work package 2, summarizes the outcomes of the simulations and investigations of the work package, which will show the requirements hydropower plants in Europe and especially in the Nordics must meet in the future.

First, extensive analyses are conducted in Chapter 2. These include a description of the development of the European power system, an investigation of the flexibility needs of the power system and its provision in genereal. In the following, an analysis of the Nordic power system, an investigation of hydropower as a flexibility option, an analysis of the volatility of supply-dependent plants, and a consideration of high-voltage direct current (HVDC) transmission in Europe is presented. These analyses provide a basis for further understanding of the studies.

Chapter 3 then presents the models developed at the Institute for High Voltage Equipment and Grids, Digitalization and Energy Economics (IAEW), which are necessary to investigate the requirements for Nordic hydropower in future scenarios. A distinction is made between a market-based model, which focuses on the time before physical fulfillment, and a dynamic model of the Nordic power system and its electrical installations, whose temporal focus is real-time operation under fault conditions.

Chapters 4 and 5 present and evaluate the results of the simulations for determining the requirements of Nordic hydropower on the European power system. Chapter 4 refers to the results of the market simulation and Chapter 5 to the results of the time domain simulations to identify possible flexibility needs in the Nordic power system im terms of maintaining frequency stability. Lastly, Chapter 6 summarzies the main outcomes.

2 Analysis

Within the scope of the analysis, the current transformation of the European power system is first described in Section 2.1 and the term flexibility is defined in Section 2.2. Following on from this, various options for providing flexibility are explained based on this definition. Furthermore, in addition to the power plant parks in Norway and Sweden, the power system of these two countries is characterized in Section 2.3. Subsequently, storage power plants as a flexibility option are analyzed in detail in Section 2.4. This is accompanied by an examination of the feed-in of RES generation units in Section 2.5. Finally, the flexibility provision by hydropower of the Nordics for the continental European power system via HVDC transmission is described in Section 2.6.

2.1 Evolution of the European power system

In the analysis of the development of the European power system, various aspects need to be considered. First, the transformation from a power system characterized by conventional, thermal generation plants to a system based on RES and the resulting status quo is decribed. Then, the political decisions and measures concerning the existing conventional, thermal power plant park and the expansion plans for the use of RES are explained. These different aspects are analyzed in Sections 2.1.1 to 2.1.3.

2.1.1 Transformation of the power system since 2000

The European power system is subject to structural change. This process has been evident since the early 2000s in the proportions of primary energy sources used in European gross electricity generation. Figure 2 shows this composition of gross electricity generation in five-year steps from 2000 to 2017. Regarding the development of the share of RES in the gross electricity production, it is noticeable that this share has more than doubled since 2000 and now accounts for more than 30 % of the production. In the same period, the generation from conventional, thermal power plants, such as coal and gas power plants as well as nuclear power plants has decreased from almost 85 % of the gross electricity generation to approximately 69 %. The various technologies have developed differently since 2000. While oil has been almost completely replaced as the primary energy source and the share of hard coal in gross electricity generation has almost halved, the share of gas-based electricity generation has increased from 17 % to 21 %.

The European development is made up of the various developments at national level. Due to different starting situations and political objectives as well as a varying availability of the different primary energy sources in the national states, the respective power plant park and the composition of gross electricity generation show significant differences. As an example, the the composition of gross electricity generation of Germany, France, Italy and Norway are compared with each other (c.f. Figure 3).

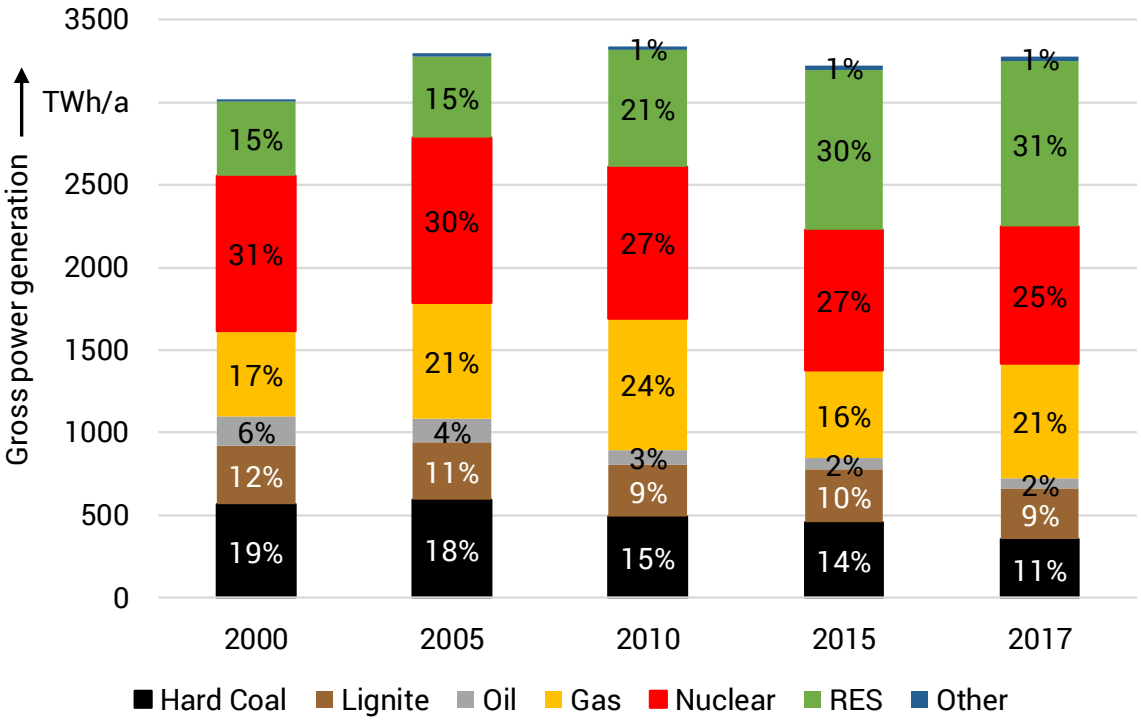

Figure 2: Development of gross European power generation (European Commission 2020; Statistic Norway 2017).

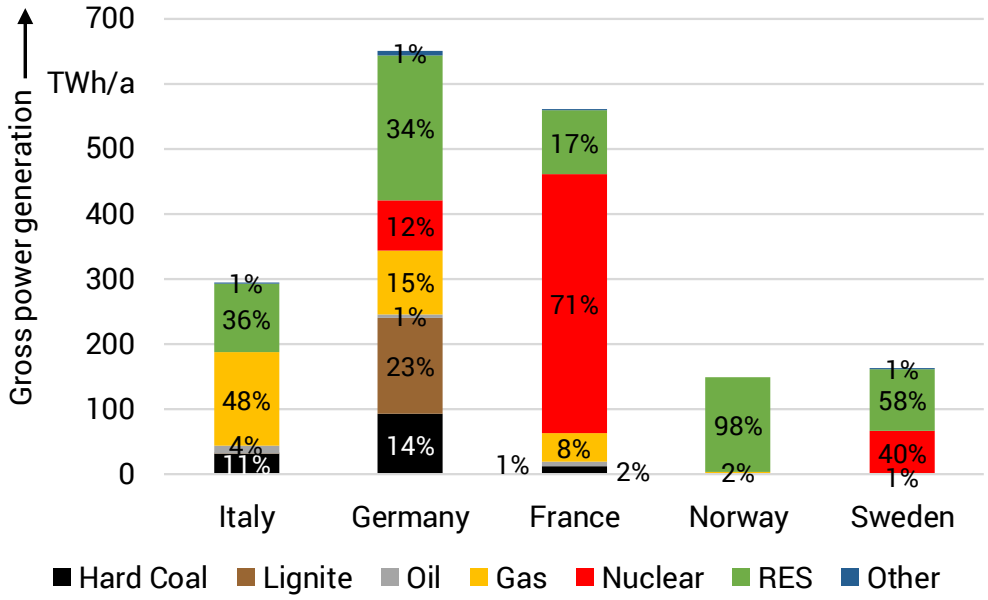

Figure 3: Gross power generation of Italy, Germany, France, Norway and Sweden in 2017, data from (Statistic Norway 2017; European Commission 2020).

In the Figure 3 above, the shares of the different primary energy sources in the gross electricity generation in 2017 are compared using the example of selected European countries. The German gross electricity generation is characterized by a high share of lignite and hard coal. These two fossil fuels account for almost 37 % of gross electricity generation, while the share of nuclear energy was about 12 % in 2017. In contrast, 70 % of the gross electricity generation in France is generated by nuclear power plants, whereas fossil fuels such as coal and gas have a combined share of only about 10 %. In Italy, gas is the dominant primary energy source with a share of approx. 50 %. Other fossil fuels such as hard coal or oil play a minor role, whereas RES make a significant contribution with more than one third. When looking at the composition of Norway's gross electricity generation, it is noticeable that the Norwegian gross electricity generation, is fundamentally different from the structures presented so far. Conventional, thermal power plants have a very small share of less than 2.5 % of the gross electricity production. Due to the geographical conditions, hydropower generation dominates in Norway with about 98 %. The situation is similar in Sweden. Here, generation from hydropower plants also takes up the largest share of gross electricity generation. Generation from nuclear power plants accounts for the second-largest share, at approx. 40 %.

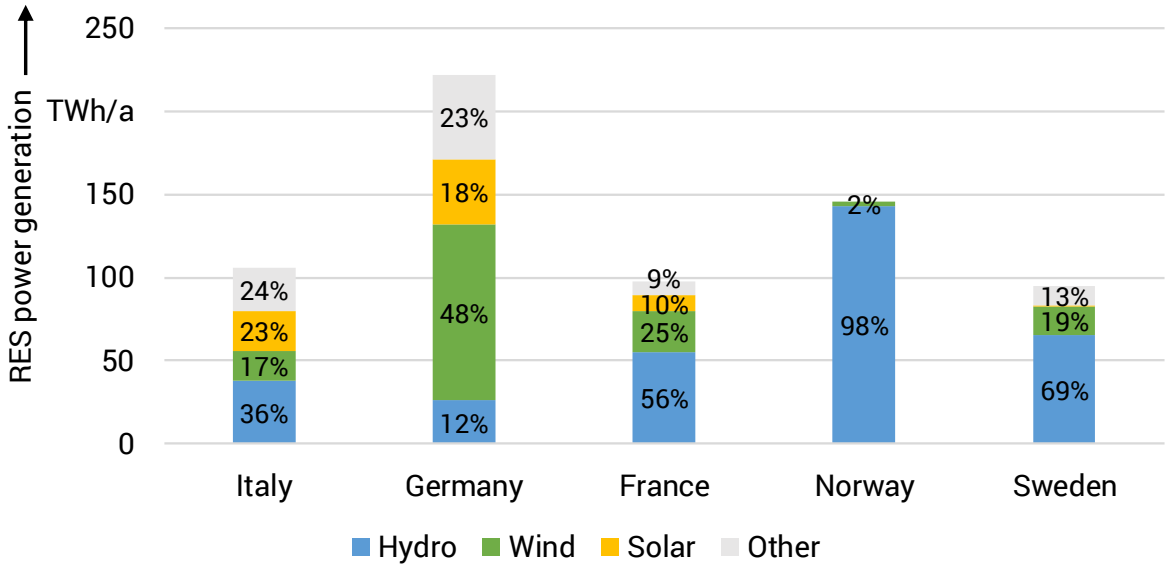

Figure 4: Composition of the RES share of gross power generation in 2017, data from (European Commission 2020; Statistic Norway 2017).

A comparison of the composition of power generation from RES (c.f. Figure 4) shows both differences and similarities between the countries. While in France, electricity generation from hydropower dominates renewable energy generation with more than 50 %, in Germany, electricity generation from wind turbines is dominating with about 47 %. Both countries have in common, however, that the production from wind turbines accounts for more than twice as much of the gross electricity production as the production from PV systems.

While similarities are still evident between France and Germany, the composition of renewable electricity generation in Norway and Italy differs fundamentally. In Italy, all three main RES sources (hydropower, wind energy and solar energy) have shares of between 17 % and 36 %, whereas Norway's electricity generation from renewable energy plants is almost exclusively based on hydropower (98 %). The RES power generation in Sweden is also mainly based on hydropower with a share 69 % due to the geographical advantages regarding generation with hydropower. It is also noticeable that in Italy - in contrast to Germany and France - electricity generation from solar PV systems clearly exceeds generation from wind turbines.

The comparison of these four exemplary selected countries shows that the generation structures in Europe are very different. While in Northern Europe wind energy and hydropower plants are used to generate electricity from RES, in Southern Europe solar PV power plants are more dominant. The consideration of Germany and France shows how different the conventional, thermal generation structures can be under comparable conditions.

2.1.2 Political decisions and objectives

With the ratification of the Paris Climate Convention in 2016, the EU has committed itself to implementing measures to limit the global temperature increase to significantly below 2°C compared to pre-industrial levels (United Nations 2016). In the course of implementing this agreement, the EU has defined three targets for 2020 and 2030. By 2020, greenhouse gas emissions are to be reduced by 20 % compared to 1990 levels and by a further 20 % by 2030. This target was tightened again at the EU summit in December 2020. There, it was decided to reduce greenhouse gas emissions internally by at least 55% net by 2030 compared to 1990. In addition, 20 % of gross end energy consumption in 2020 is to be covered by plants based on RES. By 2030, this share is expected to increase to at least 32 %. In addition to the two target indicators, greenhouse gas emissions and the share of RES units in gross end energy consumption, targets for increasing energy efficiency were defined. For the period from 2020 to 2030, the EU directives provide for an increase in energy efficiency from 20 % to 32.5 %. (European Commission, European Union 2018b, 2018a; European Commission 2014)

In the course of the political discussions on climate protection, energy system transformation and environmental protection, various decisions have been made on a national level regarding the future use of nuclear energy and coal for power generation.

Nuclear Energy

Nuclear energy is widespread in Europe and has been used there for many decades. While some countries have decided to phase out nuclear energy or to stop using this generation technology, particularly as a result of the impressions of the reactor accidents in Chernobyl (1986) and Fukushima (2011), other countries are planning to build additional or renew existing generation capacities.

As shown in Figure 5, there are very different strategies for the future use of nuclear energy in Europe. While Germany and Belgium have decided to phase out nuclear power by 2022 and 2025

respectively in the wake of the reactor accident in Fukushima, Japan, no final decision has yet been made in the Netherlands about the only Dutch nuclear power plant whose planned lifetime ends in 2033 (DutchNews.nl 2018; Pieters 2018; Deutsche-Presse-Agentur 2019; Schlandt 2019). In Switzerland, it has been decided in this context that no renewal of the existing nuclear power plants will be carried out in 2011. In addition, a referendum in 2017 decided that a nuclear power phase-out should take place. However, this phase-out is to take place without a defined target date, but at the end of the safety operating life of the power plants (Bundesamt für Energie 2017; Schultz 2017). In contrast, Austria had already become active before the Chernobyl accident in 1986 and prohibited the commissioning of a completed power plant in 1978 and later raised the Nuclear Non-Proliferation Act to constitutional status (Österreichische Nationalrat 1999; Seiser 2011).

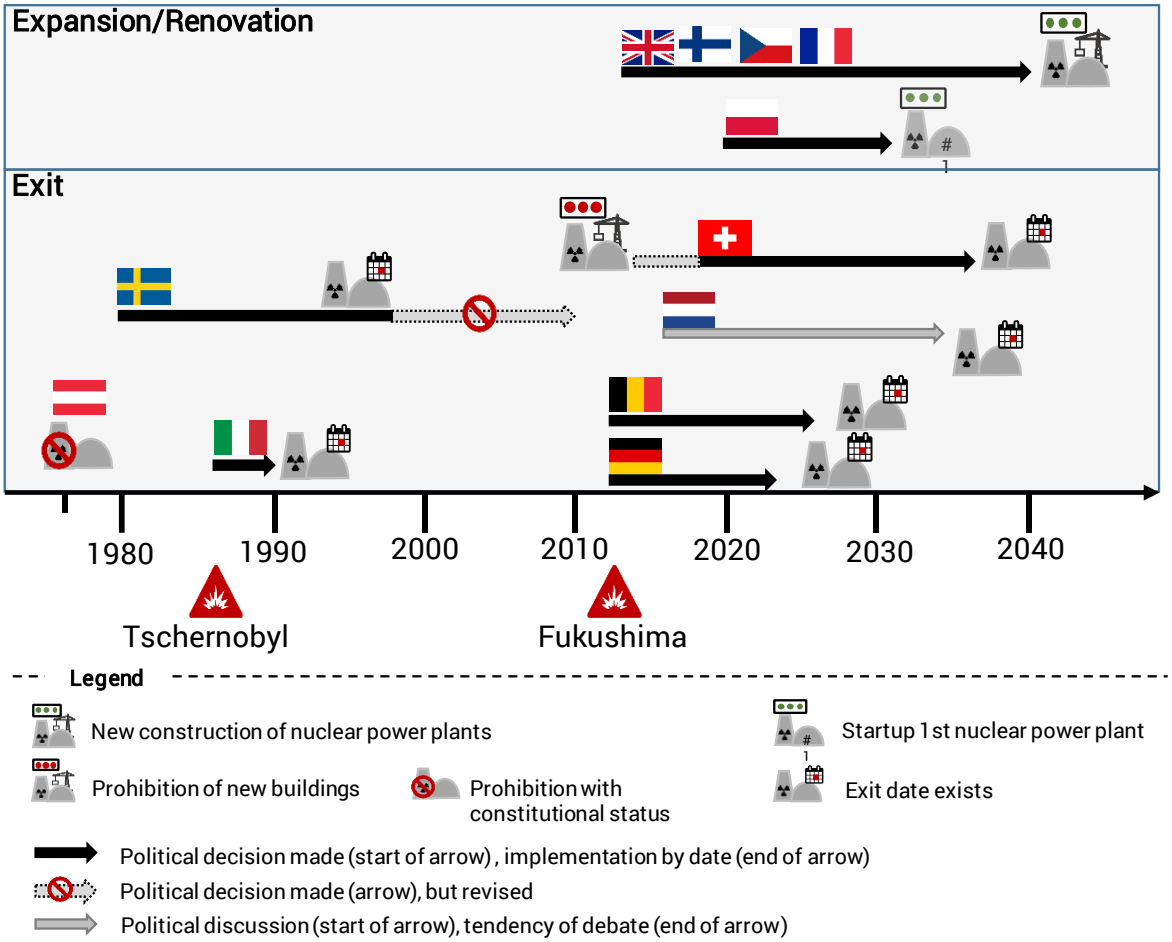

Figure 5: Overview of national decisions on nuclear energy use, own illustration[1].

[1] (Finke 2019; Chrisafis 2019; DutchNews.nl 2018; Pieters 2018; Deutsche-Presse-Agentur 2019; Donadio 2011; World Nuclear Association 2018; Schlandt 2019; Österreichische Nationalrat 1999; Seiser 2011; Anwar 2016; International Atomic Energy Agency 2014; World Nuclear Association 2019a;

The decisions in France, Sweden, Finland, the Czech Republic, Great Britain and Poland are different. While Finland, the Czech Republic and Great Britain are renewing their existing power plant parks or adding new reactors, France is planning a step-by-step reduction in nuclear power generation from currently approx. 70 % to 50 % of gross electricity generation in 2035 (Finke 2019; Chrisafis 2019; Morgan 2018; World Nuclear Association 2019c, 2019b). Poland plans to commission its first nuclear power plant in 2033 (Barteczko 2018a). In Sweden in the 1980s, the initial plan was to phase out nuclear power at the end of the lifetime of existing power plants, which would have been achieved in 2010. However, in 1997, lifetime extensions were granted and in 2010 the nuclear phase-out was formally cancelled (Anwar 2016; International Atomic Energy Agency 2014).

Coal Power

In contrast to nuclear energy, coal-fired power generation in Europe shows a much more uniform trend, but with some exceptions. Especially after the ratification of the Paris Climate Convention, various strategies and development plans have been adopted at national level to reduce CO_2 emissions from coal-fired power generation or to replace this generation technology completely with other technologies. One driver for reducing CO_2 emissions is the introduction of trading in EU emission allowances. These entitle the holder to emit 1 t of CO_2 and are only available for a limited volume. With this instrument, it is easier to manage the coal phase-out.

As shown in Figure 6, many European countries have committed themselves to phasing out coal-fired power generation in order to comply with the Paris Climate Convention. Countries with low coal shares in gross electricity generation such as Great Britain, France, Austria and Italy plan to decommission their coal-fired power plants within the next 6 years (Finke 2019; Felix 2019; Felix, Carraud, and Mallet 2019; Jewkes 2019; Radio Steiermark 2019). In contrast, countries such as Germany, the Netherlands, Denmark and Finland plan to phase out coal-fired power plants between 2029 and 2038 due to the much higher share of coal-fired generation (Morgan 2018; Goverment of the Netherlands 2019; Kommission „Wachstum, Strukturwandel und Beschäftigung“ 2019; Schultz and Traufetter 2019, 2019; Kauranen and Karagiannopoulos 2019; Jones 2017). At this point, the interactions between the decisions on coal and nuclear power must be taken into account. One of the two technologies is taken out of operation in the short term, while the share of the second technology is reduced in the long term.

Exceptions to this development are the decisions in Poland. Five new coal-fired power plants are currently being built in Poland and five more are in the planning phase. Until 2040, Poland only intends to phase out lignite-based electricity generation, while hard coal-based electricity generation is to be continued. (Barteczko 2018b; Mitteldeutscher Rundfunk 2019)

It is noticeable that countries with low generation capacities in coal-fired power generation in particular are currently planning a prompt exit. The operators of large coal-based power plant

Morgan 2018; World Nuclear Association 2019c; Barteczko 2018a; Deutsche Botschaft Prag, n.d.; World Nuclear Association 2019b; Bundesamt für Energie 2017; Schultz 2017).

parks, on the other hand, such as Germany, are planning a medium-term exit or intend - like Poland - to build further power plants. The price development of primary energies and CO_2 certificates will also have an influence on the decision when and how the coal phase-out will be implemented.

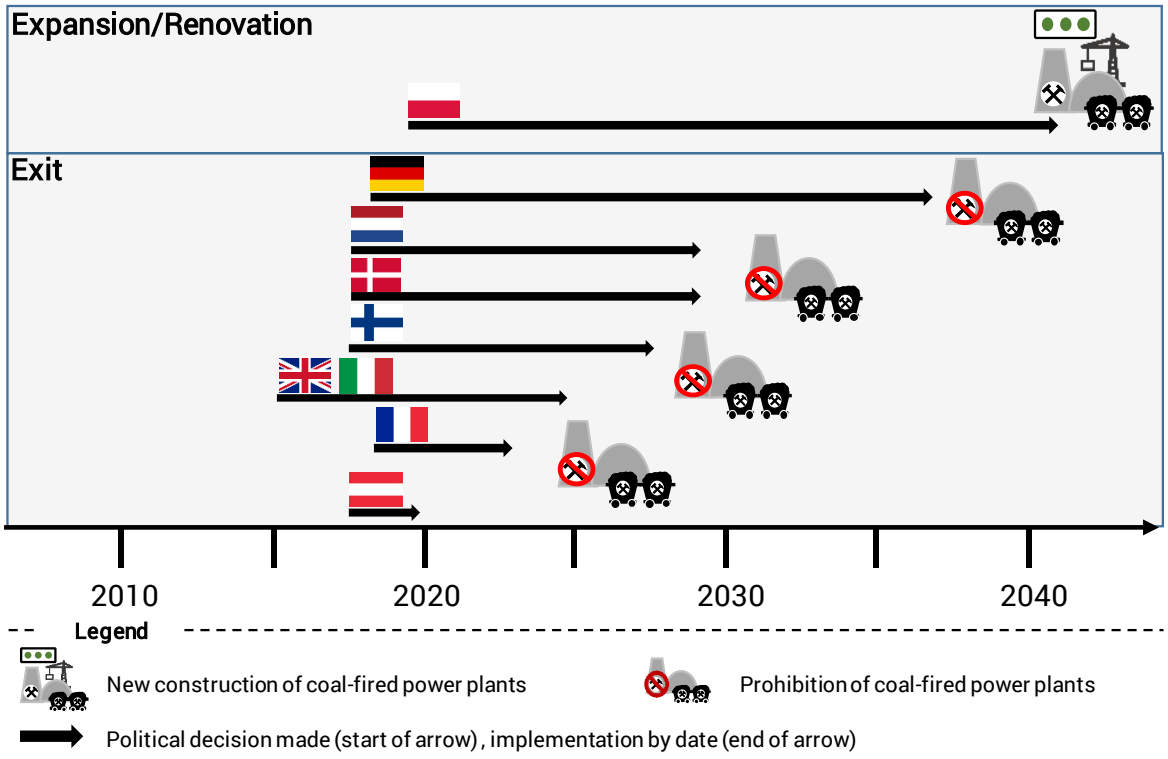

Figure 6: Overview of national decisions on coal-fired power generation, own illustration[2].

2.1.3 Expansion plans for RES plants

In order to achieve the goals defined in the Paris Climate Convention and to enable the various strategies for phasing out nuclear energy or coal-fired power generation, the capacity of RES plants increases substantially in Europe. These are mainly PV units and wind turbines. The use of wind turbines to generate electricity is increasingly being supplemented by offshore wind turbines. By the end of 2018, for example, more than 4500 wind turbines with a total installed capacity of 18.5 GW had been commissioned in the North and Baltic Seas. The majority of these plants, almost 80 % of all offshore wind turbines, have been built in Great Britain (8.2 GW) and in Germany (6.4 GW). A significant increase in generation capacity in the offshore power gener-

[2] (Finke 2019; Department for Business, Energy and Industrial Strategy 2018; Twidale, Potter, and Croft 2018; Felix 2019; Felix, Carraud, and Mallet 2019; Goverment of the Netherlands 2019; Jewkes 2019; Kommission „Wachstum, Strukturwandel und Beschäftigung“ 2019; Schultz and Traufetter 2019; Radio Steiermark 2019; Jones 2017; Kauranen and Karagiannopoulos 2019; Barteczko 2018b; Mitteldeutscher Rundfunk 2019; Martin, n.d.; Bundesamt für Energie 2015).

ation sector is also expected in the future. There are projects to expand the generation capacities of offshore wind turbines in numerous countries bordering the North and Baltic Seas. This applies in particular to the Nordic countries Sweden and Denmark. In Sweden, the installed capacity in the area of offshore electricity generation may be increased from 200 MW to 2,667 MW by implementing all currently approved projects (Newell Swedish Energy Agency). In Denmark, offshore wind farms with more than 1660 MW of installed capacity have already been commissioned (Ørsted A/S; Vattenfall AB; Vattenfall AB; Vattenfall AB 2018). In the long term, the installed capacity could multiply by 2050. The EU Commission considers capacities between 240-450 GW to be possible. (WindEurope asbl/vzw 2016; Selot, Fraile, and Brindley 2019)

As a result, the developments of the past 20 years outlined at the beginning of this section will continue. Thus, the European power system will be characterized in the future by power generation on the basis of RES, whose energy supply is supply-dependent and thus volatile, i.e. dependent on the current weather situation (Zahoransky 2019). Due to this development, the use of the remaining plannable generators, such as conventional, thermal power plants and hydro storage power plants, will no longer be determined on the basis of consumption, but on the basiagrs of residual load, i.e., the difference between consumption and generation on the basis of RES plants. With an increasing share of RES plants, this residual load can show greater rates of change than consumption, so that producers as well as consumers in Europe will have to react more flexibly in the future. (Agricola, Seidl, and Heuke 2015; Bundesnetzagentur 2017)

2.2 Flexibility in the power system

Due to the lack of ability of the grids to store electricity, a balance between generation and load needs to be maintained at any time (Konstantin 2017). As a result of the development described in section 2.1, the future European power system is expected to face an increase of supply-dependent, volatile power plants, which will lead to an additional need for flexibility (Bundesnetzagentur 2017; Agricola, Seidl, and Heuke 2015). Therefore, the following Sections 2.2.1 and 2.2.3 first define and categorize the term flexibility before presenting different technology options for providing flexibility. In Section 2.2.2 the flexibility needs in grid operation are described from a perspective of keeping a power system stable.

2.2.1 Fundamentals of flexibility from a market's perspective

The flexibility of a generation plant or consumer is the ability to change the generation output or the power consumption. This characteristic of a power plant or a consumer is described by various parameters such as the maximum power gradient or the maximum shiftable amount of energy. The maximum power gradient is the maximum possible power adjustment of a generating unit per time step. In addition, the location of the generation unit or the consumer as well as the time range in which this flexibility is applicable are essential parameters for an evaluation of the flexibility, which a generation unit or a consumer can provide for a system. (Bundesnetzagentur 2017; Union of the Electricity Industry - EURELECTRIC aisbl 2014)

Based on this definition, it is possible to characterize the flexibility of a generation unit of the electricity system in the time domain. There are three different timescales: short-term, medium-term and long-term flexibility provision.

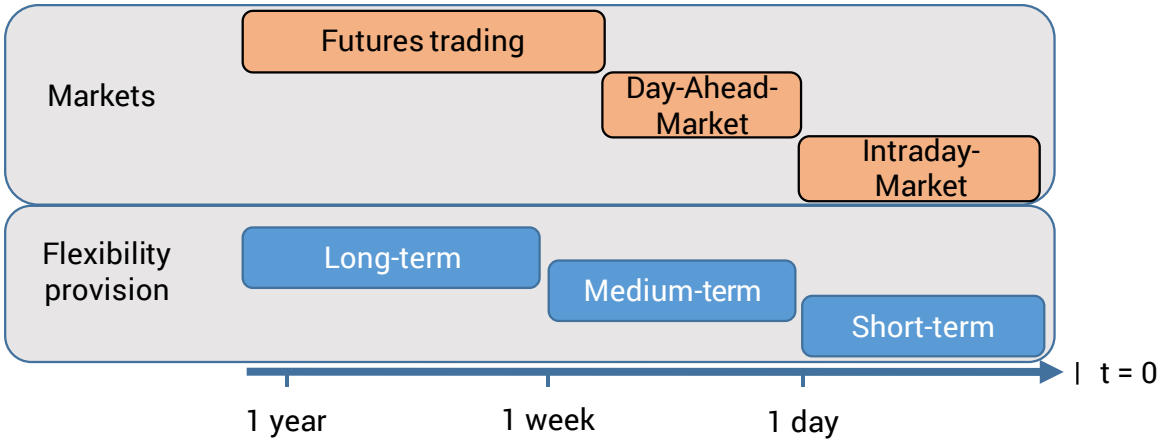

Figure 7: Characterization of flexibility in the time domain, according to (Zahoransky 2019; Konstantin 2017).

Figure 7 shows the three timescales in which flexibility provision is possible. The short-term flexibility supply serves the balancing of generation and consumption during the day. On the market side the continuous intraday trading takes place at this time, by which a short-term op-

timization of the procurement of electricity is possible. Medium- and long-term flexibility is required to compensate for longer-term changes in RES feed-in due to weather conditions such as a wind slack or a seasonally lower feed-in from PV systems in winter. Parallel to this, futures trading takes place at this time, for up to several years before the delivery date, and day-ahead trading takes place up to 36 hours before the delivery date. (Bundesnetzagentur 2017; Zahoransky 2019; Konstantin 2017)

To achieve short-term load balancing, various measures are possible, which will be referred to in the following as types of flexibility. There are four types of flexibility, as shown in Figure 8 below.

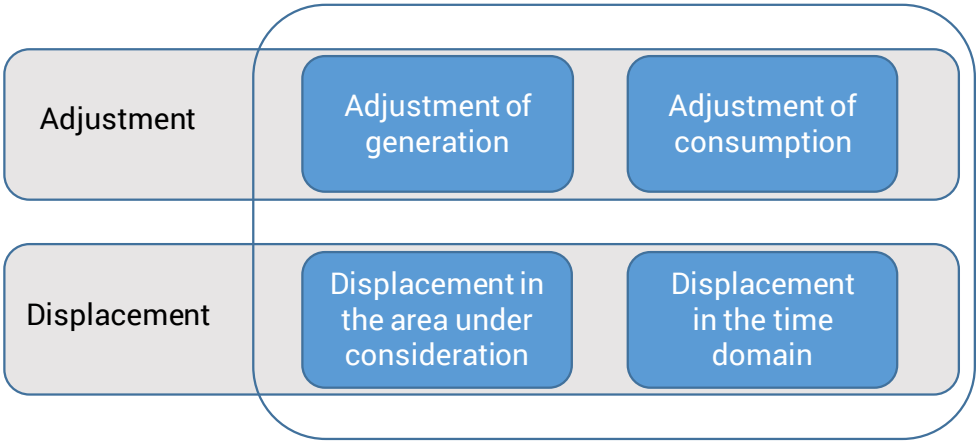

Figure 8: Types of flexibility in the power system.

These four types of flexibility can be grouped into two categories. One is the category adjustment and the other the category displacement. The category adjustment includes, for example, a generation-side adjustment of power generation by switching a generation unit on or off, or a consumer-side adjustment of consumption by means of demand side management to achieve load balancing during the day. The category displacement includes measures for shifting generation or load in the time domain by means of energy storage systems as well as the spatial shift within the area under consideration as for example by using HVDC transmission systems. (Zahoransky 2019; Union of the Electricity Industry - EURELECTRIC aisbl 2014; Siemonsmeier et al. 2018)

2.2.2 Flexibility needs in grid operation

As can be seen in Figure 9, in an interconnected system, the electrically generated power of all power plants must be equal to the load at all times, as there are no significant storage facilities in the interconnected system. (Consentec 2014)

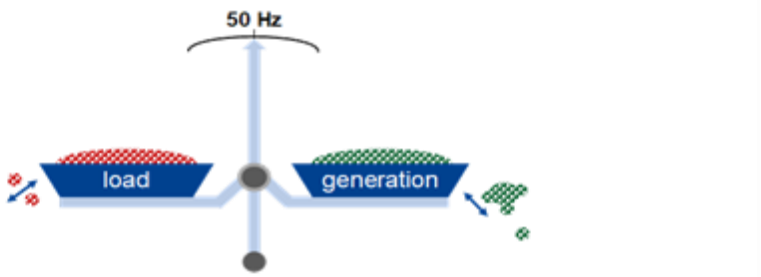

Figure 9: Balance between generation and consumption taking into account the frequency setpoint of 50 Hz (Consentec 2014).

This phenomenon is addressed by the topic of frequency stability. Frequency stability in power systems is essential for maintaining the quality of supply and security and depends largely on the demand for active power. The IEEE defines frequency stability as follows:

"It refers to the ability of a power system to maintain steady frequency following a severe disturbance between generation and load." (Kundur 1994)

If the frequency in a power system deviates upwards or downwards, this is the main indicator of a momentary imbalance between production and consumption. If the power demand exceeds the generation, the system frequency decreases. Conversely, a generation surplus means an increase in system frequency. Consequently, the system frequency fluctuates continuously in response to changing demand. It must be taken into account that it is impossible to control generation in such a way that it exactly follows the demand for power. Keeping the frequency of a power system stable is therefore a system-wide issue (Crastan 2017). Formula (2.1) illustrates – via the moment balance of all machines rotating synchronously on the mains – this relationship:

$$\mathrm{J}\,\delta = M_{gen} - M_{con} \tag{2.1}$$

The product of the moment of inertia of the rotating masses J and their angles referred to a reference point δ corresponds to the difference between the mechanical drive torque (generation) M_{gen} and the electrical counter torque (consumption) M_{con}. (Zimmer 2017)

For a power plant connected to a compound system, the electrically generated power of the power plant is composed of its turbine power P_t and an acceleration or braking power of the rotating masses, resulting from a change in speed. The turbine power must be able to cover the load and the power loss (Kleinkorte 2016). This relationship becomes apparent when formula (2.2) is converted to a current account:

$$\omega_n\,\mathrm{J}\;2\pi\,\frac{\mathrm{df}}{\mathrm{dt}} = P_t - P_{con} - P_{loss} \tag{2.2}$$

In the stationary state, the turbine power P_t covers the power consumed ($P_{con} + P_{loss}$), consisting of consumption and losses. The frequency gradient $\frac{\mathrm{df}}{\mathrm{dt}}$ is zero, since the constant nominal frequency of 50 Hz is present in interconnected operation. In case of an imbalance between generation and consumption, a frequency gradient is formed and with it a proportional acceleration or deceleration of the rotating masses. The power equilibrium is consequently restored by a temporary change of the system frequency. It is therefore necessary to first stabilize the average frequency and then return it to the setpoint. This control mechanism is called power frequency control and is shown schematically in Figure 10 ((Kleinkorte 2016; Zimmer 2017).

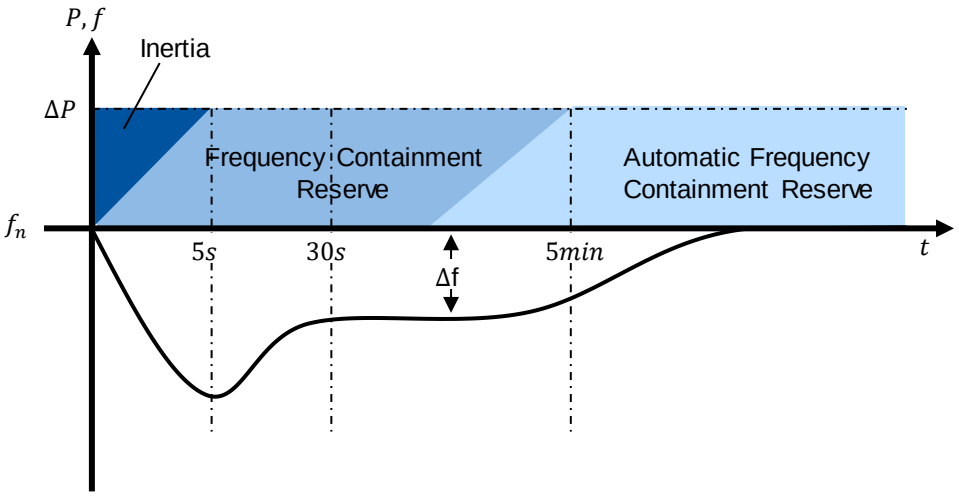

Figure 10: Frequency response after interference, according to (ENTSO-E 2013).

The diagram deals with the case of a deficit in electrical energy supply, which can result either from a generation failure or from a load increase. The effect in the period between 0 s and 5 s is called instantaneous reserve. During this period, the kinetic energy stored in the rotating masses covers the power deficit that decreases due to primary control ΔP. The instantaneous reserve is not a classical control mechanism but a physical process of energy conservation (cf. equation (2.2)), which is inherently provided by the rotating masses of conventional power plants (Dena 2016; Stein 1953). There also is the self-regulating effect of the load which has an effect during this period: In simplified terms, the load behaves like a frequency-dependent motor-inductive consumer whose power consumption depends on the frequency (Crastan 2015). At the same time a proportional speed controller, which has the frequency deviation Δf as input parameter, activates the frequency containment reserve (also called primary control reserve). This control mechanism is discussed in more detail in Sections 3.4.2 and 3.4.3. The primary control reserve aims at stopping the frequency drop and stabilizing the frequency at a constant frequency deviation. This is achieved by the power plants providing primary control power changing their operating point with the help of the activated, frequency-sensitive proportional controller, thus increasing the turbine drive torque. For each power plant, primary control takes place completely independently, uncoordinated, automatically and decentrally (Crastan and

Westermann 2018). After 30 s at the latest, the load deficit is eliminated and generation and consumption are back in balance. Nevertheless, an approximately constant frequency deviation remains in the synchronous network system. In order to prevent a renewed frequency drop, the primary control power is maintained for a period of 30 s to 15 min and successively replaced by the secondary control power (Consentec 2014). In the period from 30 s to 15 min the secondary control follows as power-frequency control (Automatic Frequency Restoration Reserve): The frequency deviation Δf, linked with a deviation of the exchange power, acts as an artificial control variable of an integral controller. The aim is to return the mains frequency to nominal frequency.

These mechanisms require flexibility in grid operation in different time periods and depend on the dynamic behavior of the electrical components and their controllers in a power system. These are addressed in Section 2.4.3 from an analytic point of view and the mathematical models are presented in Section 3.4 before the simulations on flexibility in grid operation are carried out in Chapter 5 to investigate the possible flexibility needs in terms of maintaining frequency stability.

2.2.3 Flexibility options

Flexibility in a power system is provided by a variety of different technologies. In the following, different technologies for the provision of flexibility are presented as examples.

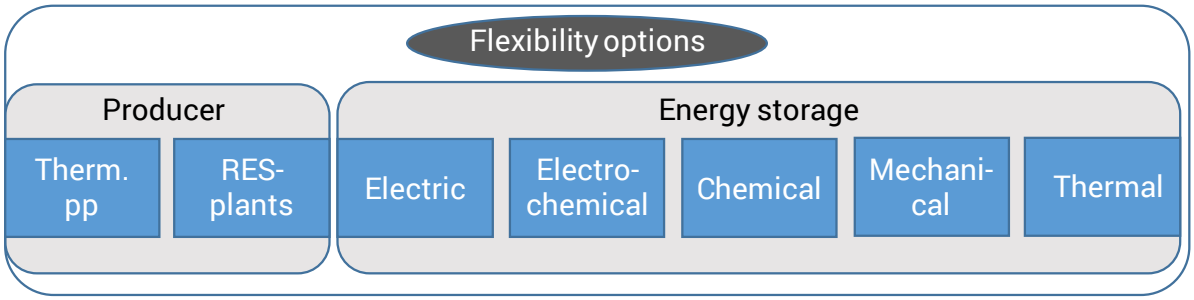

Figure 11: Classification of flexibility in the power system, according to (Bundesnetzagentur 2017; Sterner and Stadler 2017).

As shown in Figure 11, the different flexibility options are categorized on several levels. First, a distinction is made between the provision by generation units or by energy storage or sector-coupling technologies. Within this classification, it is possible to make a further subdivision according to the used technology.

In the following, four technologies for flexibility provision are presented as examples. These are the gas turbine as a technology in the generator category and three technologies from the field of energy storage and power-to-x. In addition to superconducting coils and supercapacitors as electrical energy storage devices, these are the power-to-x technology and compressed air storage as mechanical energy storage.

Gas turbines

The use of gas turbines is one way of providing flexibility on the generation side. In gas turbine power plants, the air as an operating medium is compressed by a compressor and ignited in the combustion chamber together with the respective primary energy source. The expansion of the operating gas in this process powers the downstream turbine and thus also the connected generator. (Zahoransky 2019)

Table 1: Technical data of gas turbine power plants, according to (Zahoransky 2019; Markewitz and Robinius 2017)

Parameter	Data
Startup time	Hot start (<8 h): 6 min-15 min
	Warm start (8 h-24 h): 6 min-15 min
	Cold start (>48 h): 6 min-15 min
Minimum power [% P_{nenn}]	20 %-50 %
Power change gradient [% P_{nenn}/min]	8 %-15 %

As Table 1 indicates, gas turbines are characterized by very short start-up times, regardless of their current condition. It is therefore irrelevant for which period of time this type of power plant was previously out of operation. In combination with power change gradients in the range of 8 % to 15 % of the nominal power and the low minimum operating powers, gas turbines can start up any technically permissible operating point in a comparatively short time and thus adapt their generation to the current demand. (Zahoransky 2019)

Two major disadvantages of using gas turbines to provide flexibility in the future European power system are, on the one hand, the CO_2 emissions that result from firing fossil fuels such as natural gas and, on the other hand, the comparatively high costs of procuring the primary energy source and the necessary emission rights to emit the CO_2 (Zahoransky 2019; Konstantin 2017). Due to the technical capabilities of the gas turbine described above, power plants based on this technology are highly flexible as so-called peak load power plants and allow for a load balancing during the day due to the comparatively short reaction times.

Superconducting coils and super capacitors

Superconducting coils and supercapacitors are components used in electrical engineering that are part of electrical energy storage systems. They can store electrical energy without converting it into another form, such as chemical or mechanical energy. Inside such a capacitor, the electrical energy is stored in the electrical field. Due to their high power density, they are capable of providing high power in short time ranges. In contrast, storage in superconducting coils takes

place within the magnetic field. An essential advantage of these two technologies for flexibility provision is their low losses. Due to the direct storage of electrical energy, the losses of a conversion process are eliminated. However, this technology is characterized by very low energy densities, which is why they are only suitable for short-term flexibility provision in the range of seconds and minutes. Thus, these two flexibility options only play a minor role for load balancing during the day (Sterner and Stadler 2017) but can contribute to ancillary services to ensure power system stability.

Power-to-x-technology

In contrast to the electrical storage described above, a long term storage or sector coupling is possible by converting the electrical energy into chemical energy. Different forms of this conversion, for example into gas, a fuel or heat, are summarized by the general term power-to-x technology. By using fuel or gas as the conversion product, the sectors electricity, heat and transport are linked together. Coupling with the heating sector allows to exploit the storability of heat, so that short-term shift potentials can be used. In addition, coupling with the gas sector offers the possibility to provide longer-term flexibility and to use gas infrastructure, especially gas storage. By means of gas-fired power plants, reverse power generation is then possible. (Zahoransky 2019; Sterner and Stadler 2017)

In power-to-gas plants, water is split into oxygen (O_2) and hydrogen (H_2) by electrolysers. This H_2 gas can either be used directly in fuel cell vehicles or industrial processes or converted into methane gas (CH_4) through methanization and fed into the existing natural gas network. (Zahoransky 2019; Sterner and Stadler 2017)

Table 2: Technical data of a PEM electrolyzer, according to (Sterner and Stadler 2017; Siemens AG 2017)

Parameter	Data
Electrical power	0,5 kW to 1,2 MW
Minimum power [% P_{nenn}]	20 %
Startup time	< 10 s

The electrolyser as the core element of such a plant is characterized by its high degree of flexibility, as shown in Table 2. With a start-up time of less than ten seconds and a comparatively low minimum operating capacity of 20 % of the nominal output, these plants are able to react to changes in the production situation at short notice. However, the conversion process is subject to losses. This means that the respective efficiency of the process has to be taken into account

both for electrolysis and for any subsequent methanization. For the entire process from electrolysis to the completion of methanation, efficiencies of between 49 % and 65 % are achieved. (Zahoransky 2019; Sterner and Stadler 2017)

With power-to-gas plants, it is therefore possible to provide flexibility for a short-term balance between generation and consumption by adjusting consumption.

Compressed air storage

Finally, compressed air storage is being investigated as a mechanical form of energy storage for flexibility provision. This form of energy storage stores energy in kinetic or potential form. In addition to compressed air storage, hydro storage power plants also belong to this category of energy storage. However, these are considered separately in Section 2.4.2. (Sterner and Stadler 2017)

Due to the compressibility of the ambient air, it is possible to store energy in compressed air storage power plants by means of a pressure difference. The basic structure of such a storage power plant has certain technological similarities to a gas-fired power plant. Here, as well, the core elements of this technology are a compression unit and an expansion unit, whereby the combustion chamber of the gas turbine is replaced by the gas storage unit, for example an underground empty salt cavern. Using an electrically driven compressor, the ambient air is compressed and then stored at pressures between 46 bar and 72 bar. If required, the compressed air is taken from the storage facility and expanded in a turbine unit. The energy stored in the pressure difference is converted back into electrical energy. (Zahoransky 2019; Sterner and Stadler 2017)

The following Table 3 contains technical data of two operating compressed air storage power plants. One has been located in Huntorf in northern Germany since 1978, while the other power plant has been in operation in McIntosh in the USA since 1991. These storage power plants are characterized by short reaction times, which are able to be reduced by a further 50 % in critical situations. However, when using this technology, the efficiency losses are significantly higher compared to other technologies. (Sterner and Stadler 2017)

Table 3: Technical data of two compressed air storage power plants, according to (Sterner and Stadler 2017)

Power plant	Huntorf	McIntosh
Electrical power	321 MW	100 MW
Mininmum power [% P_{nenn}]	32 %	10 %
Cycle efficiency	42 %	54 %
Stroage volume	560 MWh	2.640 MWh
Discharge duration (at full load)	approx. 2 h	approx. 24 h
Startup time (Normal operation)	14 min	12 min
Startup time (emergency)	8 min	7 min

To sum up, compressed air storage power plants are well suited for short-term intraday load balancing due to their short reaction times and relatively low minimum operating capacity. With this technology, it is possible to provide flexibility by adjusting both generation and consumption. Depending on the size of the storage facility, it is also possible to provide flexibility by shifting in the time domain.

2.3 Characteristics of the NORDEL grid

In the following Sections 2.3.1 to 2.3.2 the focus is on the hydro storage power plants in Norway and Sweden. First, the fundamentals of the two power systems are explained. Afterwards, the structure of the power plant parks is analyzed.

2.3.1 Fundamentals of the Nordic power system

The power systems in Norway and Sweden are two very renewable systems, with more than 50% of the electricity coming from RES. However, there are significant differences between the two systems, especially regarding the use of other primary energy sources.

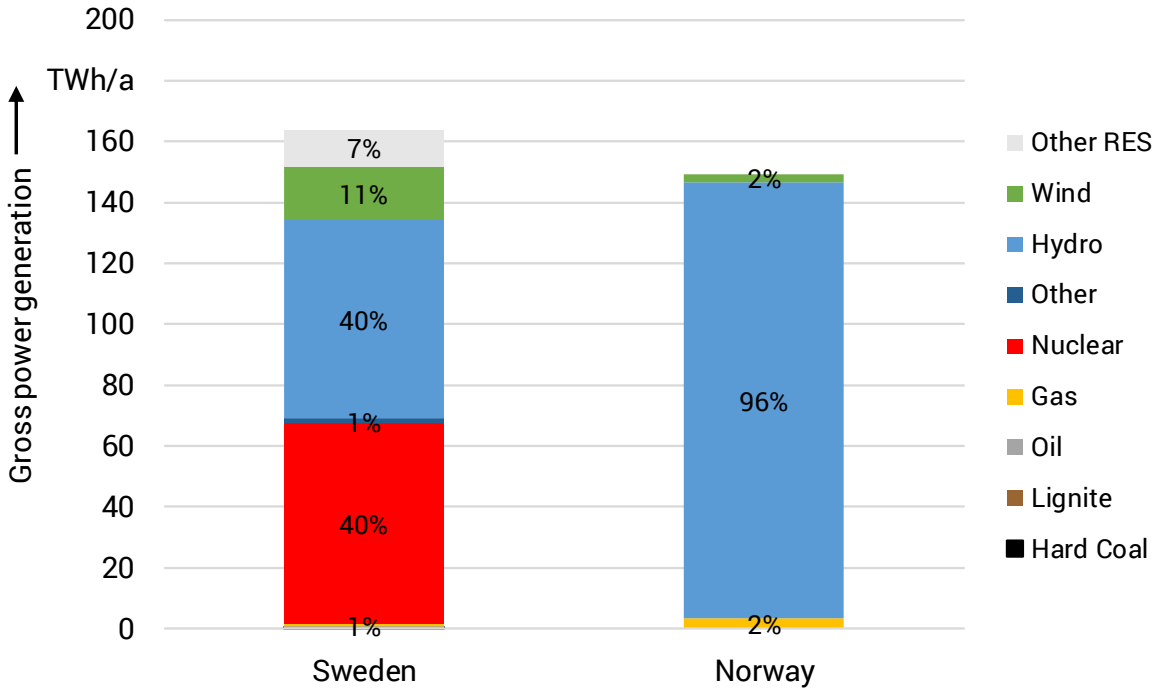

Figure 12: Gross electricity generation in Sweden and Norway in 2017, according to (European Commission 2020; Statistic Norway 2017).

While Norway's gross electricity generation is almost entirely based on hydropower, as described in detail in Section 2.1.1, Sweden has more than 60 TWh generated in nuclear power plants in 2017. Furthermore, Figure 12 above clearly shows that this amount of electricity generated in nuclear power plants of more than 60 TWh in 2017 corresponds to about 40 % of the total gross electricity generation. The rest of the gross power generation is almost exclusively generated by plants based on RES. Fossil-fired thermal power plants, such as coal- or gas-fired power plants, are of minor importance in both supply systems with shares in the low single-digit percentage range. Accordingly, these two Nordic countries are only marginally affected by the political discussions on coal-fired power generation described in Section 2.1.2.

In addition to the shares of the different primary energy sources in gross electricity generation, Figure 13 below shows their shares in the installed generation capacities.

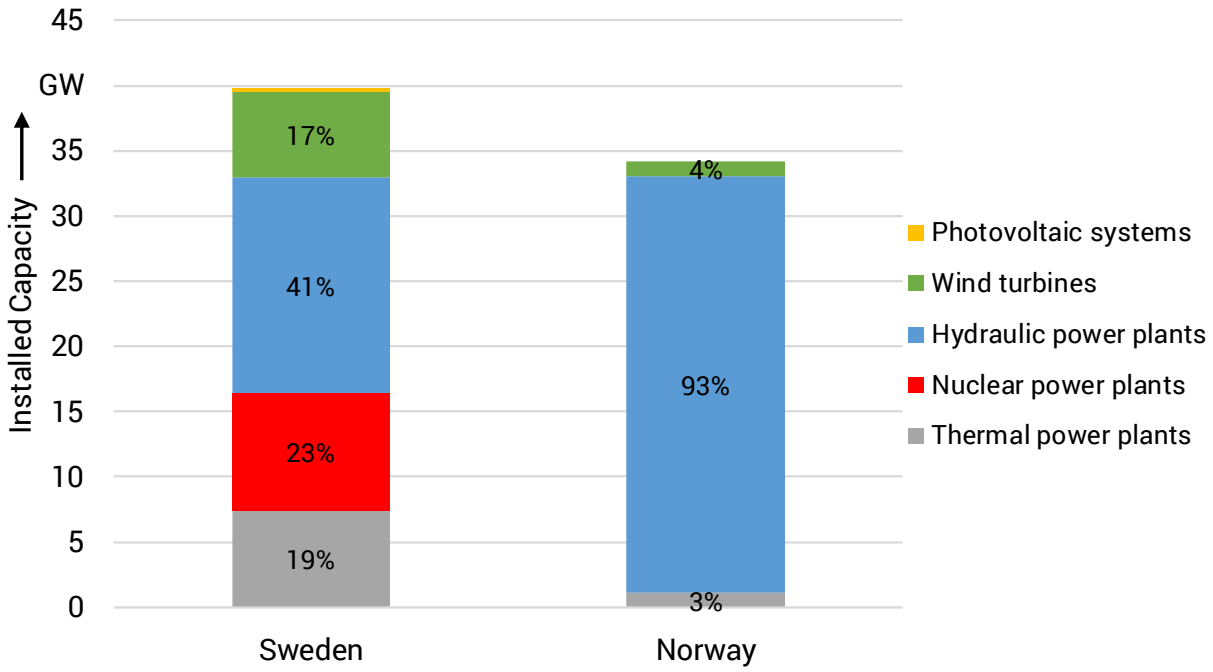

Figure 13: Installed generation capacity in Sweden and Norway in 2017, according to (Statistic Norway 2017, 2019).

In particular, considering the Swedish power plant park, it becomes apparent that conventional thermal power plants play hardly any role in actual generation, despite a share of almost 20 % of the installed generation capacities. This means that other power plants, such as nuclear power plants and hydro power plants, are primarily used to cover the load. While in Sweden hydro power plants with an installed capacity of approx. 16 GW are in operation, the Norwegian power plant park has hydro power plants with an installed capacity of approx. 32 GW. This represents over 93 % of the total installed generation capacity in Norway.

A special characteristic of the power system in Norway and Sweden is their division into up to five different bidding zones of the wholesale markets. As illustrated by the map in Figure 14, Norway is divided into five bidding zones and Sweden into four bidding zones. The layout of these bidding zones represents the main congestion management measure in these Nordic countries. While Sweden's four bidding zones exist at all times due to medium-term restrictions in the transmission system, Norway is divided dynamically. The objective of this dynamic division of Norway into different bidding zones is to take regionally different generation situations into account by creating price incentives via the market to optimize the use of the available storage capacities. In particular, different water availability in the different regions of Norway as a result of different weather conditions is taken into account. (THEMA Consulting Group 2013)

Figure 14: Bidding zone boundaries within Norway and Sweden, according to (Nord Pool AS 2019a).

The NORDEL transmission grid is shown in Figure 15. The different voltage levels are drawn in red (380 kV), blue (330 kV) and green (220 kV). In contrast to the Central European power system the Nordic transmission grid is only sparsely meshed in most parts of the Nordics, especially in the northern parts of the Nordic countries. Only in and near urban areas the grid is highly meshed.

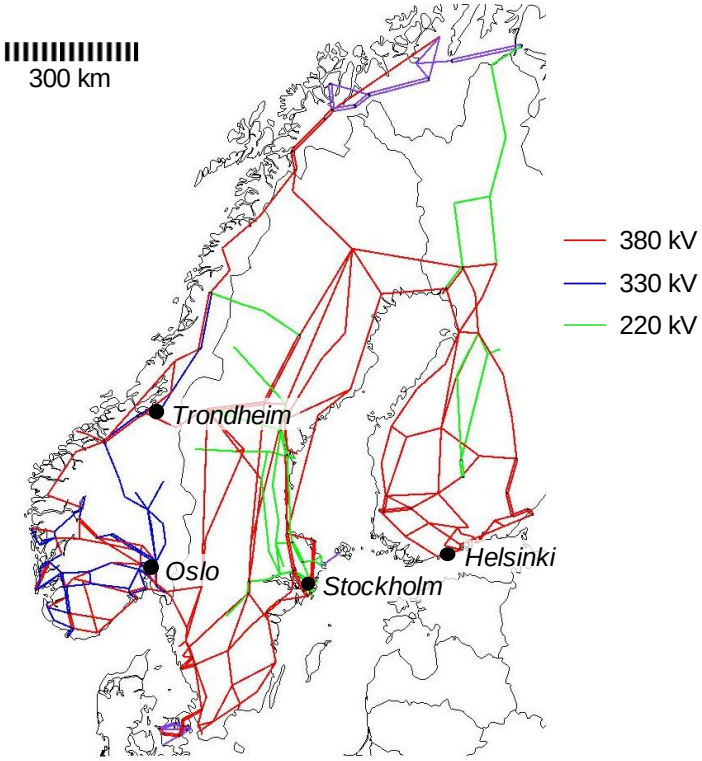

Figure 15: NORDEL transmission grid.

2.3.2 The hydro power plant park

In the following, an analysis of the structure of the hydro power plant park is carried out. Due to the long history and diversity of the hydropower plants, the considered criteria include the installed generation capacity and the age structure. Due to a lack of data on technical parameters of the plants, turbine-specific parameters cannot be analyzed in the folliwing. These are interpolated and calculated in Section 3.3.1.2 as part of the modeling process.

In the following analysis, power plants with a nominal capacity of less than 10 MW and run-of-river plants are not considered. Accordingly, about 75 % of the hydro generation capacity in Sweden and about 90 % in Norway is examined in more detail (ENTSO-E 2018). The absolute number of hydropower plants considered is 341 in Norway and 85 in Sweden with a generation capacity of 29.1 GW and 12.4 GW respectively (c.f. Figure 16). A classification into power categories and their frequency distribution is shown in Figure 17. In this chart it is noticeable that Sweden tends to use larger plants, while the frequency distribution in Norway is highest in the power category between zero and 50 MW with 43.1 %.

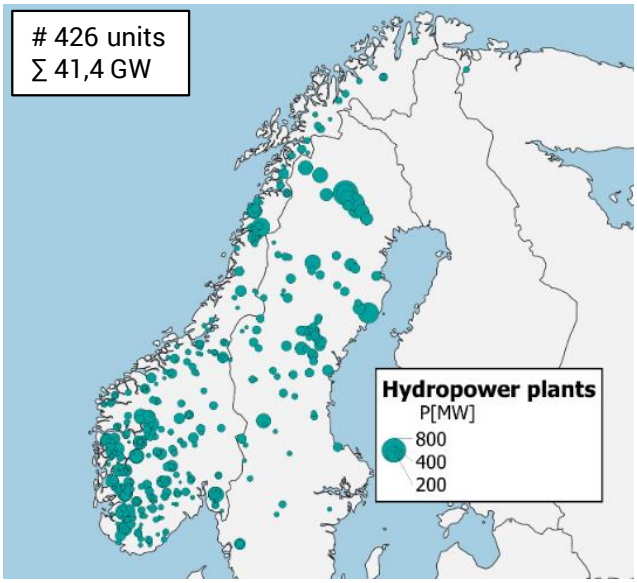

Figure 16: Nordic hydropower plant park.

Figure 18 shows the frequency distribution of the different age categories of hydro power plants. The figure indicates that the power plants in Sweden are on average significantly older than those in Norway. In Sweden about 45 % and in Norway about 27 % of all plants are older than 60 years. Furthermore, the share of newly comissioned plants within the last 15 years is only about 1 % in Sweden and about 8 % in Norway.

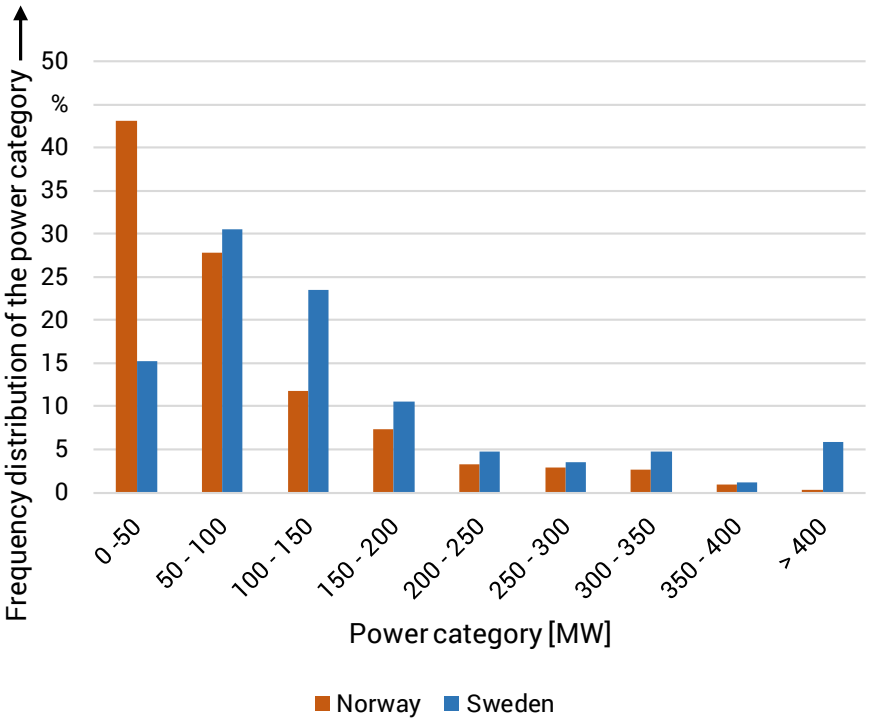

Figure 17: Frequency distribution by number of turbines allocated to different power categories, according to own research.

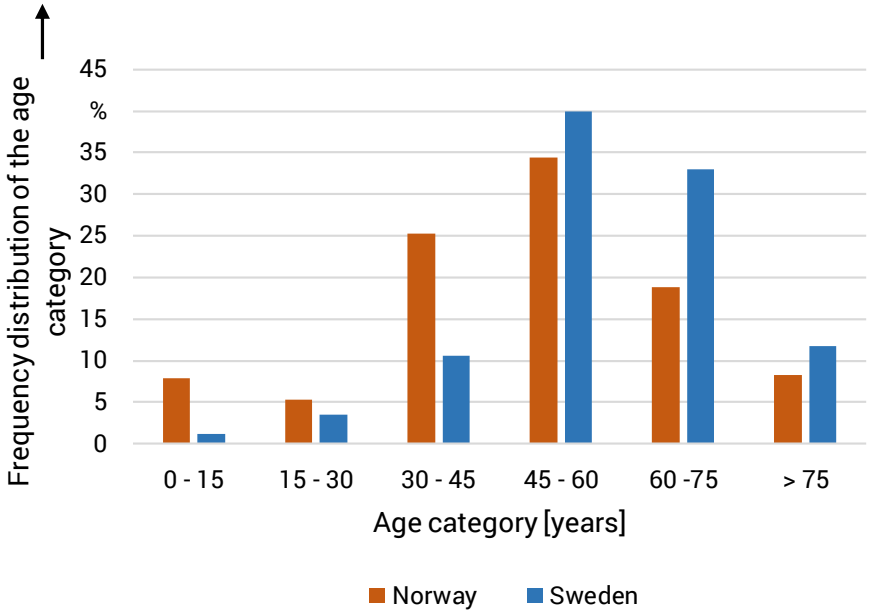

Figure 18: Frequency distribution by number of turbines assigned to different age categories, according to own research.

2.4 Hydropower as a flexibility option

Since the focus of this study is on the provision of flexibility by hydro storage power plants, the structure and operation of this flexibility option ist considered individually in the following chapter. First, the operating mode of two exemplary storage power plants will be considered on the basis of their operation in two months in 2018. Then, the structure, function and flexibility provision by hydropower is described. After that, the dynamic behaviour of hydropower is analyzed.

2.4.1 Current use of hydro storage power plants in Sweden

In the following section, the current operation of hydro storage power plants will be examined using two power plants in Sweden for the months January and July 2018 as an example. The power plants in focus are the generation plants Porjus and Stornorrfors. The two selected power plants are two of five power plants that were defined as reference power plants, so-called reference sites, within the HydroFlex project (Hydroflex 2019). The following Table 4 contains the most important technical data of these two power plants.

Table 4: Technical data of the Porjus and Stornorrfors power plants, according to (Vattenfall AB 2019a, 2019b)

Power plant	Porjus	Stornorrfors
Max. power [MW]	430	599
Commissioning	1975	1958
Turbine type	Francis	Francis
Number of turbines	2	4

In the following, different parameters are considered to describe the current operation mode. These are the average generation by the two power plants in January and July 2018 as well as the maximum number of start/stop cycles[3] that one of the two respectively four turbines of the power plants has run on one day during the period under consideration. Power plant usage data from ENTSO-E, the European Association of Transmission System Operators for Electricity (ENTSO-E), which is available on their transparency platform, was used for this purpose.

As shown in Table 5, both power plants are utilized at less than 40 % during the considered period, which in the case of the Porjus power plant corresponds to less than 125 GWh of electricity production. In July, both power plants are operating at less than 30 % of nominal capacity. This corresponds to 91 and 114 GWh of electricity production respectively. While the maximum number of start/stop cycles of a turbine of the power plant Stornorrfors does not change compared

[3] A start/stop cycle is defined as a process from one start-up of the generator to the next start-up.

to both months, the number of start/stop cycles at the power plant Porjus increases to up to three cycles per day in July.

Table 5: Key parameters of the current operation of the Porjus and Stornorrfors power plants, according to (ENTSO-E 2019)

Power plant	Porjus	Stornorrfors
Generation (January)	124,69 GWh	180,42 GWh
Generation (July)	90,75 GWh	114,1 GWh
Maximum number of cycles of a turbine per day (January)	2	2
Maximum number of cycles of a turbine per day (July)	3	2

In the following, the generation profile of the two power plants in July 2018 is examined more in detail.

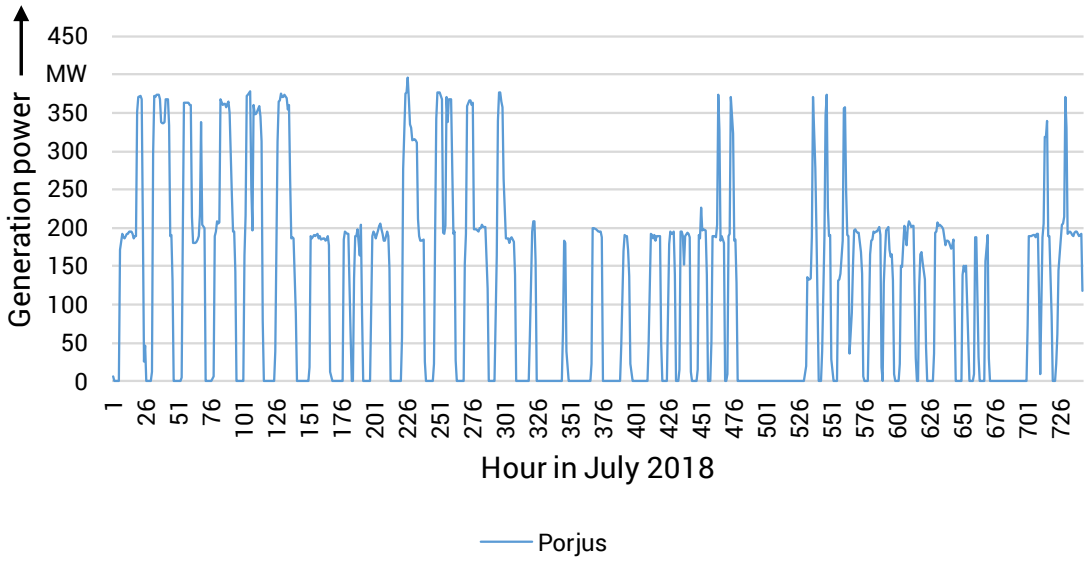

Figure 19: Generation profile of the reference power plant Porjus in July 2018, according to (ENTSO-E 2019).

Figure 19 shows the hourly production of the Porjus power plant in July 2018. It is noticeable that the two turbines of the power plant were out of operation in more than 40 % of the hours. The power plant never operated at nominal capacity during the month under consideration. In only 14 % of the hours the power plant was used to more than 50 % capacity.

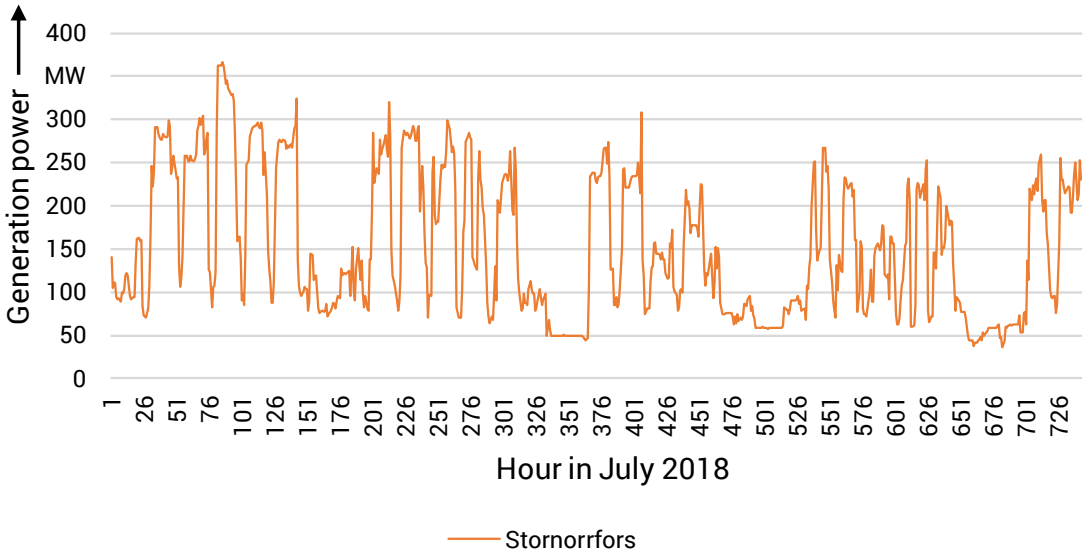

Figure 20: Generation profile of the reference power plant Stornorrfors in July 2018, according to (ENTSO-E 2019).

Figure 20 illustrates the corresponding generation profile for the Stornorrfors power plant. It shows that the power plant was out of operation at one point in time in July 2018, but was operated at less than 25 % of the nominal capacity in more than 55 % of the hours. Similar to the Porjus power plant, the Stornorrfors power plant was never operated at nominal capacity, but was only utilized to a maximum of 61 %.

For both reference power plants, it is important to point out that rarely or never all two or four turbines of the power plants are operated simultaneously. Furthermore, by considering the less amount of start/stop cycles, it seems that these hydro power plants were only operated as flexible generation units to a limited extent at the present time.

2.4.2 Flexibility provision by hydro storage power plants

In addition to the possibilities for providing flexibility already described in the Section 2.2.3, there is also the option to provide flexibility by hydro storage power plants. Due to the focus of this study on this flexibility option, this technology is explained in detail in the following. First of all, the different types of power plants will be discussed, before the operational and technical restrictions are presented.

2.4.2.1 Types of hydro power plants

Hydropower plants convert potential energy resulting from height differences into kinetic energy via a pressure pipe. The kinetic energy is then transformed into mechanical energy by means of water turbines and finally converted into electricity by means of a generator. All different types of hydropower plants have in common that they have at least one turbine. Depending on whether

the power plants also have a pump or whether there are storage reservoirs from which the turbines are fed, a distinction is made between storage or pumped storage power plants and run-of-river power plants. Tidal and wave power plants represent further possibilities for generating energy from hydropower. Howewer, these types of power plants will not be considered in detail here.

Run-of-river power plants

In contrast to storage power plants, run-of-river power plants do not have storage reservoirs, as they are used in streams where damming up is not possible, for example, because navigability has to be guaranteed, or where the gradient is too low. The height difference between the inlet to the turbine and the outlet from the turbine of a run-of-river power plant is comparatively small compared to the height difference in storage power plants. Because the turbine is fed directly from the running water, the operation of these power plants depends on the water supply of the watercourse and are therefore not able to provide flexibility. Thus, run-of-river power plants usually operate as base load power plants. Compared to storage power plants, run-of-river power plants are not designed for the maximum possible water volume flow, but for the average value. This is mainly for economic reasons. (Zahoransky 2019)

Storage and pumped storage power plants

Storage power plants and pumped storage power plants have a basically comparable design. In contrast to storage power plants, however, pumped storage power plants also contain at least one pump. In these power plants, electricity is generated by converting potential and kinetic energy of the water into electrical energy. (Strauss 2016)

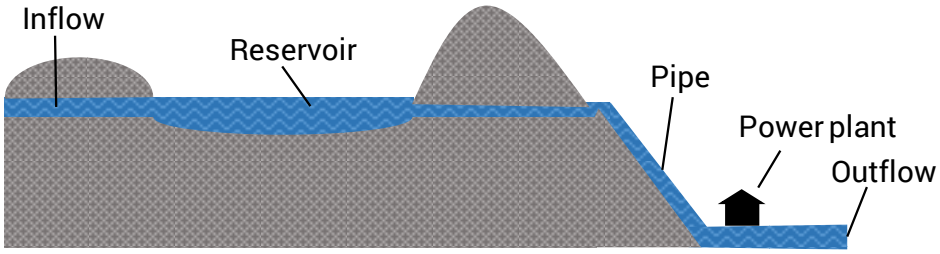

Figure 21: Hydro storage power plant, according to (Schwab 2017).

Figure 21 shows the schematic structure of a hydro storage power plant. Characteristic for these power plants are the two very different height levels within the generation plant. On the upper level is the storage basin and its inlet. The water within this storage basin has potential energy due to the difference in height to the outlet. To generate electricity, the water is transferred from the storage basin through pipes to the lower level outlet and drives the turbine and the connected generator. The head of the water, i.e. the difference in height between the storage basin and the power plant, has a significant influence on the power generation. For this type of power plant three components are of particular importance, which is why their function is described in more detail in section 2.4.2.2. In addition to one or more storage basins, these are the

turbine and - if the special case of a storage power plant is a pumped storage power plant - the pump. (Strauss 2016; Schwab 2017)

2.4.2.2 Components of hydro storage power plants

After the basic description of the two most important types of hydro power plants, the three main components of a hydro power plant are explained more in detail below. First, the turbines and pumps are examined. Then the function of the storage basin is described.

Turbine

The turbine is the core element of a hydro storage power plant. It converts the kinetic energy of the water falling from the higher located storage basin through pipelines into rotational energy. A generator is connected to the turbine to convert the rotational energy into electrical energy. Normally Kaplan, Francis or Pelton turbines are used in hydro power plants. Due to a development of the turbines adapted to the head of the water and the volume flow, they have different characteristics.

Table 6: Technical characteristics of the most common water turbines, according to (Moser 2018)

Parameter	Kaplan turbine	Francis turbine	Pelton turbine
Head [m]	6-70	20-900	100-1770
Max. power [MW]	300	800	500
Max. efficiency [%]	94	95	90

As Table 6 shows, Francis or Pelton turbines are particularly suitable for use in storage power plants with high heads. These allow generation capacities of up to 500 MW per Pelton turbine or 800 MW per Francis turbine. In contrast, the Kaplan turbine is used with a maximum output of 300 MW per turbine at low heads between 6 m and 70 m, as is mainly the case in run-of-river power plants. When considering the maximum efficiency of the different turbine types, significant differences are noticeable. The Francis turbine has the best efficiency of 95 %. A special characteristic of the Kaplan turbine and the Francis turbine is their ability to be used as pumps. (Zahoransky 2019; Konstantin 2017; Moser 2018)

Pumps

While kinetic energy is converted into electrical energy in turbines, the corresponding opposite process takes place in pumps. By using one or more pumps, pumped storage power plants are able to pump water from a river or another storage basin as run-off water into the higher located reservoir. It is then possible to use the water for power generation at a later time. (Schwab 2017)

Reservoirs

Basically, every turbine or pump in a hydro power plant requires an inlet and an outlet. In hydro storage power plants, there is usually a storage basin between the inlet, for example a river, and the turbine. The turbined water is discharged through a river or another storage basin, the lower basin. Only the use of an upper basin makes a temporal decoupling of the inflow and the generation possible. The maximum shift of the generation in the time domain by storage of the inflow in the upper basin is determined by its storage capacity. The larger the storage basin is dimensioned, the longer the generation can be shifted in the time domain. (Zahoransky 2019; Schwab 2017)

2.4.2.3 Operational restrictions of hydro storage power plants

One of the basic requirements for the operation of a hydro storage power plant is the availability of water. Operation is not possible without a sufficient filling quantity of the storage basin. The availability of water is essentially dependent on two variables. On the one hand, the natural inflows and on the other hand the inflows and outflows resulting from the interconnection of several hydro storage power plants by waterways.

An example of a natural inflow to hydro storage power plants is a river that flows into the constructed upper reservoir. However, this inflow is not constant at all times, but is subject to seasonal fluctuations. These must be taken into account in the operational planning to prevent the basin from running empty. (Konstantin 2017)

In addition to the natural inflow, the amount of available water and thus the operation of the hydropower plant may depend on other hydro power plants. If several hydro power plants or their storage reservoirs are connected to each other via waterways, this is called interconnection. In Figure 22, such a linkage of different power plants is shown using the example of a power plant group in Norway.

It is clear that the Moflåt power plant, for example, can only turbine if one of the two upstream power plants, Såheim or Mår, is also in turbine operation. In contrast, the Vermork power plant is not permanently tied to the operation of the upstream Frøystul power plant, as the Skardfoss reservoir between the two power plants enables the two operating modes to be decoupled. This section of the Norwegian hydro system clearly shows that the use of a hydro storage power plant may depend on other power plants due to interconnection (The Norwegian Water Resources and Energy Directorate 2019).

Besides the limitation of operation due to water availability, other aspects during operation have to be considered, since reservoirs are usually used for other purposes in addition to electricity generation. For example, they are used to supply cities or industry with water or to regulate the level in downstream waters, for example to make navigation possible. (Sterner and Stadler 2017)

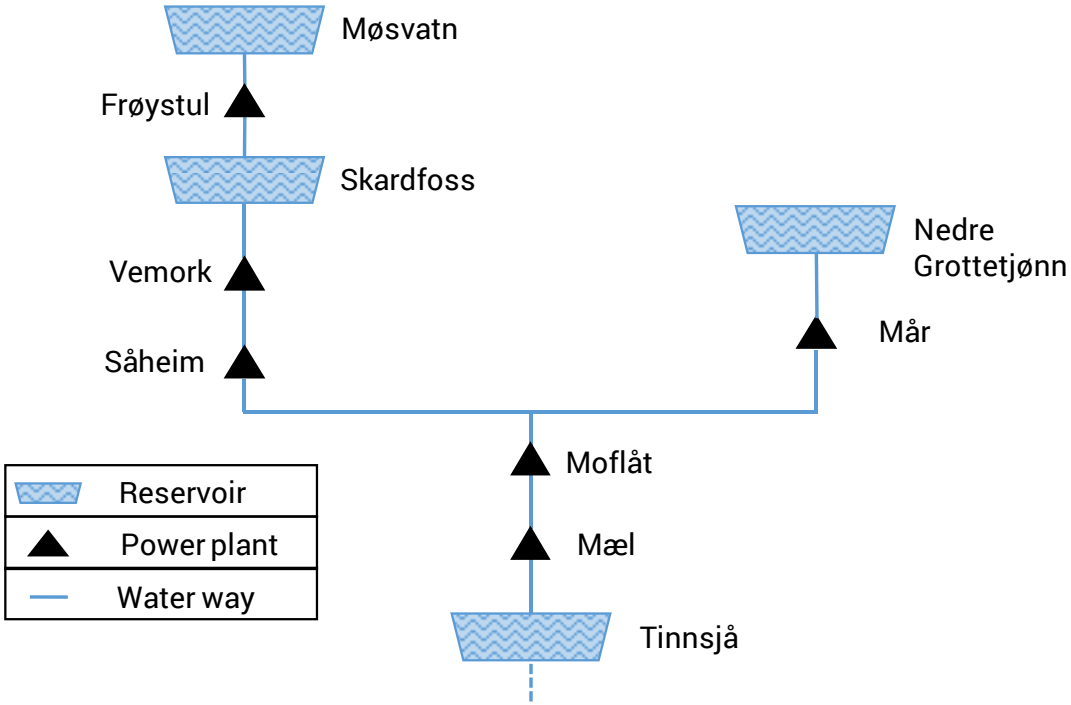

Figure 22: Interconnection of hydro storage power plants using the example of a Norwegian power plant group, according to (The Norwegian Water Resources and Energy Directorate 2019).

2.4.2.4 Technical restrictions of hydro storage power plants

After the operational restrictions have been considered in Section 2.4.2.3, the technical restrictions of hydro storage power plants are discussed in the following. The focus is on restrictions of power plant operation to reduce the stress of the different components of the power plant. The reason for this is that due to the large water masses flowing through the power plant, its components are subjected to high dynamic, mechanical and thermal loads (Sterner and Stadler 2017). In principle, it is possible to use the power plants in a very flexible manner, since the start-up time is one minute or less (Schwab 2017). However, every start-up process involves stress for the mechanical components. As a result, each of these starts reduces the lifetime of the power plant and its components by 15 hours (Nilsson and Sjelvgren 1997). In order to consider and reduce these stresses in daily operation, the power plant operator can define minimum operating times, minimum downtimes or a maximum number of start-up processes. The minimum operating time specifies how long the power plant must remain in operation after a start-up process before it is permitted to shut down again. Depending on the power plant operator and turbine, typical minimum operating times range from two to six hours. Thus, the flexibility potential of hydro storage power plants is limited by these technical restrictions to reduce mechanical stress and wear. (Nilsson and Sjelvgren 1997)

After explaining the structure, the function as well as the operational and technical restrictions of hydro power plants in the previous Sections 2.4.2.1 to 2.4.2.4, this flexibility option is classified according to the types of flexibility provision defined in Figure 8.

As a controllable generation unit, hydropower plants are able to provide flexibility by adjusting generation. If the considered power plant is a pumped storage power plant, it is also possible to influence the consumption in the power system by adjusting the pump operation, thus providing a second type of flexibility. Due to their storage basin in the turbine inlet, hydro storage power plants are able to provide a third type of flexibility. By decoupling generation from the inflow, these power plants are able to shift generation in the time domain. To summarize, hydro storage and pumped storage power plants are capable of providing flexibility to the power system in a variety of ways.

2.4.3 Dynamic behaviour of hydropower plants

Although hydropower plants are considered RES, they are classified as conventional power plants in the same way as thermal power plants, which generate electricity from thermodynamic energy conversion processes. This can be explained as follows: Hydro (large-scale) power plants in their classic design with a grid-connected synchronous generator and the associated speed control system have a similar dynamic behavior to conventional power plants. (Zimmer 2017; Heuck 2013; Crastan and Westermann 2018; Hutarew 1969)

Figure 23 shows schematically the elements of a (pumped) storage power plant, which are important to analyze the dynamics of hydropower plants. Accordingly, mathematical models differentiate between a conglomerate of turbine model and a model of the water column in the pressure pipeline as well as a speed governor. The regulator consists of control and actuating devices to vary the flow rate. The flow rate can be used to control the turbine torque from standstill to full load within a certain speed range. (Naghizadeh 2014)

In the following, a brief introduction is given to the variables that are important for the analysis of the different turbine models and for the differentiated consideration of the dynamic behaviour of the water column.

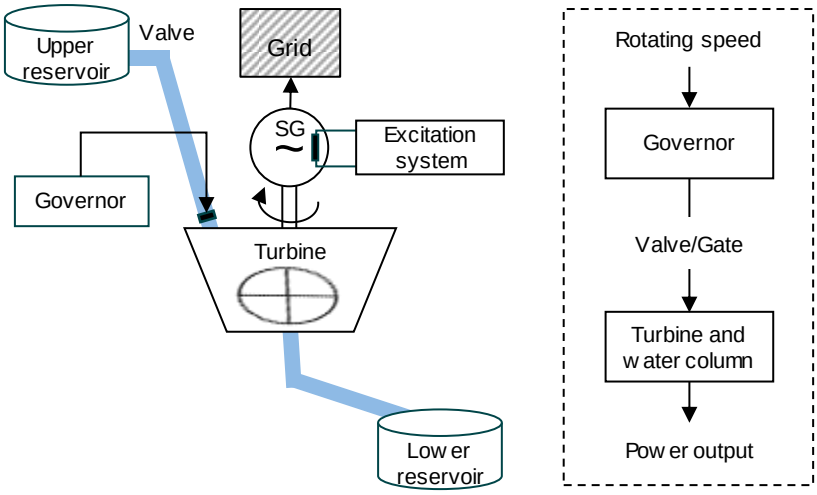

Figure 23: Components of a hyraulic power plant (Zimmer 2017).

Figure 24 illustrates the hydraulic coupling between the upper reservoir and the turbine. The hydraulic coupling between the reservoir and the turbine takes place, among other things, via one (or more) penstock(s). A penstock is a pressurised pipeline that is completely filled with water and under pressure, which reduces frictional losses (Kaltschmitt 2013; Detering 2018). Pressure fluctuations occur when opening or closing the valve. A distinction is made between short-wave and long-wave pressure fluctuations: Short-wave pressure fluctuations result from the compressibility of water and the elasticity of the pressure tube, while long-wave pressure fluctuations are a consequence of mass inertia (Giesecke and Heimerl 2014). If, for example, a change in the valve position is considered, the turbine flow follows with a time delay due to the inertia of the water. In addition, progressive pressure waves occur, which cause water hammer within the elastic pipe. (Singh 2011)

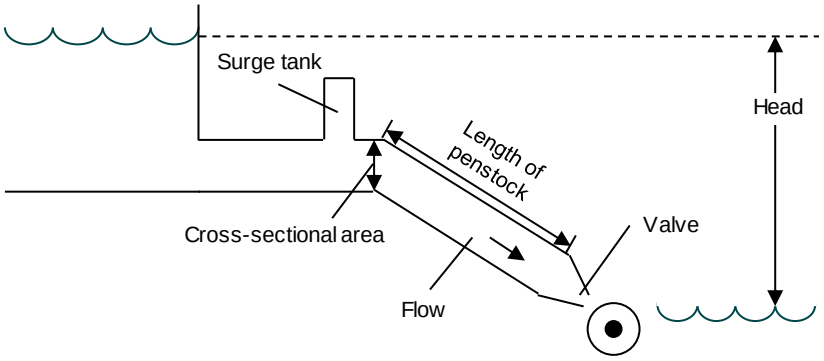

Figure 24: Characteristic values of a water turbine.

Storage power plants usually have a surge tank to dampen the long-wave pressure fluctuations almost completely. Short-wave pressure fluctuations and their reflection are only partially dampened. It should therefore be emphasised that a surge tank leads to greater stability in the control loop, since a quasi-stationary state is reached earlier and the water start-up time (cf. Chapter 2.4.1) is reduced. (Giesecke and Heimerl 2014)

Figure 25 schematically shows the step response of a water turbine to a valve opening to increase the turbine output. In the first moment after opening the valve, an inverse behaviour can be seen, as the entire water column in the pressure pipe starts moving with a time delay. This behaviour of the pressure wave is called all-pass behaviour and results from the high mass inertia of water. In the course of time, the power increases logarithmically to the new operating point after an initial short-term dip. The transient water column primarily influences the dynamic behaviour of the turbine output. (Schwab 2017)

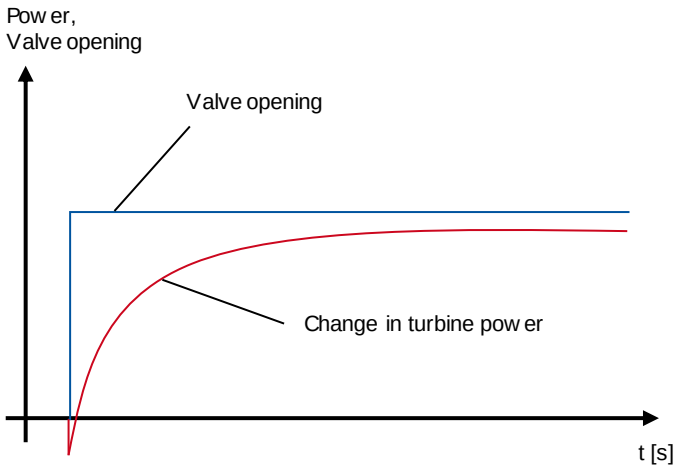

Figure 25: Step response of a water turbine to an increase in the valve position (Schwab 2017).

To investigate the flexibility needs in grid operation (cf. Section 2.2.2) for all kind of disturbances in the power system it is necessary to perform a time domain simulation to adequately represent the dynamic behavior of the electrical equipment. There are different types of models to represent the dynamic behavior of electrical equipment in power systems and especially hydropower plants, which are addressed in Section 3.4.

2.5 Volatility of supply from renewable energy plants

As generation from volatile, supply-dependent RES plants will play a central role in the future, the provision of flexibility will become increasingly important to ensure security of supply. In order to determine the level of flexibility to be provided, it is necessary to analyze the volatility of RES plants' generation. Using the method developed in this analysis to describe the volatility of RES plants, conclusions about the use of hydro power plants can be drawn in the further course of the exemplary investigations.The method for the analysis of volatile time series is first presented in Section 2.5.1. Subsequently, in Section 2.5.2 quarter-hourly wind time series of some German wind farms are compared with the hourly extrapolated time series of these quarter-hourly time series. This analysis can be used to determine the effect of interpolation or extrapolation of volatile time series, which is relevant for further investigations in this study. Furthermore, a comparison of the wind time series of a single wind turbine with an aggregated wind generation time series over Germany is carried out. After that, in Section 2.5.3 volatility of PV systems is examined.

2.5.1 Methods for analyzing volatile time series

In this section a method to analyze and characterize volatile time series is presented. The method is illustrated graphically in Figure 26.

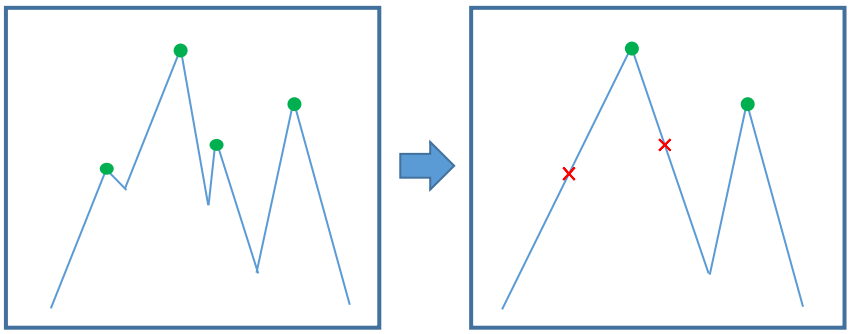

Figure 26: Schematic illustration for the determination of power changes of a certain quantity.

A measure for characterization is the number and size of power changes or local peaks of the time series. A power change is defined in the following as the minimum distance of a high point to the nearest low points. The counting of peaks of a time series is determined by the first derivative of the time series. This indicates whether there is a rising or falling edge between two points, depending on whether the derivative is positive or negative. In order to determine the loss of volatility when considering an hourly instead of a quarter-hourly time series, the magnitude of the change in power between a high and a low point is also decisive. For this reason, a method for measuring the magnitude of power changes has been developed within the framework of the analysis. With the help of the method it is possible to count all high points whose difference to the nearest low points corresponds to a fixed minimum size. The power changes smaller than the predetermined size are therefore ignored. After localization of the local high and low points via the derivative, the difference of these points to each other is determined with

an iterative approach. If the difference between two points lies below the defined limit, the neighboring high and low points are deleted and the difference between the previously considered high or low point and the next one is calculated retroactively. If this difference is again below the defined limit, these high and low points are also deleted for counting.

Thus a small-step iteration of the previously defined size, which describes the minimum size of the power change, allows to calculate the number of all peaks in certain intervals. The number of resulting local peaks for different power change sizes is used in the following as a measure to describe the volatility.

2.5.2 Volatility of feed-in from wind turbines

2.5.2.1 Comparison of the volatility of quarter-hourly and hourly wind time series

In the following, wind time series of some German wind turbines (c.f. Figure 27) are compared with quarter-hourly and hourly resolution. The hourly time series correspond to the linear extrapolation of the quarter-hourly time series. Thus, the temporal resolution is reduced by considering only one value per hour. The focus is on the resulting loss of volatility when considering an hourly instead of a quarter-hourly resolution of a time series. This loss is determined with the help of the method presented in Section 2.5.1.

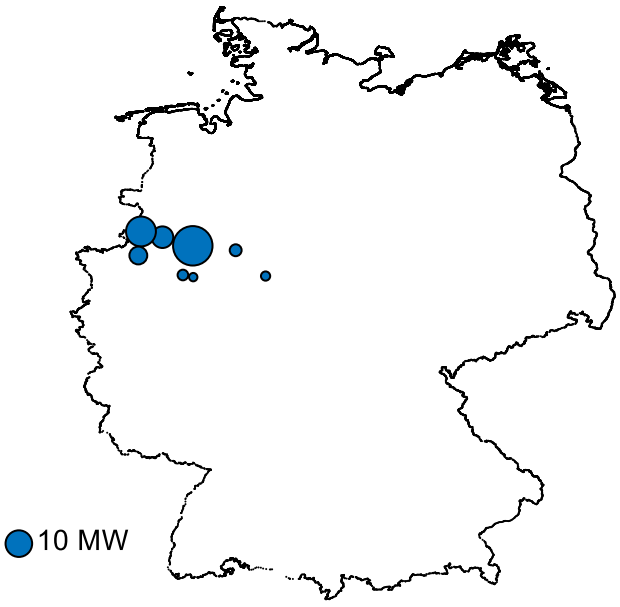

Figure 27: Locations and installed capacities of the German wind turbines under consideration.

The average number of local peaks of the considered German wind time series per year in quarter-hourly and hourly resolution is shown in Figure 28. It becomes clear that the hourly time series with an average of about 2200 peaks per year show only about 30 % of the number of peaks of the quarter-hourly time series with about 7500 peaks per year.

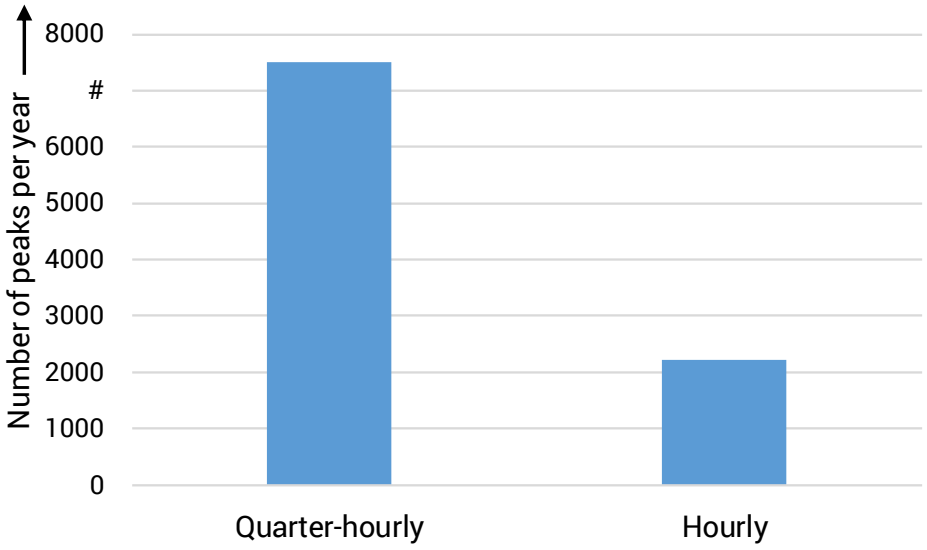

Figure 28: Average number of peaks per year of selected German wind time series in quarter-hourly and hourly resolution.

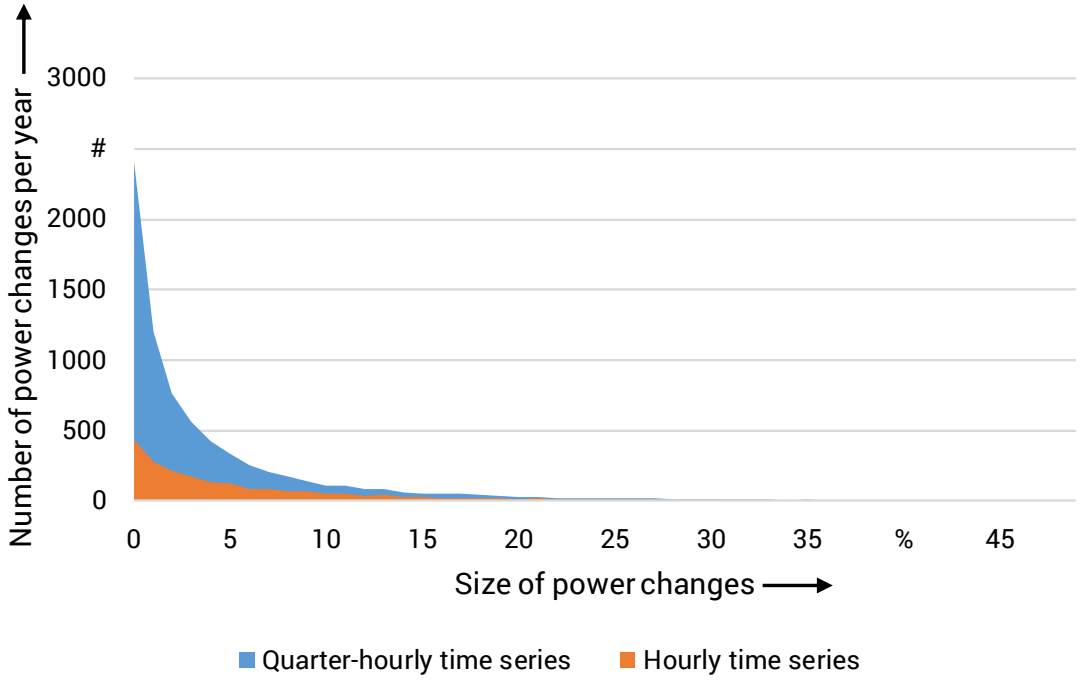

Figure 29: Average number and size of power changes of selected German wind time series per year in quarter-hourly and hourly resolution.

Figure 29 shows the average number of peaks per year as a function of the magnitude of the power changes in quarter-hourly and hourly resolution. The time series as well as the size of the power changes are normalized to the nominal power of the respective plant. It is noticeable that most of the power changes of the quarter-hourly and hourly time series are in the single-digit

percentage range of the nominal power. For the quarter-hourly time series, approx. 75 % of the total power changes are smaller than 5 % of the nominal power, for the hourly time series approx. 60 %. This also means that the majority of the power changes of the quarter-hourly time series are below the 5 % mark. Thus, essentially only relatively small peaks are lost when looking at an hourly time series compared to a quarter-hourly time series.

2.5.2.2 Comparison of the volatility of power generation from a wind turbine and from the aggregated wind time series of a country

After comparing quarter-hourly and hourly time series of individual wind turbines in Germany, this section compares the hourly time series of the turbines with an aggregated time series for Germany. In this analysis section the method for volatility analysis presented in Section 2.5.1 is also used.

Figure 30 shows the number of peaks per year of the hourly wind turbine time series and an hourly aggregated German wind time series. With approx. 800 peaks per year, the aggregated German time series shows significantly less power changes than the time series of the individual wind turbines with approx. 2200 peaks per year. Due to the aggregated consideration, the total volatility is reduced due to the missing correlation of the volatility of the individual turbines to each other.

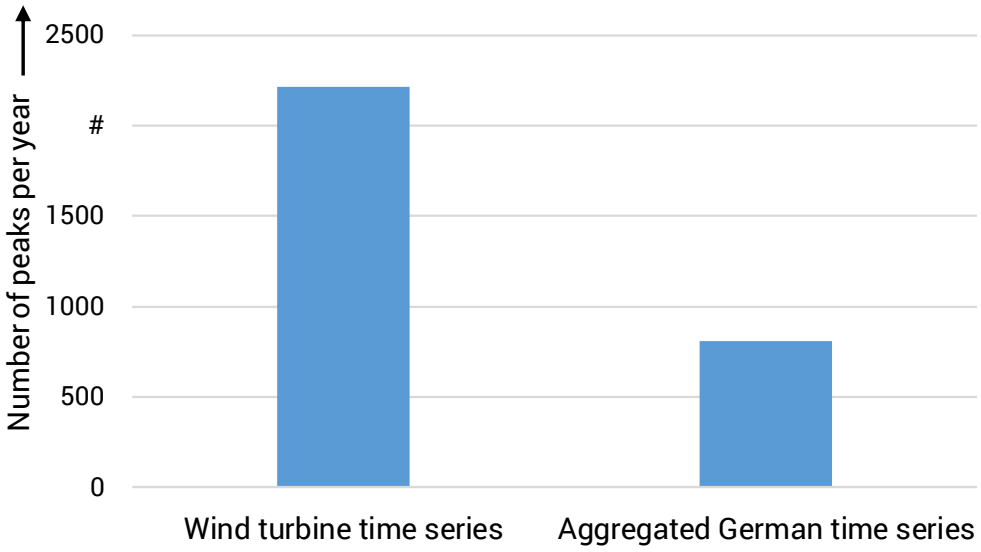

Figure 30: Average number of peaks per year of selected German wind time series in hourly resolution and an aggregated time series of Germany.

In the next step, the time series are now also compared based on the size of the peaks. Figure 31 shows, analogous to Figure 29, the average number and size of power changes of the time series of some German wind turbines and the number and size of power changes of wind generation in aggregated time series of Germany. Both for the time series of the individual wind turbines and for the aggregated Germany time series, about 75 % of the relative size of the power

changes are in the single-digit percentage range. This graph also shows the decreasing volatility due to the aggregation of wind time series. However, the size distribution of the power changes remains similar.

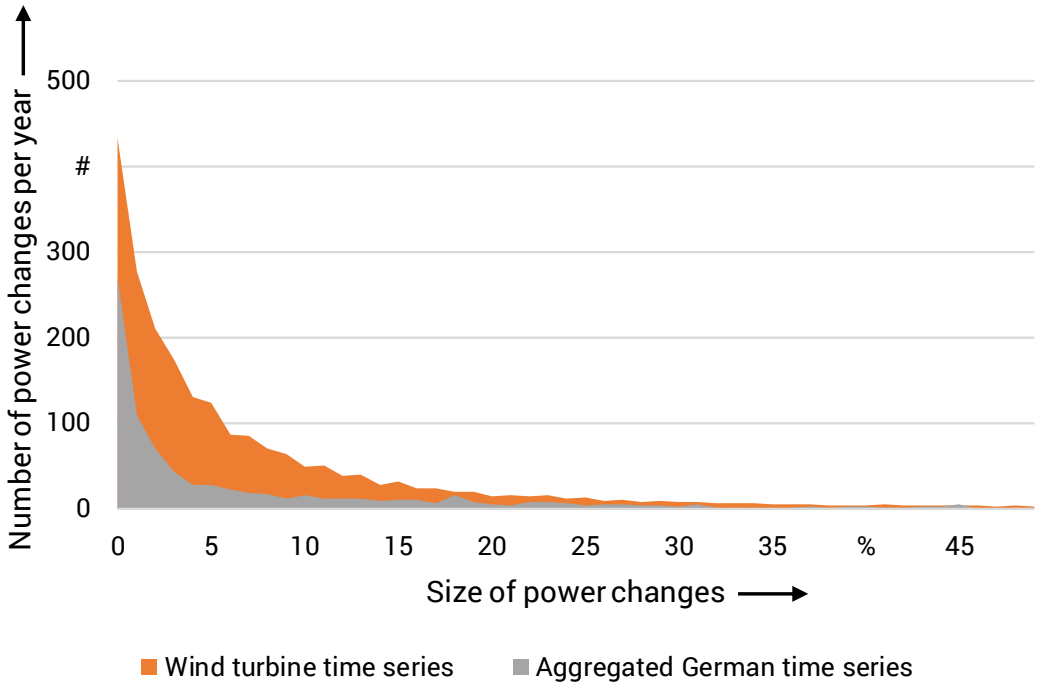

Figure 31: Average number and size of power changes of selected German wind time series per year and of an aggregated wind time series of Germany in hourly resolution.

2.5.3 Volatility of feed-in from photovoltaic plants

The volatility of the feed-in from PV systems can be analyzed by Figure 32. This shows an historical aggregated generation time series from PV plants in Germany for a period of two weeks. It is noticeable that the number of peaks per day is one. The volatility of the PV plants is therefore only defined by the maximum generation output and not by the number and size of the power changes in the time series as is the case with wind energy plants.

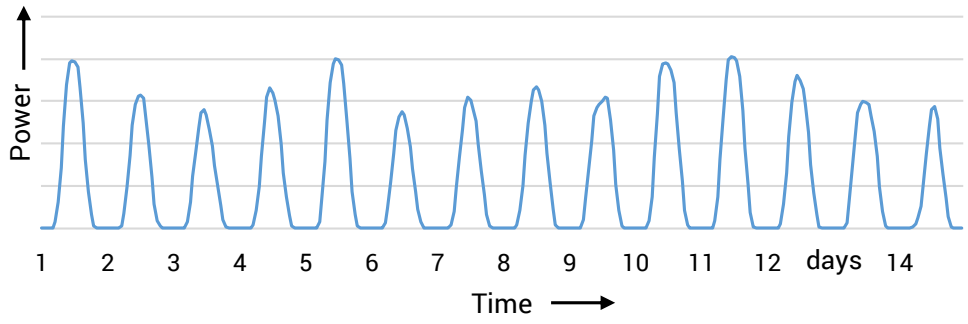

Figure 32: Aggregated generation time series from PV plants in Germany for a period of two weeks.

2.6 High voltage direct current transmission

Now that it has been shown that hydraulic power plants are technically capable of providing short-term flexibility and are in use in large numbers in Norway and Sweden, it is necessary to investigate to what extent this flexibility can also be provided to other European countries than the Nordics. This requires a transfer from the Nordics to continental Europe. These two regions, NORDEL and Central Western Europe, are connected via high-voltage direct current (HVDC) transmission since they are two asynchronous power systems. In the following, this technology is therefore examined in more detail. The focus is on the technological fundamentals, current and planned routes, and the mode of operation of these facilities.

2.6.1 Fundamentals

Generally, three-phase systems are used for transmission in the high-voltage grid. However, there are applications where direct current transmission makes sense from both a technical and an economic point of view. This is particularly the case when transporting over distances of more than 600 km or when using submarine cables with a length of more than 30 km, as is the case between Germany and Sweden, for example. In addition, this technology can be used to connect offshore wind farms or to couple two interconnected systems that are not synchronized with each other. (Konstantin 2017; Schwab 2017)

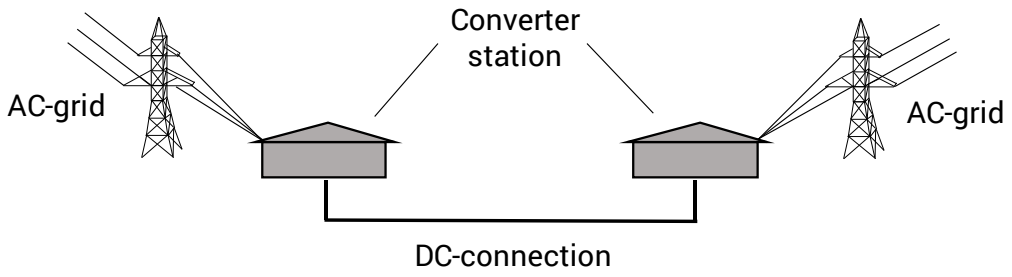

Figure 33: Schematic structure of an HVDC link between two AC networks, according to (Amprion GmbH 2019).

As shown in Figure 33, an HVDC system consists of three main components: The two converter stations at the connection points to the three-phase grid and the DC interconnector between the two converter stations. Within the first converter station, a rectifier converts the alternating current and alternating voltage into direct current and direct voltage. Similarly, in the second converter station, the reverse transformation is done with the help of an inverter. (Amprion GmbH 2019; TenneT TSO GmbH 2019a)

The connection between the two converters can be either symmetrical (bipolar) or asymmetrical (monopolar). In the case of a bipolar connection, two separate lines or cables between the two converter stations with different voltages with respect to the ground potential exist. If there is a failure of one of the two conductors, the HVDC link can continue to operate as a monopolar link

with half the transmission capacity, since in this case the earth is used as the return conductor. (Konstantin 2017; Schwab 2017)

An HVDC link, as shown in Figure 33, is also referred to as a point-to-point link. In addition to the so-called point-to-point connections, a distinction is made between back-to-back connections and multi-terminal HVDC connections. Back-to-back connections basically have the same structure as point-to-point connections. The only difference is, that the distance between the converter stations of back-to-back connection is very small, i.e. the converters are located at the same place. In contrast to these two connection types, more than two converter stations are connected to each other when a multi-terminal connection is used. (Konstantin 2017; Crastan and Westermann 2018)

The main advantage of HVDC over three-phase transmission is that it is possible to use cables even for long transmission distances, as is necessary for transmission across water areas. Due to the high capacitive charging power occurring in cables in AC transmission, they can only be used in high voltage for short transmission distances without additional compensation facilities. In addition, with HVDC transmission no reactive power is required for the transmission of electrical energy. However, in HVDC schemes with line-commutated converters, reactive power is required for commutation at the converter stations. Due to the pure active power transmission and the associated lack of reactive power components, only ohmic losses occur in this form of transmission. In addition, interconnected systems can be coupled in this way without the need for synchronization of the two systems. HVDC interconnections allow power flow control by means of power electronics and can thus have a positive effect on the performance and flexibility of the AC-grid. (Konstantin 2017; Crastan and Westermann 2018; ABB AG Energietechnik-Systeme)

However, in addition to the HVDC transmission line, converter stations, which represent the connecting element between the HVDC route and the three-phase systems at the ends of the HVDC line, are required. These operating resources are associated with corresponding additional costs. Furthermore, the protective devices, such as circuit breakers, for high-voltage direct current technology are more complex to develop and therefore more cost-intensive. Short-term overloading of the operating equipment is possible only to a very small extent with HVDC technology. (TenneT TSO GmbH 2019a; Jovcic and Ahmed 2015)

Within HVDC technology, a distinction is made between two different variants based on the power electronic converters used and their mode of operation. On the one hand, the line-commutated converter technology with externally or grid-operated converters and, on the other hand, the voltage-source converter technology with self-operated converters. These different technologies are described in the following Sections 2.3.1.1 and 2.3.1.2.

2.3.1.1 Line-Commutated converter

In line-commutated converter technology (LCC), thyristors form the core element of rectification. These are semiconductor components that can conduct current in only one direction. When

switched on, they behave similarly to a diode, which is why thyristors are also called controllable diodes. However, the thyristors can only be switched off when the AC current is at zero crossing. Thus, LCC HVDC systems can be turned on at any point in time but cannot be turned off. (Crastan and Westermann 2018; Jovcic and Ahmed 2015)

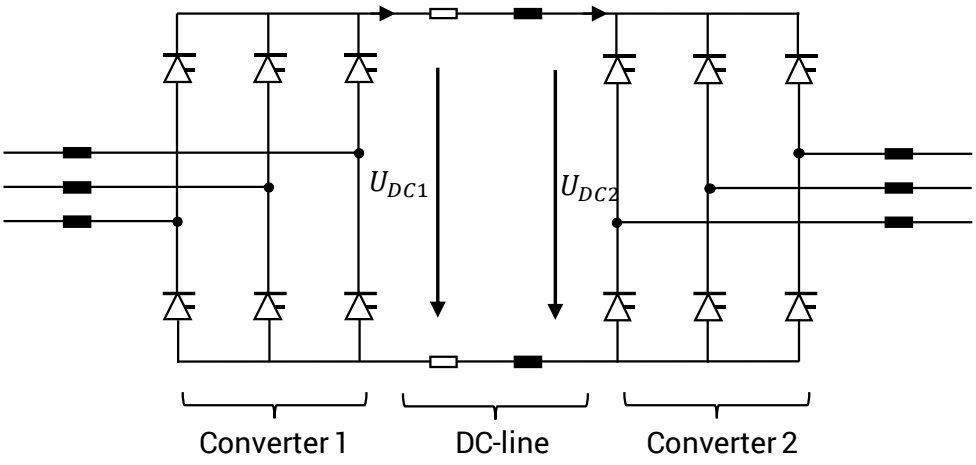

Figure 34: Structure of the LCC converters, according to (Moser 2015).

To rectify both the positive and negative portions of the three-phase system, at least one six-pulse bridge circuit is required in each converter, as shown in Figure 34. In practice, twelve-pulse bridges are commonly used. These can be implemented by connecting two six-pulse bridges in series with a phase shift of 30°. (Crastan and Westermann 2018; Jovcic and Ahmed 2015)

Each of the six thyristor valves of an inverter shown in Figure 34 consists of hundreds of individual thyristors connected in series. Basically, only one of the thyristor valves is conducting at any time. An exception is the commutation process, i.e. the period in which the current flow changes phase. By means of an appropriate control, sections of the same polarity from the different phases of the AC voltage are cyclically connected to the DC link so that a voltage with the lowest possible ripple is present there. (Crastan and Westermann 2018)

The operation of line-commutated converters is only possible with an AC current lagging the voltage of the feeding AC network, so that the current reaches zero crossing and the thyristor switches off before the next thyristor starts to conduct. Reversing the DC voltage within the converter is necessary to change the direction of the power flow across an HVDC transmission line. (Crastan and Westermann 2018)

In addition to the thyristor valves, other components such as filters for eliminating various harmonics or such as power factor correction systems for providing the required reactive power are used in practice to prevent negative repercussions of the system on the three-phase grid. Their additional space requirements must be taken into account when dimensioning the converter stations. (Crastan and Westermann 2018; Jovcic and Ahmed 2015)

Table 7: Technical information on LCC HVDC technology, according to (Crastan and Westermann 2018)

Parameter	Data
Max. voltage level	+/- 800 kV (+/- 1100 kV in development)
Space requirement converter station	25 m^2/MW
Reactive power demand [% $P_{converter}$]	50 % to 60 %
Minimum operating power [% $P_{nominal}$]	10%
Grid connection condition	$S_k > 2 \times P_N$
Power flow inversion	Reversal of DC voltage

Table 7 above contains the most important technical information of LCC HVDC technology. Thus, LCC HVDCs can be operated with voltages up to +/- 800 kV and, at the same time, can be continuously controlled with respect to the active power flow from 10 % load. At the same time, this technology requires approx. 25 m^2/MW of installed power, among other things due to the capacitor banks for reactive power compensation. However, grid connection requirements exist for these systems. For example, the short-circuit power needed to exceed the rated power of the inverters by a factor of two to three. (Crastan and Westermann 2018)

2.3.1.2 Voltage source converter

In contrast to line-commutated converters, the converters used in so-called voltage source converter (VSC) technology are capable of being switched on as well as off at any time. For this purpose, Insulated Gate Bipolar Transistors (IGBTs), developed in the 1990s, are used instead of thyristors. Because of their operation independent of the grid, these converters are also referred to as self-controlled converters. (Jovcic and Ahmed 2015)

The DC voltage is adjustable to any value by the use of high-frequency pulse width modulation, in the range above 1 kHz. In addition, VSCs require little to no filtering equipment to remove harmonics or power factor correction equipment. This significantly reduces the size of VSC stations compared to LCC stations for the same power. (Crastan and Westermann 2018; Jovcic and Ahmed 2015)

Table 8: Technical information on VSC HVDC technology, according to (Crastan and Westermann 2018; Jovcic and Ahmed 2015; ABB)

Parameter	Data
Max. voltage level	about. +/- 640 kV
Space requirement converter station	10 m^2/MW
Reactive power demand [% $P_{converter}$]	0%
Minimum operating power [% $P_{nominal}$]	0 %
Grid connection condition	No particular requirements
Power flow inversion	Reversal of the direct current direction

Compared to line-commutated converters, self-commutated converters have several advantages. As shown in Table 8, VSCs do not require reactive power for operation and can also control active and reactive power independently. Thus, the converter stations can contribute to voltage stability in the connected three-phase AC-system. In addition, when using VSC technology, the power flow direction can be modified without adjusting the dc voltage direction, by reversing the dc direction. (Jovcic and Ahmed 2015)

However, VSCs are costlier to install and have higher losses than the LCCs. In addition, the IGBTs have a lower overcurrent capability compared to the thyristors of the LCCs. In addition, LCC technology makes it possible to realize much higher transmission powers per converter station. Thus, transmission capacities of up to 10 GW per station and circuit are expected for this technology in the future, while VSC HVDC will be limited to a few gigawatts per station according to the current status. (Crastan and Westermann 2018; Jovcic and Ahmed 2015)

2.6.2 HVDC transmission lines in Europe

After the basics of HVDC have been presented in the previous section, this section discusses the HVDC transmission lines that are currently in operation or under construction between Continental Europe, Great Britain and the Nordics.

At the present time, as shown in Figure 35, eight HVDC transmission lines between Central Europe and the Nordics are in operation. These are the so-called Storebaelt link between West Denmark (DKW), which is synchronous with Continental Europe, and East Denmark (DKE), which is synchronous with the Nordics, the NorNed link between the Netherlands and Norway, the Skagerrak link between DKW and Norway, the Konti-Skan link between DKW and Sweden, the KontTek link between Germany and DKE, the Baltic Cable as a link between Germany and Sweden, the NordLink between Germany and Norway and the North Sea Link between Norway and

United Kingdom. These links provide a total transmission capacity of over 7,4 GW. (ABB; ABB; ABB; Statkraft Markets GmbH 2010; TenneT TSO GmbH 2019b)

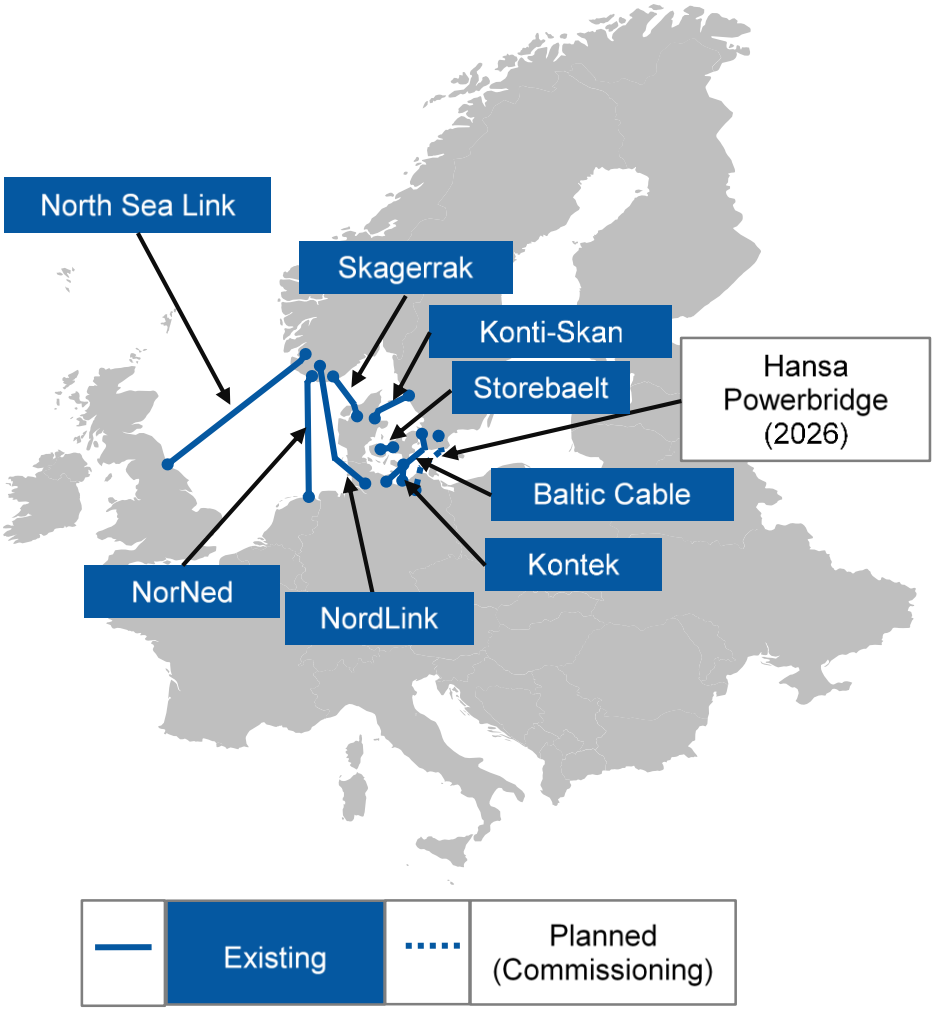

Figure 35: Overview of existing and planned HVDCs in Northern Europe[4].

In addition, the link between Germany and Sweden called Hansa Powerbridge I is currently under construction. This is scheduled for operation in 2026 with 700 MW of transmission capacity. (50 Hertz Transmission GmbH; Bundesnetzagentur für Elektrizität, Gas, Telekommunikation, Post und Eisenbahnen 2019; Stattnet SF 2019)

[4] (ABB, n.d.; ABB, n.d.; ABB, n.d.; 50 Hertz Transmission GmbH, n.d.; Bundesnetzagentur für Elektrizität, Gas, Telekommunikation, Post und Eisenbahnen, n.d.; Statkraft Markets GmbH 2010; Stattnet SF 2019; TenneT TSO GmbH, n.d.).

Overall, transmission capacities between Central Europe and the Nordics will almost double within the next few years.

2.6.3 Operation of HVDC transmission lines

In the following, the operating mode of HVDC transmission lines is analyzed. First, the technically possible mode of operation is considered, followed by the mode of operation required by the transmission system operator and the market. Finally, their actual use is analyzed on the basis of two selected transmission line paths.

2.6.3.1 Technically possible mode of operation

Due to the power electronic components used, HVDC systems are basically capable of switching to another operating point in a relatively short time. Thus, start-ups are possible within fractions of a second. However, this responsiveness may be limited due to restrictions imposed by the three-phase system, in which case the start-up process may take several minutes. These restrictions may exist because an exporting HVDC link with several hundred megawatts of power acts like an additional load in the exporting three-phase system. Accordingly, an increase in transmission power can lead to a generation deficit in the exporting system and is thus comparable to a power plant outage and the corresponding impact on frequency in the AC grid. In addition, a change in transmitted power in this power range has an impact on the power flows that occur in the AC grid. These interactions must be taken into account when planning the operation of the HVDC link. Shutdown of an HVDC system is possible in a similarly short time. Thus, current and voltage can be controlled to zero within 300 ms. The duration of the change in power flow direction within the HVDC link depends on the technology used. While a change of the flow direction is possible within 50 to 100 ms with VSC, this process takes five to ten times as long, i.e., about 500 ms, for LCC. (Jovcic and Ahmed 2015; Kundur 1994)

Thus, HVDC connections are at least theoretically capable of transferring the flexibility of Nordic storage power plants to Central Europe through flexible operation, regardless of the technology involved and are capable of providing positive or negative Frequency Containment Reserve.

2.6.3.2 Operating mode required by law and the market

In addition to the technical characteristics of the converter stations and the lines, legal requirements and the energy market influence the operation of an HVDC system. In the case of the legal requirements, the grid connection requirements are a particular influencing factor.

Within the framework of a European Commission regulation, grid connection conditions for HVDC systems have been laid down that apply to the entire European Economic Area. As far as the controllability of the active power flow is concerned, the HVDC systems must adjust their operation on the instructions of the responsible transmission system operator (TSO). In principle, the operator can specify the step size in which the adjustment of active power must take place and the minimum operating power that the system must provide if it is in operation. The reversal of the transmission of the maximum active power from one direction to the opposite

direction with maximum transmission power must take place as quickly as possible - in compliance with the technical operating limits of the equipment - and may take a maximum of two seconds. If the system requires longer for this process, this shall be justified by the system operator to the responsible TSO. (European Commission 2016)

Besides the already presented requirements for the operation of HVDC systems, the same regulation describes further criteria for the operation of HVDC and authority of the TSO towards the system operator regarding reactive power control, short-circuit contribution in case of a fault and other aspects, which are not further considered here. (European Commission 2016)

On the market side, the operation of the HVDC link is influenced by the Net Transfer Capacities (NTC) allocated to the energy market. These available transfer capacities are determined as the difference between the total transfer capacity (TTC) and a safety margin, the so-called transmission reliability margin (TRM) for each connection on an hourly basis. The TTCs are dimensioned in such a way that full utilization of this transmission capacity does not lead to any limit violations in either of the two bidding zones. The safety margin is kept within the continental European interconnected system, the UCTE area, among other things for the transmission of reserve capacity. For the HVDC links between the UCTE area and NORDEL region, this margin does not apply. Thus, the TTCs generally correspond to the traded NTCs. An adjustment of the transmission capacities may occur, for example, as a result of a high wind energy feed-in in Germany. In this case, for example, the transmission capacity for the connection between Germany and Sweden, the Baltic Cable, is limited. To limit the repercussions of a change in transmission capacity on the power flows in the connected AC networks, maximum power changes per hour are defined for the HVDC links between the Nordics and Continental Europe. (Nord Pool AS 2018, 2019d)

Compared to the technically possible operating limits presented in Section 2.6.3.1, it is noticeable that the maximum duration of active power flow reversal specified by the legislator is significantly longer than the technically possible duration. Thus, the regulatory requirements do not restrict the operation of HVDC systems regarding the flexibility of their operation.

2.6.3.3 Actual operation in practice

In the following, the actual operation of currently existing HVDC transmission lines is examined in more detail using two exemplary transmission lines. These are the NordNed and Baltic Cable connections already mentioned in Section 2.6.2. While the NorNed HVDC links Norway with the Netherlands and has a transmission capacity of 700 MW, the Baltic Cable link provides 600 MW of transmission capacity between Germany and Sweden (Statkraft Markets GmbH 2010; TenneT TSO GmbH 2019b). Since no detailed operational data is available on the operation of these HVDC transmission lines, the mode of operation is inferred from the hourly exchange between the two bidding zones that the HVDC connects. However, such derivation is only possible if the link under consideration is the only link between the two bidding zones. These requirements are met by the two connections mentioned above, which is why the exchange services between these four countries and their hourly variation correspond to the operation of the two HVDC

transmission lines. As an example, the hourly exchange services in January 2019 are considered in the following.

Figure 36 shows the hourly exchanges between Sweden and Germany in January 2019 via the Baltic Cable. It is noticeable that especially in the second half of January the operation of the HVDC link varies significantly and even several power flow reversals occur within one day. This happened, for example, on January 24. On that day, the power flow direction was changed a total of eight times, maintaining the new direction three times for only one hour before changing it again. (Nord Pool AS 2019c)

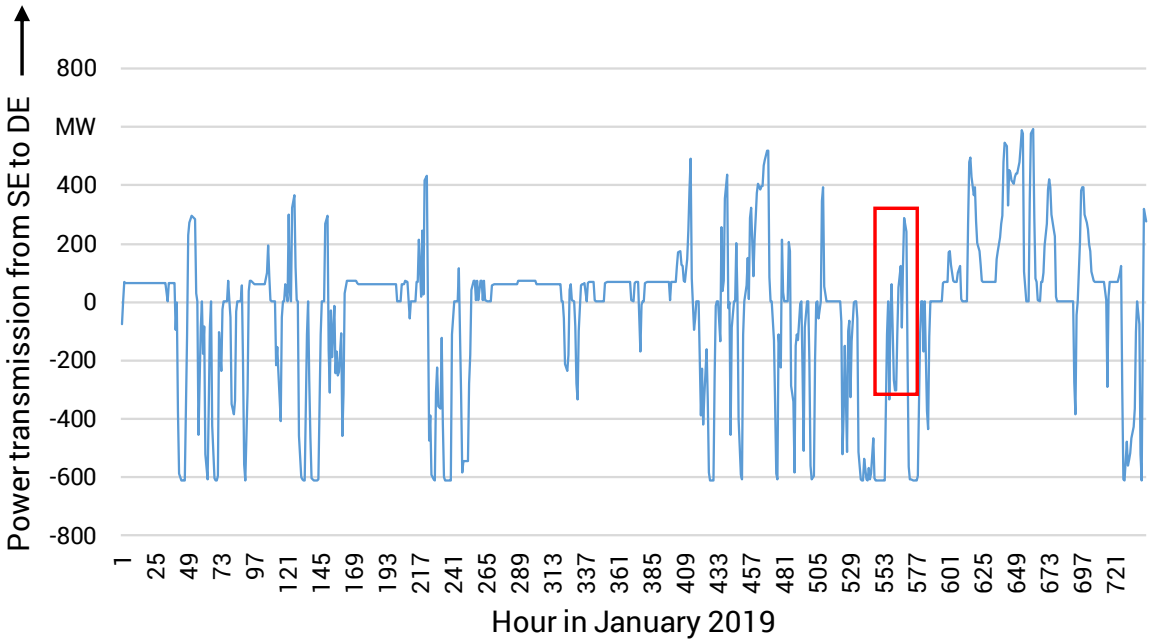

Figure 36: Hourly exchange capacity between Sweden and Germany in January 2019, according to (Nord Pool AS 2019c).

Considering the hourly exchange capacities between Norway and the Netherlands (c.f Figure 37), it is noticeable that especially towards the middle of the month, the power transmitted via the HVDC link varies significantly more frequently than at the end of the month. In contrast to the Baltic Cable connection, hours with high utilization are more frequently followed by hours with high utilization in the reverse power flow direction. (Nord Pool AS 2019b)

Thus, it becomes clear that both HVDC links under consideration temporarily use parts of their flexibility potential in current operation and thus the exchange capacities can vary significantly in the hourly observation.

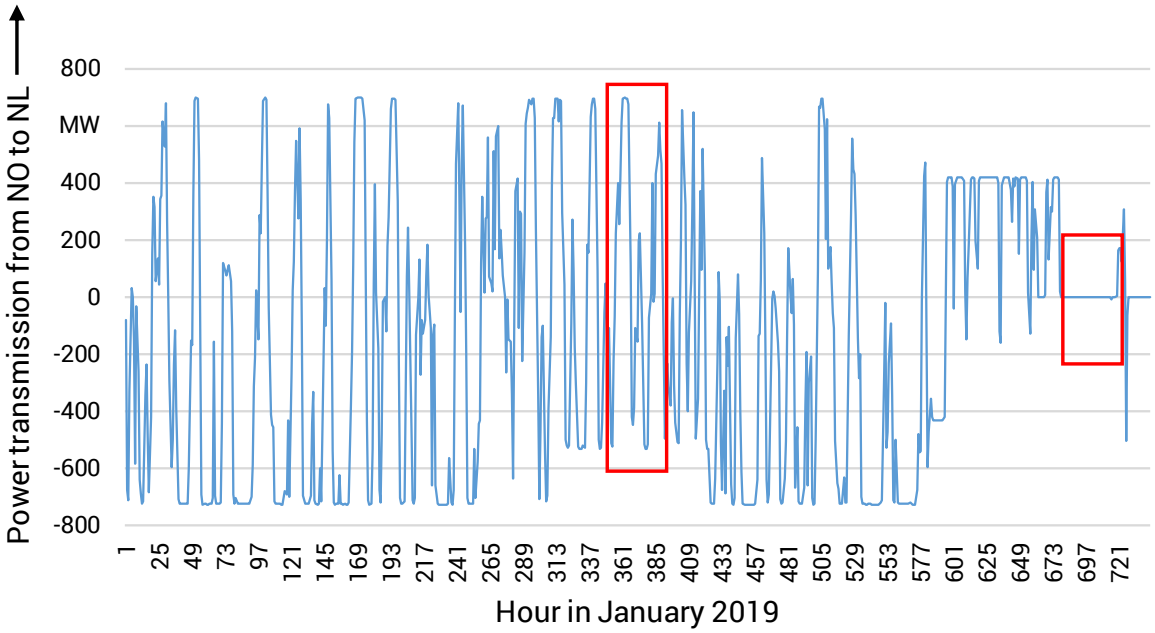

Figure 37: Hourly exchange capacity between Norway and the Netherlands in January 2019, according to (Nord Pool AS 2019b).

In conclusion, it can be stated that HVDC transmission is technically capable of transferring flexibility in terms of Frequency Containment Reserve provided at short notice by hydraulic storage power plants in the Nordics to the continental European power system. However, the operation of HVDCs is also dependent on the performance of the three-phase networks and the corresponding NTCs, so that currently the technical potential of HVDCs in terms of flexible operation is not fully exploited. Flexibility can also be provided on the market side via HVDC lines. A detailed evaluation of flexibility provision depending on power plant deployment in the European context for future scenarios is given in Chapter 4.

3 Methodology

In this chapter, the toolchain used for simulating the deployment of highly complex hydropower networks and investigation of the flexibility needs in grid operation is presented. First, an overview of the process is given in Section 3.1. Then, in Section 3.2 and Section 3.3, a detailed description of the two-step market-based model is given. Section 3.4 describes the dynamic models used for time domain simulations of grid operation after a grid fault occurred to investigate the flexibility needs and frequency stability in a future Nordic power system.

3.1 Overview of the methodology

The toolchain is shown in Figure 38 and can be divided in three main steps: market, grid operation and stability investigation methods.

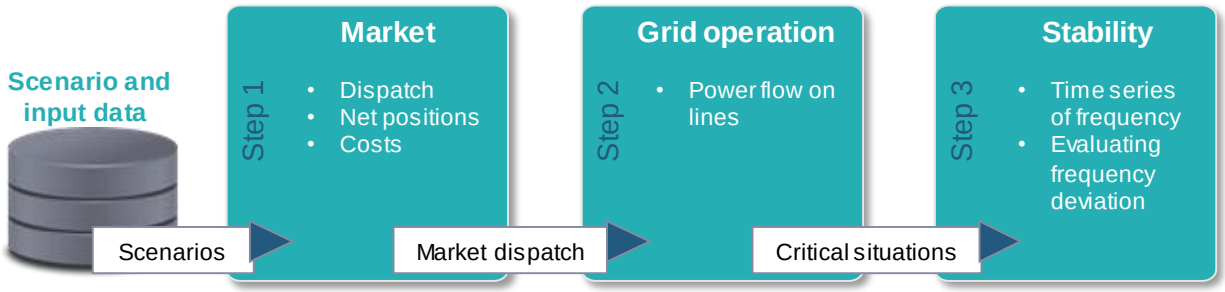

Figure 38: Toolchain used for investigations in this work.

The method for the market simulation of hydropower plant operations is divided into two steps (c.f. Figure 39). The first step is a fundamental European market simulation existing at the Institute for High Voltage Equipment and Grids, Digitalization and Energy Economics (IAEW) (Drees 2015). The aim of the market simulation is to simulate the wholesale market in order to determine the power plant operation. Therefore, the objective function of the optimization problem of the market simulation is the minimization of the overall electricity generation costs. The market simulation covers the day-ahead and intraday market. The input data includes, inter alia, the power plant parks, transmission capacities, bidding zones, time series of RES units, load time series and fuel prices. The results provide, among other things, power plant schedules, exchanges, costs of electricity generation, and bidding zone prices.

Due to its high degree of interconnection by waterways in some bidding zones, hydropower plant parks are accompanied by a high complexity, which enormously increases the computation time of market simulations. Therefore, hydropower plants are aggregated in bidding zones with strongly interconnected hydropower plant parks in the market simulation. Furthermore, the market simulation is carried out in hourly temporal resolution to reduce the computing time. The aggregated hydraulic systems are assumed to have maximum flexibility. This estimation towards the more flexible side ensures that the overall result does not underestimate the flexibility required. However, the assumed flexibility must be taken into account in the second step of the method.

The resulting aggregated hydropower plant schedules are then used as input data for the hydraulic unit commitment model, the second step of the method. The hydropower plant park is disaggregated and simulated in detail in this process step. The objective of this algorithm is the optimal operation of the plants with regard to their technical restrictions and the aggregated scheduling from the first process step, the market simulation. These include the consideration of the minimum operating time (MOT) and minimum downtime (MDT) to comply with operational restrictions and the power/flow ratio to minimize water consumption. The final result is the detailed hydraulic unit commitment with a quarter-hourly temporal resolution.

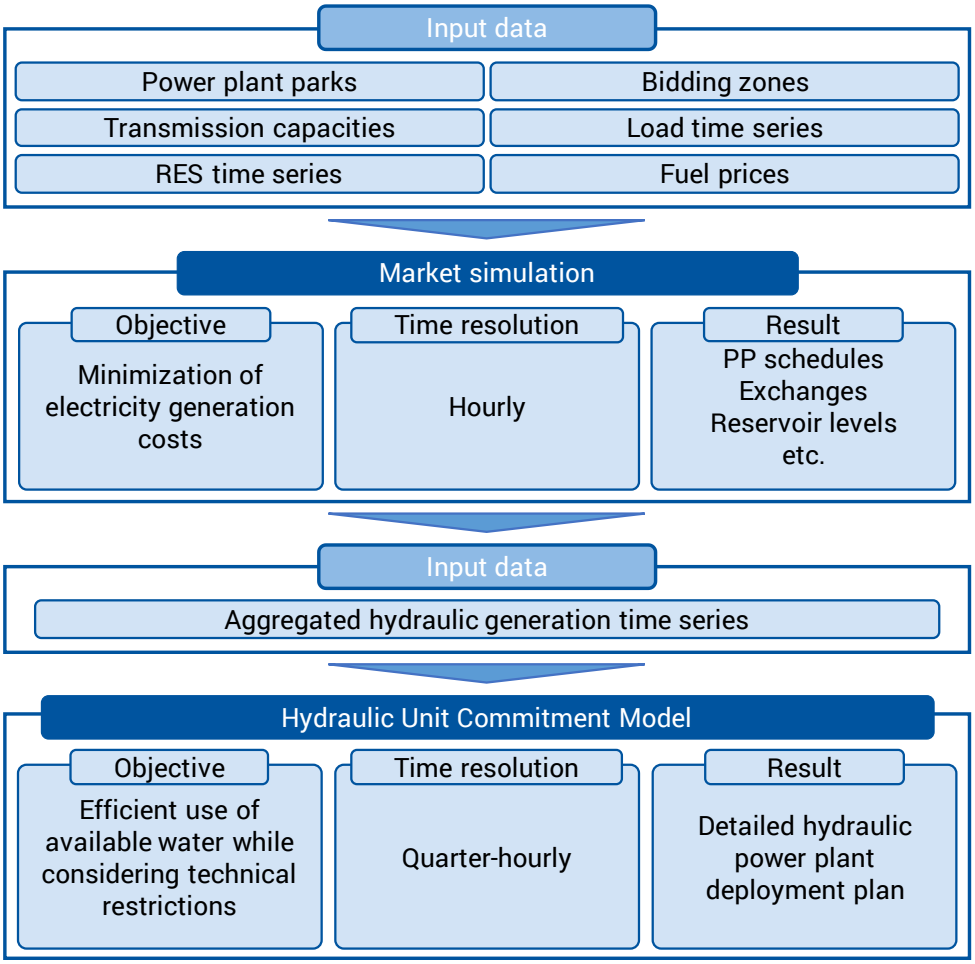

Figure 39: Overview of the method for simulating future power systems.

The second and third step from Figure 38 refer to the point of the physical fulfilment of the results of the market simulation and are performed by the method presented in Figure 40. The quarter-hourly temporal resolution of the infeed by hydropower plants from the unit commitment model is used to investigate the grid operation by calculating the corresponding power flows on the power lines. Because of the high degree of detail of the dynamic models of the electrical components and the resulting computing times for time domain simulations of large power systems it is not practicable to simulate periods of more than a few seconds or minutes. Therefore,

it is necessary to identify critical situations in grid operation first which can be further investigated in case a fault occurs. This is necessary to cause a maximum amount of stress to the power system to get close to a worst case situation and to investigate power system stability to derive er flexibility needs in the future if needed. Since the aim of this work is the investigation of possible flexibility needs in terms of active power power provision a frequency stability analysis is carried out.

The model input parameters consist of the grid model, loads and feeders to define the power system as a result of the market simulations and the hydro commitment model. Another parameter is the disturbance which is applied to the power system within the time domain simulation to trigger netting effects. Next, a steady-state initialization is performed by a power flow calculation. These results are used for the initialisation of the dynamic components as starting solution of the time domain simulation. The output for each power plant site are time series of the frequency for the corresponding bus in the power system. By the time series values as the evaluation rate of frequency deviation and the rate of change of frequency can be analyzed to derive possible flexibility needs.

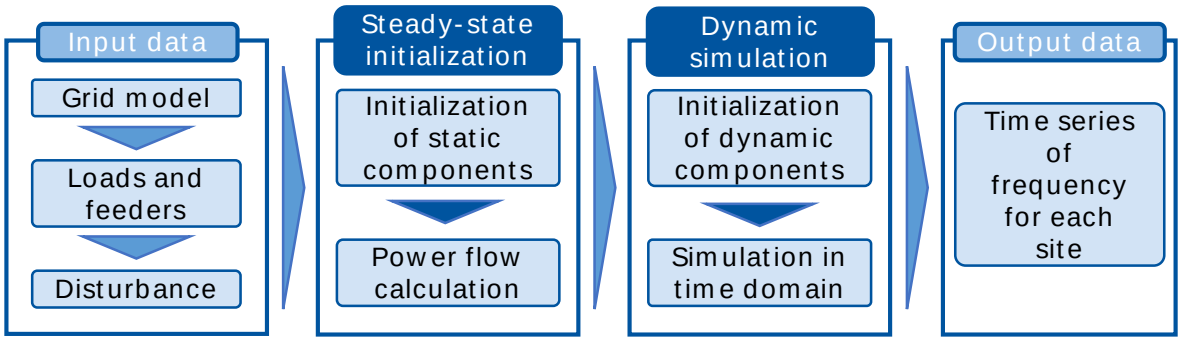

Figure 40: Overview of the method for investigation of frequency stability.

3.2 Market simulation

The market simulation aims to simulate electricity generation in Europe for future scenarios. The maximization of the contribution margin of each market participant at day-ahead and intra-day markets is transferred to an optimization problem minimizing the generation costs in the whole generation system. The simulation differentiates between three different types of generators. These include thermal power plants, RES and separately hydropower plants. Furthermore, the demand for electricity can partly be regulated by using demand-side management. The scope of the market simulation is divided into several bidding zones. These are characterized by an individual producer and consumer structure. The bidding zones are usually connected to other bidding zones via interconnectors, so that an exchange between the bidding zones is possible to a certain capacity. Within optimization, the technical restrictions of the different types of generation and storage facilities, the coverage of the load, the provision of primary control reserve and the available transmission capacitites are integrated using auxiliary conditions. (Drees 2015)

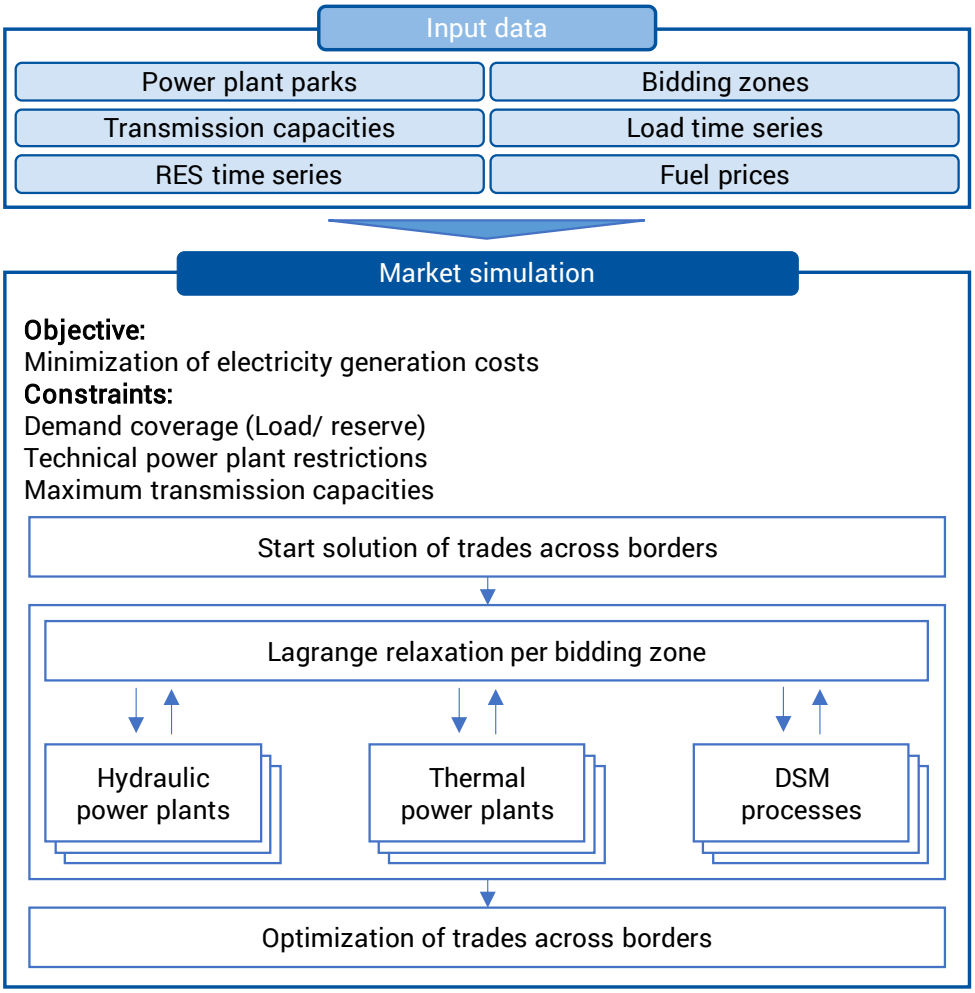

Figure 41: Overview of the market simulation method.

Due to the complexity of the optimization problem set up within the scope of the market simulation, it is divided into three stages. First, a simplified, linear optimization model is used to calculate a starting solution for the exchanges between the bidding zones and the generation marginal costs. For this purpose, the heat consumption curves of the thermal generation units are linearized with the aid of a heat consumption coefficient, and switch-on decisions and minimum shutdown and minimum operating times are neglected. Then, in the next stept, the switch-on decisions of the thermal power plants are determined taking the calculated exchange capacities and marginal costs into account. The determined initial solution serves as input data set for the subsequent process step. (Drees 2015)

The core of the method used is a Lagrangian decomposition and relaxation. This approach allows a decomposition in the time domain as well as in the system domain. The subsequent iterative solution of the resulting subproblems is coordinated with the help of Lagrange coordinators so that an overall optimal solution can be determined. Specialized methods and dynamic programming are used to solve the subproblems of the operation of thermal generation units, storage units and DSM processes. The determined optimal switch-on and operation decisions for generation units and storage facilities are transferred to the subsequent process step, in which the switch-on decisions are adopted and improved again with linear optimization. Furthermore, a determination of the operating points as well as the redetermination of the cross-border exchange takes place in this step. (Drees 2015)

The market prices calculated within the simulation are fundamentally based on the marginal costs of individual power plants plus start-up costs. Accordingly, the prices serve only as a measure for the calculation of the power plant dispatch schedule, which is the focus of the simulation.

As a result of the power plant dispatch optimization carried out, the hourly resolved schedules of the block-specific generation units and storage facilities, the trading balances of the bidding zones considered and the generation costs are obtained. (Drees 2015)

Since hydraulic generation plants are the focus of the study, the model of hydropower plants is discussed below more in detail. The following hydraulic characteristics are taken into account by the optimization by means of constraints:

- Reservoir filling levels of the storage reservoirs
- Inflows and outflows
- Head of water
- Flow rate of the turbine
- Turbine efficiency
- Hydraulic connections to other hydropower units

Hydropower plants are often interconnected due to geographical conditions. The model for hydraulic systems consists of storage basins and waterways. Waterways are interconnections from and/or to storage basins and can be natural inflows or outflows, overflows, turbines or pumps. Waterways are, therefore, degrees of freedom for the optimization such as turbines or pumps or given by time series. The large number of basins and waterways in the power system results in a large number of constraints and dependencies. Since the complexity increases significantly due to these linked constraints, simplifications must be made to reduce the runtime of the simulation. The storage basins are assumed to be flat so that the head is independent of the level of the basin and the efficiencies are assumed to be constant despite their non-linear dependence on the head and the flow at each operating point. (Drees 2015)

3.3 Hydraulic unit commitment model

The hydraulic unit commitment model is used for the detailed calculation of the schedules of complex interconnected hydraulic systems, which were previously considered aggregated in the wholesale market simulation. The model is divided into the three parts data preparation, parameterization of the hydropower plants and rule-based algorithm. The rule-based algorithm represents the main part of the model.

3.3.1 Data preparation

In the market simulation, the first step of the process, the calculation was performed with an hourly resolution in order to reduce the complexity and the computing time. In this first step of the hydraulic unit commitment model, the data preparation, the resulting time series with an hourly temporal resolution of the market simulation are interpolated to a quarter-hourly resolution, since this corresponds to the temporal resolution of the intraday market and, thus, increases the significance of the results.The impact of the time resolution is already described in section 2.5, in which volatile RES time series with different time resultion are analyzed. Furthermore, in this part the detailed hydro power plant characteristics of the bidding zones previously considered in aggregated form are loaded and processed. In particular, the turbine-specific power-flow characteristic curve required for the model is determined.

3.3.1.1 Temporal interpolation of volatile time-series

By interpolating feed-in time series to increase their temporal resolution, the volatility of time series from intermittent feed-in units needs to be taken into account. A linear interpolation causes the time series to lose its original volatility, as stated above. Other common interpolation methods, such as spline interpolation, which is intended to achieve a rounded transition between neighboring data points (McKinley), are also unsuitable for interpolating volatile time series (Fickel 1996). For this reason, a method for the interpolation of volatile time series has been developed within the framework of the model, in order to produce a representative image of hourly resolved wind time series with a quarter-hourly resolution. The method is based on (Fickel 1996).

Using this interpolation method, a stochastic roughness is added between the hourly points. The degree of vertical compression is determined by a freely selectable vertical factor. This can either be the same for each time step or, for example, a random factor can be applied. The value range of the vertical factor is between [-1; 1]. Within this study, the vertical factor is defined by using the results of the volatility analysis regarding the comparison of wind power plant time series with different temporal resolutions (c.f. section 4.3).

The described interpolation is applied to the aggregated generation time series from wind energy of the respective bidding zones considered, because these varies most by the view of the feed-in time series with hourly and quarter-hourly time resolution (c.f. section 2.5). The vertical factor for interpolation is chosen so that the total energy produced in the hourly time series over one year is equal to the new quarter-hourly time series. To ensure that the energy balance in each time step remains unchanged from the hourly market simulation result, it is assumed that

the added volatility of the wind time series is compensated by flexibility-providing technologies. For this purpose and to ensure balance between load and demand, the difference between the linearly interpolated wind time series and the volatile interpolated wind time series is added to the linearly interpolated time series of the flexibility-providing technologies. In the Nordics these technologies are mainly hydropower plants. In order to not underestimate the flexibility provision of hydropower there, this difference is added completely to the aggregated hydropower feed-in time series.

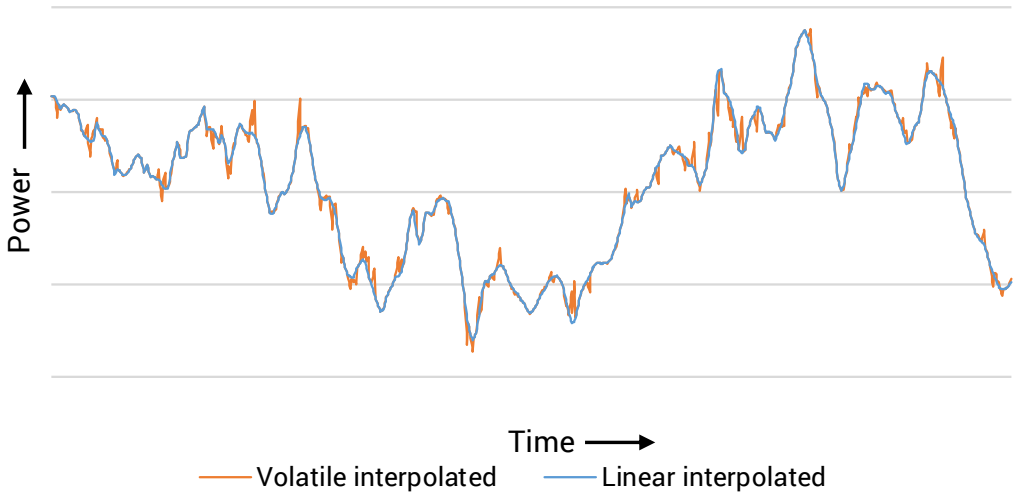

Figure 42: Example of a volatile interpolation of a time series with exemplary vertical factor.

3.3.1.2 Interpolation of turbine-specific power-flow characteristic curve

In the rule-based model developed as part of the research work, turbine-specific power-flow characteristic curves are used. As mentioned in Section 2.3.2, the turbine specific characteristics are not available for most of the turbines considered in this simulation. Therefore, these characteristics need to be calculated within the framework of this study. In order to take the non-linear relationship between the flow rate and the efficiency and thus the generation power into account, the turbine-specific power-flow characteristic curve is approximated by a piecewise linear function. This has four grid points, referred to below as P_{min}^{T1}, $P_{limit,1}^{T1}$, $P_{limit,2}^{T1}$ and P_{max}^{T1}.These parameters have been determined on the basis of four exemplary efficiency curves using the parameters age and size of the turbine. The interpolation method used for this purpose is described in more detail below.

For each of the three turbine types, Kaplan, Francis, Pelton turbine, four exemplary efficiency curves are available, which differ with respect to the age and size of the turbine. An overview of the age and the corresponding installed power belonging to the respective characteristic curve is given in Table 9.

Table 9: Overview of the technical data of the exemplary efficiency curves

Labeling	Age of the turbine	Size of the turbine
Characteristic curve Q1	0 a	0 MW
Characteristic curve Q2	119 a	0 MW
Characteristic curve Q3	0 a	800 MW
Characteristic curve Q4	119 a	800 MW

Based on the four turbines with the characteristic data, the efficiency curve can be estimated depending on the age and electrical power. These four characteristics for each turbine type are used to define a solution space for each grid point of a turbine in which the turbine-specific grid point is located. Each corner of the solution space, i.e. the power of the turbine in the grid point when using the exemplary efficiency characteristic, can be calculated under the assumption that the turbine under consideration matches one of the four reference characteristics in the criteria age and size. Figure 43 shows an example of such a solution space.

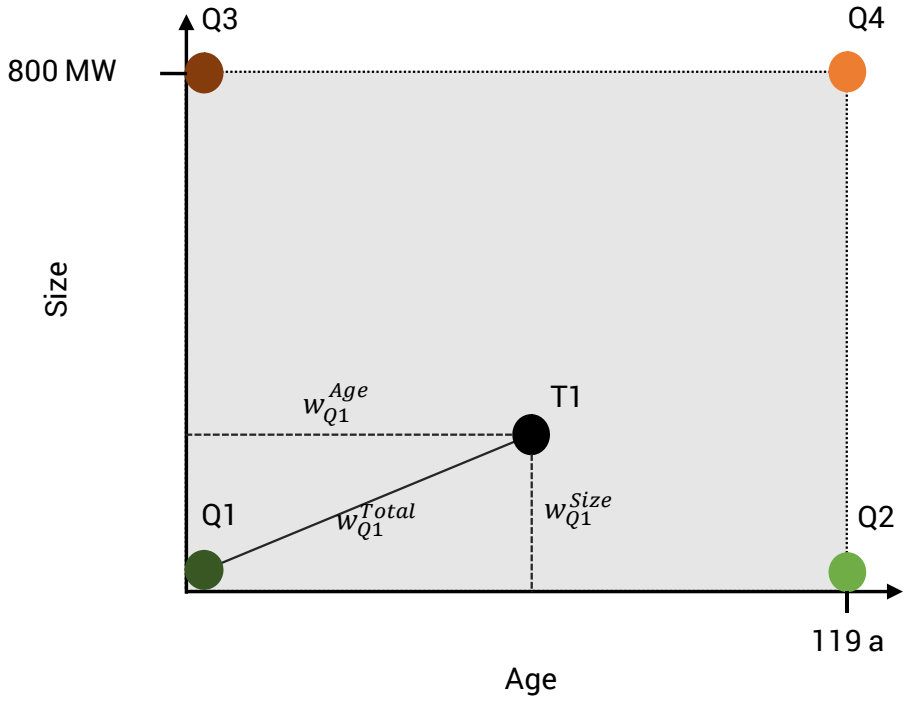

Figure 43: Schematic representation of the solution space.

For the calculation of the turbine specific grid point power, T1, the inverse distance weighting method is used. The reason for this is that a smaller distance between the actual turbine characteristics and one of the grid reference points, as in Figure 43 between T1 and Q1, corresponds to a higher comparability of the efficiency curves. Thus, smaller distances should be weighted more heavily than larger distances. In general, for inverse distance weighting according to Shepard, the relationship from the formula below holds for nonzero distances. (Shepard)

$$f(p) = \frac{\sum_{i=1}^{N}(d_i)^{-u} \cdot z_i}{\sum_{i=1}^{N}(d_i)^{-u}} \tag{3.1}$$

In the scope of this modeling, the exponent $u = 1$ is chosen. In this context, the variable z_i corresponds to the grid point power of reference point i. Due to the four available reference characteristics for each turbine type, $N = 4$. The variable $f(p)$ corresponds to the turbine-specific power resulting from the inverse distance weighting of the reference points.

From the solution space shown in Figure 43, the following correlations for the distances and the corresponding weighting result. With the help of the correlations in (3.2) and (3.3) it is possible to calculate the total distance d_{Q1}^{Total} according to (3.4).

$$d_{Q1}^{Size} = (P_{T1} - P_{Q1}) \tag{3.2}$$

$$d_{Q1}^{Age} = (A_{T1} - A_{Q1}) \tag{3.3}$$

$$d_{Q1}^{Total} = \sqrt{\left(d_{Q1}^{Size}\right)^2 + \left(d_{Q1}^{Age}\right)^2} \tag{3.4}$$

While the variables P_{Q1} and $A_{Q1}$are the power and age of the turbine belonging to reference point Q1, P_{T1} and A_{T1} correspond to the power and age of the turbine under consideration T1. Analogous to the total distance d_{Q1}^{Total}, the total distances to the reference points Q2 to Q4 can also be calculated.

Using the previous formulas, the general formula for inverse distance weighting from (3.1) can be applied to the calculation of the power of the first grid point of turbine T1. This results in the relation (3.5) for the minimum power of the turbine.

$$P_{min}^{T1} = \frac{1}{\sum_{i=1}^{4}\frac{1}{d_{Q_i}^{Total}}} \cdot \left(\frac{P_{min,i}^{Q1}}{d_{Q1}^{Total}} + \frac{P_{min,i}^{Q2}}{d_{Q2}^{Total}} + \frac{P_{min,i}^{Q3}}{d_{Q3}^{Total}} + \frac{P_{min,i}^{Q4}}{d_{Q4}^{Total}}\right) \tag{3.5}$$

The other three turbine-specific grid point powers $P_{limit,1}^{T1}$, $P_{limit,2}^{T1}$ and P_{max}^{T1} can be determined analogously using the respective reference grid point powers also via formula (3.5).

3.3.2 Parameterization of the hydropower plants

In the section parameterization of the plants, a dynamically adjustable flexibilization and change of the minimum operating time and minimum downtime of the plants is possible in order to be

able to analize different flexibilization scenarios. When flexibilizing plants, it is possible to choose between different flexibilization rates and flexibilization criteria. The flexibilization rate indicates the percentage of the nominal power of the flexibilized plants in relation to the total nominal power of the generation. The flexibilization criterion specifies according to which characteristic the plants are to be flexibilized up to a certain flexibilization rate. The selectable flexibilization criteria include:

- The power-to-flow ratio (descending and ascending)
- The nominal power (descending and ascending)
- The age
- The number of violations of the minimum operating time and minimum downtime based on previous calculations (violation criterion)

3.3.3 Rule-based algorithm

The aim of the rule-based algorithm is to simulate a detailed hydraulic unit commitment while ensuring efficient use of the available water and taking technical restrictions into account. Figure 44 shows the flow chart of the rule-based algorithm.

In the rule-based algorithm, the power plant feed-ins are calculated for each time step in an iterative process until the load is covered. First of all, the hydropower plants whose minimum operating time has not yet been reached are selected. A pre-selection of flexible and inflexible turbines based on a short-term forecast to detect load fluctuations follows. The forecast is used to determine the demand for flexibility and the related share of flexible plants. This guarantees that the number of operational violations is minimized. Then, the most efficient plants with the highest power/flow ratio at the optimum operating point are selected to ensure efficient use of the available water. The plants whose minimum downtime has not yet been reached in the time step under consideration are not taken into account in the selection. The algorithm ends with the load coverage in each time step.

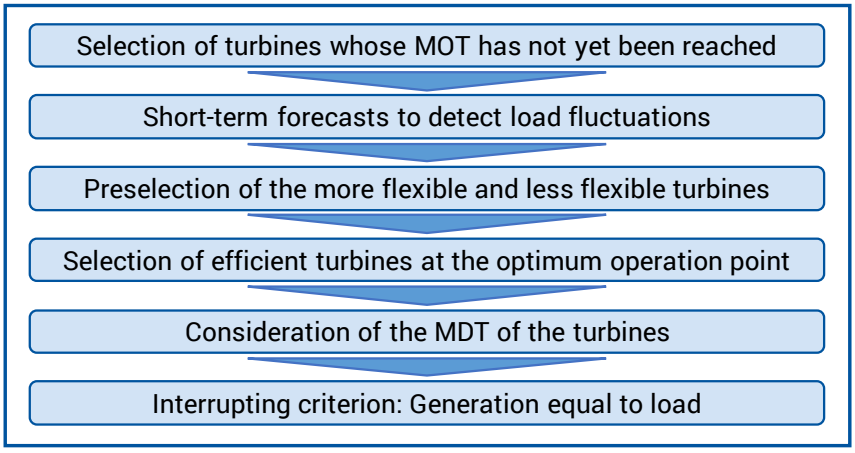

Figure 44: Flow chart of the rule-based algorithm.

The decision on the share of flexible and inflexible plants in use is explained more in detail in Figure 45. An ideal use of the flexible and inflexible plants is guaranteed if the advantage of the flexible plants, which are capable of a high number of start/stop cycles without operational violations, is used optimally. To achieve this ideal use, flexible plants should cover the peak load. The inflexible plants can, then, mainly cover the base load, which leads to a minimization of the operational violations of the inflexible plants.

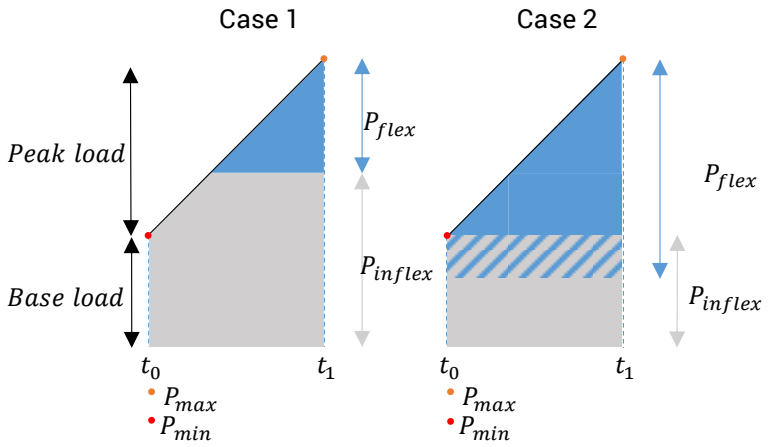

Figure 45: Schematic illustration of the rule-based algorithm in the unit commitment model.

In Figure 45, t_0 describes the considered time for which the power plant schedule must be calculated. The time span t_1-t_0 specifies the forecast duration. The forecast duration corresponds to the maximum MOT or MDT of the inflexible plants, because this is the maximum needed foreseeable time span to avoid operational violations of the inflexible plants. The difference between the maximum and minimum describes the capacity that must be covered by flexible plants.

If the capacity of the flexible plants is not sufficient to cover the peak load, as shown in case 1 in Figure 45, the inflexible plants are also used to cover the peak load. In the case of a strong load change after time t_1, operational violations can occur, if the capacity of the flexible plants and the inflexible plants, which cover the base load, is not sufficient to handle the abrupt load change. If the difference between the maximum and minimum over the period under consideration is less than the available capacity from the flexible plants, as shown in case 2 of the figure, the peak load is completely covered by the flexible plants. In order to cover the base load, the most efficient plants of the flexible plants not yet in use and inflexible plants are used. After calculating the required power from flexible and inflexible plants, these are selected according to the highest power/flow ratio until the load is covered.

3.4 Dynamic models of electrical equipment

Since this work investigates the provision of flexibility in terms of active power provision the corresponding investigation on power system stability is a frequency stability analysis (cf. section 3.1). Figure 46 illustrates the time behaviour of different compensation processes, which are divided into electro-magnetic, electro-mechanical and thermo-dynamic processes. Hence, the focus is on the area of electromechanical compensation processes. The time range relevant for the observation thus extends from milliseconds to a few seconds to simulate the fast provision of flexibility. Consequently, the dynamic modelling and simulation of the network elements inverter, generator and turbine, as well as the corresponding controller models and the connected dynamic consumers are of particular importance. Therefore, the dynamic models for the relevant parameters of a power system are explained in the following sections.

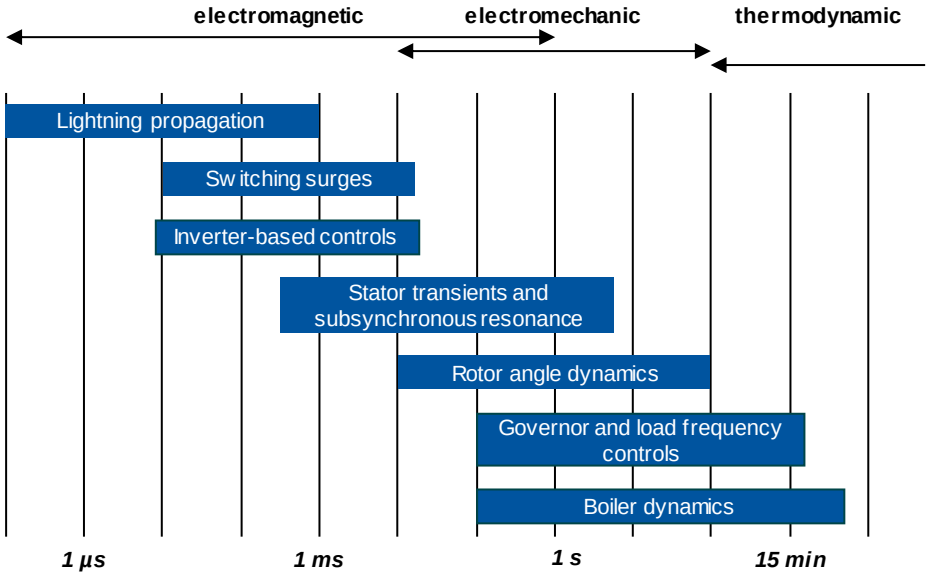

Figure 46: Time ranges of the dynamics in power systems (IEEE/CIGRE Joint Task Force on Stability Terms and Definitions 2004).

3.4.1 Basics of power plant modelling

First, the conventional generation units in the grid are analysed, which include thermal (nuclear, coal, gas and biomass) and hydropower plants. Usually a power plant is composed of several, largely independent machines or groups of generators. Figure 47 shows the structure of such a group (Machowski, Bialek, and Bumby 2012). In a turbine, thermal or kinetic energy is converted into mechanical energy. The shaft transfers mechanical power to the synchronous generator, which is fed into the grid as current and voltage via the generator. (Boldea 2016)

In the following subchapters, the components relevant in the time domain are first analysed separately. Largely independent of the power plant type under consideration, the investigation of the synchronous generator, the excitation system and the grid is considered. In sections 2.4 and 2.5, the different turbine types with their respective power frequency controllers are then

analysed in detail. The excitation voltage U_f represents externally controllable parameters. Indirectly influenced by the speed of the synchronous machines, the average frequency f.

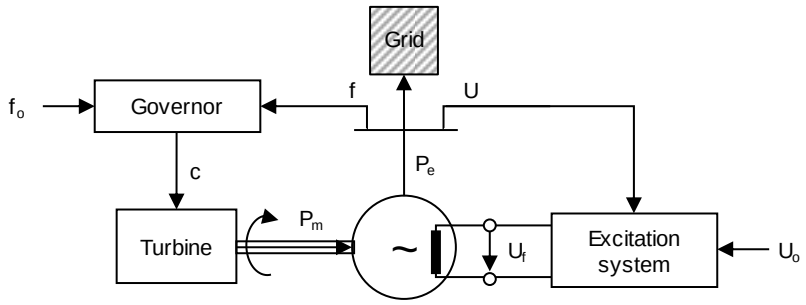

Figure 47: Block diagram of a generator group (Lehnen 2014; Machowski, Bialek, and Bumby 2012).

3.4.1.1 Synchronous Generator

The conversion of mechanical energy into electrical energy in conventional (large-scale) generation units is carried out by means of three-phase synchronous generators. Three-phase synchronous generators are therefore also described as electromechanical energy conversion machines. In addition, three-phase asynchronous generators are used to a small extent: Wind generators or small hydropower plants, which are operated without personnel (on site), are to be listed here as examples. Since this work mainly deals with large hydropower plants, reference is made to (Crastan 2015, 2017) for supplementary information on three-phase asynchronous generators. The focus is on the dynamic modelling of synchronous generators to represent the overall behaviour of the grid. (Plassmann and Schulz 2013; Schwab 2017).

In power systems – regardless of the location and condition under consideration – there should be an approximately constant frequency (cf. Chapter 2.2.3). Synchronous machines have a direct influence on the electrical mains frequency via their rotor angular velocity. The rotor angular speed depends largely on the turbine speed, which in turn depends on the generation technology under consideration. As a result, a distinction is made between limb pole and full pole generators, whose area of application depends on the speed n applied. These differ in their rotor geometry with regard to the number and design of the poles p and the arrangement of the excitation winding (Skolaut 2018). The full pole generator is used in thermal power plants. Due to its high speed (for $p = 1: n = 3000$; for $p = 2: n = 1500$) it is also called a turbo generator. The salient-pole generator is used with higher numbers of pole pairs at speeds less than 1200 rotations per minute. (Skolaut 2018)

Figure 48 shows the rotor cross-section of a full pole generator (turbogenerator) with a rotationally symmetrical rotor on the left and a limb pole generator with pronounced poles on the right. The limb pole generator as a low-speed generator is typically used in hydropower plants. To describe the basic functioning of the leg pole generator and the previously mentioned relationship to the frequency of the power system, the relationship between the electrical angular frequency and the mechanical angular frequency is shown below (cf. formulae (3.6) and (3.7)). (Crastan 2015)

$$\omega_m = \frac{2\pi n}{60s}\ (mech.angular\ frequency) \tag{3.6}$$

$$\omega = 2\pi f\ with\ f = \frac{np}{60s}\ (elec.angular\ frequency) \tag{3.7}$$

The relationship between the frequencies is described by the speed n (in rpm) and the number of pole pairs p.

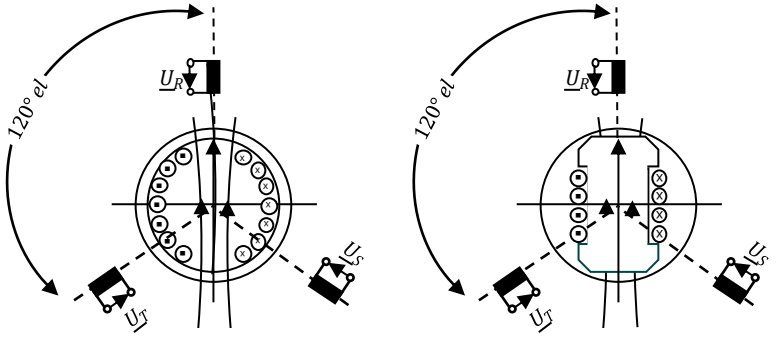

Full pole generator $(p = 1\ o.2)$ Shank pole generator $(p = 1 \ldots 50)$

Figure 48: Synchronous generator types according to (Schwab 2017).

Due to the large number of pronounced poles, the rotor geometry can be regarded as rather disc-shaped. As can be seen in the graph, the rotor is surrounded by three windings offset by $120°/p$ corresponding to the three phases of a three-phase system R, S, T. The terms rotor, pole wheel and rotor are used synonymously for both the full pole generator and the limb pole generator.

The conversion of the mechanical energy of the drive torque into electrical energy is effected by induction: a direct current flowing through the excitation windings. The direct current produces a magnetic direct field which rotates synchronously with the mechanical circular frequency. The rotational movement causes the excitation field to be non-constant and induces an alternating voltage in the three stator windings. (Crastan 2015)

Park-Transformation

The 0dq or Park transformation is a linear and time-variant modal transformation that transforms the instantaneous values of the three-phase system (electrical and magnetic quantities) to the two axes of the rotor. The stationary stator windings R, S and T are substituted by two substitute windings d and q rotating synchronously with the pole wheel and a zero sequence system. The d-axis is located in the field direction of the excitation winding and the q-axis is phase-shifted perpendicular to it by 90°. The zero sequence system is assumed to be currentless and can therefore be neglected. Formula (3.8) describes the parking transformation based on the 0dq-transformation mathematically:

$$\boldsymbol{T_{0dq}} = \frac{2}{3}\begin{bmatrix} 1/2 & 1/2 & 1/2 \\ \cos(\omega t + \vartheta) & \cos(\omega t + \vartheta - \frac{2\pi}{3}) & \cos(\omega t + \vartheta + \frac{2\pi}{3}) \\ -\sin(\omega t + \vartheta) & -\sin(\omega t + \vartheta - \frac{2\pi}{3}) & -\sin(\omega t + \vartheta + \frac{2\pi}{3}) \end{bmatrix} \tag{3.8}$$

The polar wheel angle ϑ describes the position of the rotor field in relation to the strator rotating field. The parking transformation as such is power invariant (Werner 2018). Due to the p.u. system (per unit system) and thus the use of dimensionless variables, the operating behaviour of the synchronous generator can be described with a few specific variables and simple relations between these variables can be established. The physical quantities are converted into related quantities by division with the appropriate reference quantities (typically nominal values). (Bonfert 1962)

Dynamic Model of a Synchronous Machine

The dynamic model of a synchronous machine comprises the stress equations (electrical component), the flux linkage equation (magnetic component) and the equation of motion (mechanical component). The following sections briefly introduce the equation of motion and the necessity of modelling. For more detailed explanations, please refer to (Milano 2010)

The equation of motion describes the balancing processes occurring during a power imbalance in the course of the instantaneous reserve (cf. section 2.2.2). Thus, there is a direct relation to frequency stability and polar wheel angular stability (Crastan and Westermann 2018). The following differential equation describes the relationship between the mechanical drive torque and the mechanical braking torque of the generator as well as the damping torque across the air gap:

$$\dot{\omega} = \frac{1}{2H}\left(\tau_m - \tau_{el} - D(\omega - \omega_s)\right) \tag{3.9}$$

H represents the inertia constant and is an indicator of how long the generator can deliver its nominal power purely from the kinetic energy stored in the rotating masses. The differential equation (3.10) represents the changes in the pole wheel angle due to balancing processes:

$$\dot{\vartheta} = \Omega_b(\omega - \omega_s) \tag{3.10}$$

If there is a difference between the speed of the rotor field and that of the stator rotating field, this leads to an increase or decrease in the electrical pole wheel angle ϑ.The term $\Omega_b = 2\pi f$ is necessary to transform between the SI system and the p.u. system, since the synchronous circuit frequency $\omega_s = 1\ [p.u.]$ is given in the per unit system. (Milano 2010; Morren 2006)

To map the transient and subtransient dynamics of a synchronous machine description of the electrical and magnetic components also would be necessary. Since this is not directly related to frequency stability in terms of this work it is not presented here. Further literature explicitly dealing with the modelling of the magnetic component is (Morren 2006; Milano 2010)

The literature recommends a 4th order model the representation of electromechanical compensation processes in system studies of frequency stability. Hence this work uses a corresponding model (Milano 2010). Electromagnetic, transient and subtransient processes are not considered. The two-axis model according to Park is used, which enables the transfer of partial differential equations into a system of ordinary differential equations. This provides a reduction of the fundamental wave model and the electromagnetic torque on longitudinal and transverse axis (Göbel 2010).

Formulae (3.11) and (3.12) exemplarily represent the electrical stator equations. These illustrate the frequency dependence of the synchronous machine.

$$-\omega\psi_q = \mathrm{r}_a \mathrm{i}_d + v_d \tag{3.11}$$

$$\omega\psi_d = \mathrm{r}_a \mathrm{i}_q + v_q \tag{3.12}$$

The parameterization of the two-axis synchronous machine model is carried out depending on the primary energy source used and the rated apparent power using the parameter sets provided by Pai in (Sauer and Pai 1998). The "per unit" data of the parameter sets refer to the rated apparent power. If no clear allocation is possible via the rated apparent power, the mean value between two successive parameter sets is used. Due to the consistent allocation of the parameters of the conventional power plants, the synchronous generator behaviour can be precisely represented in the course of a more dynamic simulation. The parameter sets used are shown in Table 10.

Table 10: Parameter set for synchronous generator from (Pai 1989)

Parameter	1	2	3	4	5	6	7	8	9	10
$H\ [s]$	500.0	30.3	35.8	28.6	26.0	34.8	26.4	24.3	34.5	42.0
$\mathrm{R}_A\ [p.u]$	0.0	0.0	0.0	0.0	0.0	0.0	0.0	0.0	0.0	0.0
$\mathrm{x}_d\ [\mathrm{p.u}]$	0.02	0.295	0.25	0.262	0.67	0.254	0.295	0.290	0.211	0.1
$\mathrm{x}_d^{'}\ [\mathrm{p.u}]$	0.006	0.07	0.053	0.044	0.132	0.05	0.049	0.057	0.057	0.031
$\mathrm{x}_q\ [\mathrm{p.u}]$	0.019	0.282	0.237	0.258	0.62	0.241	0.292	0.280	0.205	0.069
$\mathrm{x}_q^{'}\ [\mathrm{p.u}]$	0.008	0.170	0.088	0.166	0.166	0.081	0.186	0.091	0.059	0.008
$\mathrm{T}_{d0}^{'}\ [\mathrm{s}]$	7.0	6.56	5.7	5.69	5.4	7.3	5.66	6.7	4.79	10.2
$\mathrm{T}_{q0}^{'}\ [\mathrm{s}]$	0.7	1.5	1.5	1.5	0.44	0.4	1.5	0.41	1.96	0.0

3.4.1.2 Excitation System

In order to carry out an adequate stability investigation in the power system, especially considering the dynamic behaviour of synchronous generators, a modelling of the excitation system used is necessary. The IEEE standard 421.5 defines three types of excitation systems: AC excitation systems, DC excitation systems and static excitation systems. A comprehensive description can be found in (Zimmer 2017). For the correct implementation of the models presented in IEEE 421.5, it is necessary that the excitation models of the power plants to be mapped are at least schematically known. If no information is available on the type and design of the real excitation model in a power plant, ENTSO-E recommends the use of the Simplified Excitation System (SEXS). This is a highly simplified, generic excitation system with voltage regulator that cannot be assigned to the AC, DC or static excitation systems. The basic structure of the simplified block diagram (cf. Figure 49) corresponds to the IEEE model AC4C. (Semerow 2018)

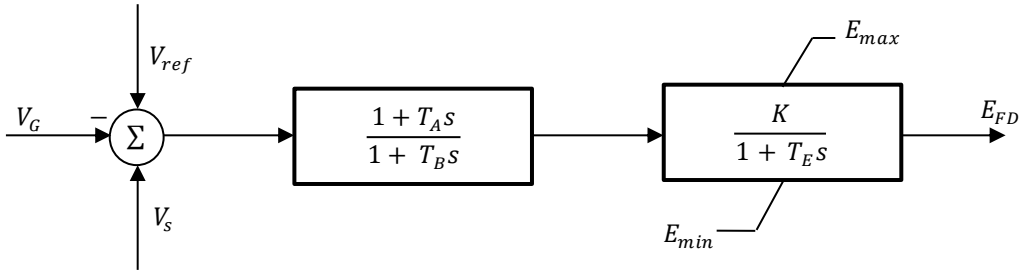

Figure 49: Simplified Excitation System (SEXS) model (Neplan AG 2015).

The field voltage E_{FD} in the reference system of the excitation system is the output variable of the model and flows into the magnetic equations of the synchronous generator. The reference voltage V_{ref}, the terminal voltage V_G of the synchronous machine and the output voltage of the Power System Stabilizer (PSS) V_S serve as input variables. The PSS (also called pendulum damping device) prevents unintentional control oscillations which can be caused by fast voltage regulators. The resulting damping of the system would lead to small signal instability. The PSS counteracts this effect and provides an additional stabilising signal for the voltage regulator. The power system becomes more robust because electromechanical oscillations are damped. The output voltage of the PSS is non-zero only in the case of equalization processes. (Schwab 2017; IEEE Power & Energy Society 2016)

The transfer function of the SEXS model consists of a lead-lag compensator, a gain constant and a PT1 delay element. The lead-lag compensator is modelled by the time constants T_a and T_b and represents the voltage regulator. It enables a reduction of the transient gain and can provide excitation voltages with sufficient accuracy over a wide frequency range. It is therefore often referred to as a correction element in control engineering. Depending on the parameterisation of the time constants a different control behaviour can be generated. For the parameterisation $T_A > T_B$ a lead compensator with differentiating behaviour follows. The lead compensator raises the phase position in the range $\omega_A = \frac{1}{T_A} \leq \omega \leq \frac{1}{T_B} = \omega_B$ and reduces the amplitude response at low frequencies. For $T_A < T_B$ follows a lag compensator with integrating behaviour.

The lag compensator lowers the phase position in the range $\omega_B = \frac{1}{T_B} \leq \omega \leq \frac{1}{T_A} = \omega_A$. The proportionality factor K represents the total gain of the control system.

The excitation system itself is modelled as a PT1 element with the excitation time constant T_E, which mathematically describes the delay of the excitation system. The output of the PT1 element is limited by upper and lower limits to take into account the minimum E_{Min} and maximum E_{Max} excitation voltage. (Zimmer 2017)

The use of the SEXS model and thus a simplified representation of the excitation system is therefore permissible, since the exact voltage behaviour is not relevant for frequency investigations. The SEXS model maps the most important dynamic characteristics of modern excitation systems without causing design limitations (IEEE Power & Energy Society 2014). Table 11 shows three different parameter sets for the SEXS model.

Table 11: Parameter sets for the SEXS model (Neplan AG 2015; European Network of Transmission System Operators for Electricity 2013; Kou 2014)

	ENTSO-E	EASTERN	NEPLAN
K	200.0	100.0	20.0-100.0
$T_A\ [s]$	3.0	1.0	0.25-20.0.0
$T_B\ [s]$	10.0	10.0	5.0-20.0
$T_E\ [s]$	0.05	0.1	0.0-0.5
$E_{max}\ [s]$	4.0	5.0	3.0-6.0
$E_{min}\ [s]$	0.0	-4.0	0.0

3.4.2 Hydropower plants

As shown in section 2.3, the modelling of hydropower plants is of particular importance for the investigation of frequency stability in the Nordic power system. The following sections present the models used for water turbines and speed controllers within this work.

3.4.2.1 Turbine model

In water turbine modelling, a distinction is made between a linear water turbine model and a non-linear water turbine model, regardless of the type of turbine under consideration. In addition, a distinction is made between turbine models that assume the water column to be elastic and those that assume an inelastic water column. The models differ particularly in their complexity and in the required data requirements.

The dynamic transfer behaviour of a hydraulic system is significantly influenced by the characteristics of the turbine and the penstock. In particular, the effects of water inertia, water compressibility and pipe wall elasticity on the dynamic behaviour must be taken into account. Traditionally, the linearised model is used in computer models. Linearised models are typically used for the analysis of small-signal stability and apply only for small deviations of the system frequency from the nominal frequency. Due to the fact that the linearisation takes place around an

operating point, only usual valve positions of large power plants can be considered. Extreme values, however, are not taken into account (Naghizadeh 2014; Argonne National Laboratory 2013). At this point it should be noted that the overscore "‾" indicates a standardisation to a stationary operating point. G is defined as the relative valve position. Figure 50 illustrates this relationship, which is also quantified in formula (3.13).

$$\bar{G} = A_t \bar{g} = \frac{1}{\bar{g}_{FL} - \bar{g}_{NL}} \bar{g} \tag{3.13}$$

The real position is normalised to a range of values between zero and one and thus transformed into a relative valve position by including the idle position $\bar{g}_{NL}$ and the valve position at full load $\bar{g}_{FL}$. (Naghizadeh 2014).

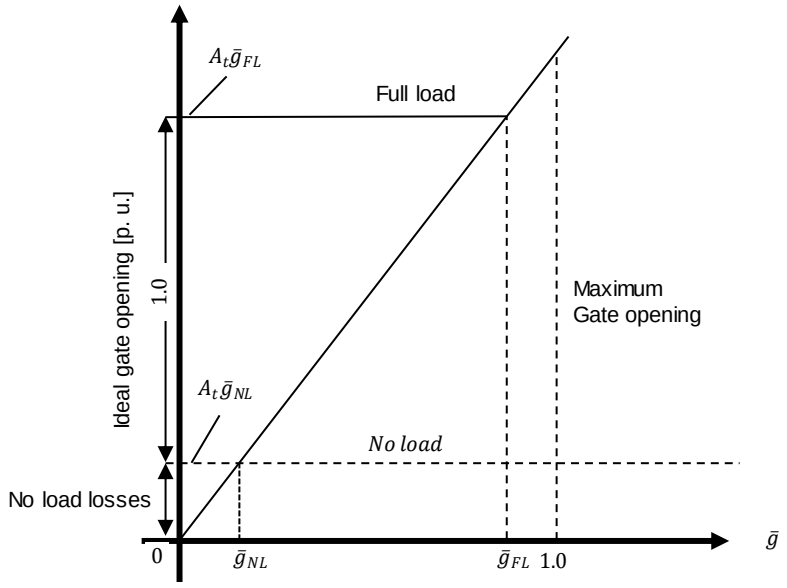

Figure 50: Relationship between relative and ideal valve position (Kundur 1994).

The linear model is shown in Figure 51. The transfer function of the idealised turbine representation depends on four constants a_{ij} and also on the time constant of water T_w. The valve position (also gate valve) of the pressure pipe $\bar{g}$ serves as the input variable.

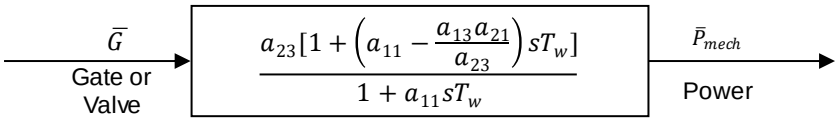

Figure 51: Linear turbine model (IEEE Power & Energy Society 2013).

The coefficients a_i represent partial derivatives according to the gate position or the head. The coefficients a_{11}/a_{21} are partial derivatives of the flow, whereas the coefficients a_{13}/a_{23} represent partial derivatives of the turbine power. If the coefficients $a_{11} = 0{,}5$, $a_{21} = 1{,}5$ and $a_{13} = a_{23} = 1$ are set, an ideal, loss-free water turbine is modelled. (Kundur 1994)

T_w is defined as the water start-up time required to accelerate the flow in the downpipe to nominal velocity after an abrupt change in head from standstill. The water start-up time constant T_w is calculated according to formula (3.14), taking into account the cross-section A and the length of the pressure pipe L (IEEE Power & Energy Society 2013). At this point it should be noted that the acceleration time was calculated neglecting the losses due to pipe friction. (Lehnen 2014)

$$T_W = \left(\frac{L}{Ag}\right)\left(\frac{U_{initial}}{h_{initial}}\right) \tag{3.14}$$

T_w represents a lower time limit which must at least elapse in order to reach the operating flow rate at nominal speed. The water start-up time is of essential importance for the control accuracy. Characteristic for the linear model is that the user has to recalculate the value of T_w for each load level of the hydraulic power plant, as it is highly sensitive to a change in load and the associated changed flow conditions. If, for example, a change from full load to half load is considered, the flow U is approximately halved, while the head remains approximately constant (Kundur 1994). In addition, a model extension is conceivable, which takes into account the compressibility of the water and the pipe's elasticity of change. In this way, the dynamic interaction between the hydraulic and the electrical system can be represented in a simplified way (Naghizadeh 2014). You can draw the conclusion that linear models with their simple structure can take into account basic characteristics of the hydraulic system and are therefore useful for tuning the control system using linear analysis techniques. Linear models are unsuitable for large variations in output power and mains frequency. (Argonne National Laboratory 2013)

The more flexible, non-linear inelastic turbine model shown in Figure 52 is more suitable for the investigation of larger disturbances.

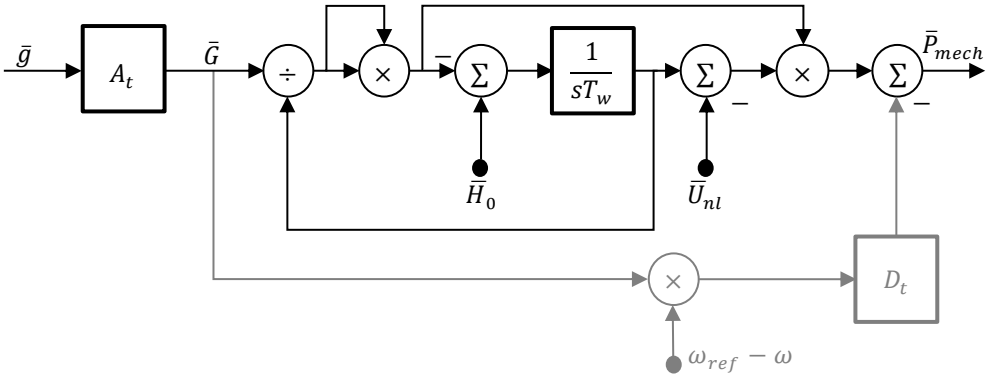

Figure 52: Non linear, inelastic water turbine model (Naghizadeh 2014; Kundur 1994).

In this model, the pressure waves and the compressibility of the water are neglected. The lower – grey-shaded – forward loop is not always considered in the literature. It describes a turbine self-regulation term D_t, which depends on both the speed change and the flow, can be included via a forward loop (IEEE Power & Energy Society 2013) The non-linearity of the model results from the non-linear relationship between the valve position and the turbine output (Sauer, Pai, and Chow 2017). Analogous to the linear model, the influence of the valve position is considered

via the constant A_T. This is calculated according to formula (3.13). In addition, the stationary head $\bar{H}_0$ and the offset resulting from the flow in idle mode $\bar{U}_{nl}$ are calculated. Accordingly, the turbine model presented in Figure 52 – assuming an inelastic water column – is sufficient for hydropower plants with a short or medium-length penstock (IEEE Power & Energy Society 2013, 1992b). The previously mentioned offset describes power losses resulting from the no-load flow. Not the entire flow rate contributes to power generation. $\bar{U}_{nl}$ is calculated from formula (3.15) assuming a stationary idling condition. (Kundur 1994)

$$\bar{U}_{nl} = \frac{1}{\bar{g}_{FL} - \bar{g}_{NL}} \bar{g}_{NL} \sqrt{\bar{H}_o} \tag{3.15}$$

In addition to the inelastic, non-linear turbine model (cf. Figure 53), there are turbine models in the literature that depict the elasticity of the water column. The elastic turbine model takes the compressibility of the water and the elasticity of the pressure pipeline into account.

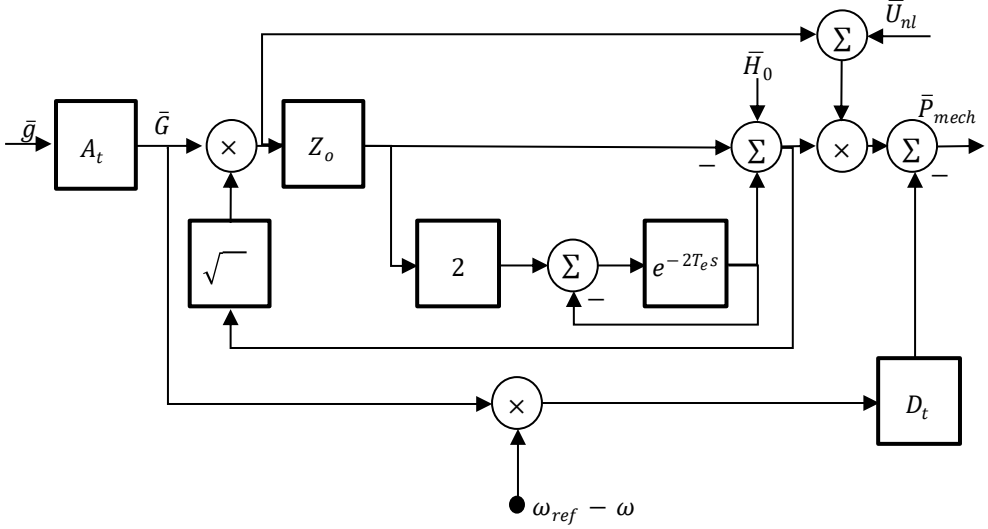

Figure 53: Non linear water turbine model under consideration of shock waves (IEEE Power & Energy Society 2013).

The input variable of the non-linear, elastic model also represents – in accordance with the models described above – the relative valve position (cf. formula (3.13)). In addition, there is also a parallel forward branch in this model, which describes the turbine self-regulation. Additional constants used in this model are the characteristic impedance of the pressure pipe (Z_0) and the wave propagation time (T_e). Z_0 is calculated according to:

$$Z_o = \frac{U_{FL}}{H_{static}} \cdot \frac{1}{\sqrt{g \propto}} \tag{3.16}$$

U_{FL} is defined as the flow that occurs when the valve is fully open. H_{static} is the total static head. It is defined as the difference in height between the reservoirs (Crastan 2017). The acceleration due to gravity $g = 9{,}81\ m/s^2$ is also included. Formula (3.17) describes the auxiliary quantity $\propto$.

$$\propto = \rho g \left(\frac{1}{K} + \frac{d}{fE}\right) \tag{3.17}$$

The variable ρ describes the density of water and K the compression module. The pressure pipeline is described by the variables d, f, E: d is the (inner) diameter, f the wall thickness and E the Young's modulus (IEEE Power & Energy Society 2013). The compression module represents the change in volume of the water due to hydrostatic pressure.

$$K = -V\frac{\partial p}{\partial V} \tag{3.18}$$

The Young's modulus describes a relationship between stress and strain due to elastic deformation (Giancoli 2010). Formula (3.19) quantifies the wave travel time can be quantified by means of the wave velocity.

$$T_E = \frac{l}{a}, with\ a = \sqrt{\frac{g}{\propto}} \tag{3.19}$$

It should be pointed out at this point that the elastic, non-linear model provides a precise representation of the turbine and water column dynamics. However, its application is not absolutely necessary, since the water column model only influences the results of frequency investigations under certain conditions and the necessity must be assessed according to the situation. A lower ratio between the water start-up time constant (T_W) and the wave propagation time (T_E) increases the influence of the elastic model. The tuning of the controller to the hydropower plant under consideration is also of importance. If the controller is designed for a fast response, differences between the models can occur, especially if oscillations of remote network blocks (within a network system) with impermissible frequency and power oscillations (inter area oscillations) have to be considered (Kundur 1994; IEEE Power & Energy Society 2013). Hence inter area oscillations are not in focus within this work, the inelastic model is sufficient for frequency analysis within the frame of this work.

3.4.2.2 Governor

The task of the governor or speed or frequency controller is to react to a frequency deviation resulting from a generation/consumption imbalance (cf. 2.2.2) and to adapt the active power generated to the current demand. (Anderson 2002)

In order to take into account the inverse reaction of the turbine output to a change in valve position, which is characteristic of a hydroturbine, transient statics must be considered in addition to the permanent statics of a power plant: Transient statics refers to a fast power-frequency control for short-term, transient frequency deviations. If there is a frequency deviation in the steady state, a high amplification of the control error in combination with a slow response of the controller is necessary. Therefore, permanent statics is defined as the speed drop under steady state conditions necessary to move the valve from the minimum to the maximum valve position (IEEE Power & Energy Society 1992b). A high transient static is required in conjunction with a long reset time so that the mechanical power can follow the flow of water influenced by the frequency deviation. It is possible to classify speed controllers according to their design. The

literature distinguishes between a more direct turbine control, which is mechanical-hydraulic, and a turbine control, which is auxiliary. These are analogue or digital electro-hydraulic controllers (Kaltschmitt 2013). Whereas mechanical-hydraulic controllers were mainly used in the past, today electro-hydraulic controllers are state of the art (Kundur 1994). Figure 54 shows the block diagram of a two-stage mechanical-hydraulic speed governor. Due to their robust design, mechanical turbine governors are extremely durable. Since the limited change of the valve/turbine gate is mechanically translated via a linkage, flexible and fast control is only possible to a limited extent and the control accuracy is limited (IEEE Power & Energy Society 1992b). Table 12 shows the physical meaning of the parameters used.

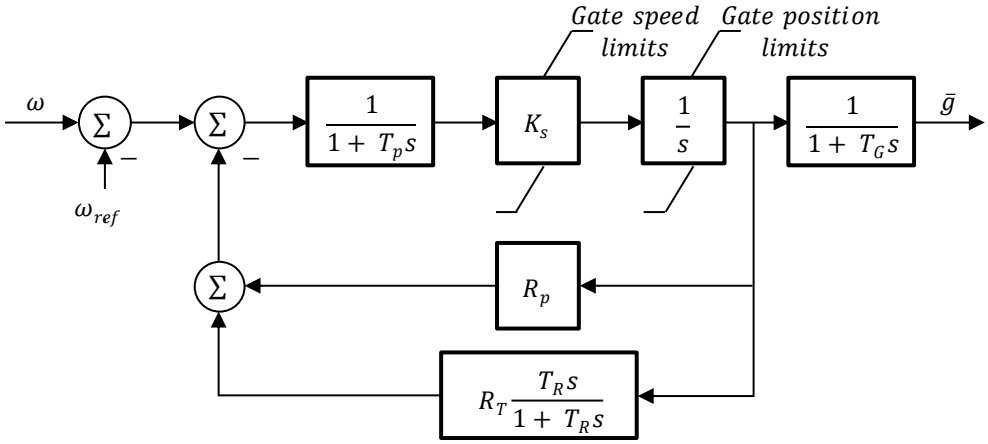

Figure 54: Mechanical-hydraulic controller (Kundur 1994).

Table 12: Parameter of the mechanic hydraulic Controller (IEEE Power & Energy Society 1992a)

Parameter	Explanation
T_p	Time constant of the servo motor for the pilot valve
K_S	Servo motor gain factor
T_G	Time constant of the servo motor for the inlet
R_P	Permanent droop
R_T	Transient droop
T_R	Reset time

The mechanical-hydraulic controller consists of two servo motors that regulate the pilot valve and the inlet. The servo motor of the pilot valve is composed of the PT1 element with the time constant T_p and the gain factor K_s. To prevent damage to the downpipe due to water hammer, which can occur when the valve or turbine gate is abruptly closed, the gain factor K_s limits the rate of change of the pilot valves. Abrupt pressure drops are avoided as the flow is gradually reduced. This has the additional advantage of a damping of the valve opening or closing is guaranteed (Kundur 1994). To represent the inertia of the water, the output of the pilot valve is negatively fed back: the proportional feedback models the common statics, while the feedback via

the PT1 element with the differential element provides a correction term for the influence of the transient statics (Machowski, Bialek, and Bumby 2012). The servo motor of the inlet (also main servo motor) also consists of a PT1 element with the time constant T_G.Also the main servo motor is modeled by two limiters. The valve position is limited between fully open and fully closed (Machowski, Bialek, and Bumby 2012). Different configurations of electro-hydraulic controllers are analysed below. A distinction is made between analogue and digital turbine controllers. Due to the high control quality, the almost arbitrary parameterisation and the simple integration into existing control systems, digital turbine controllers are used almost exclusively today. The functionality of electro-hydraulic controllers is similar to that of mechanical-hydraulic controllers. However, the electrical components offer greater flexibility and improved accuracy in terms of dead time ranges and time delays (Kaltschmitt 2013).

Figure 55 visualizes the basic version of an electro-hydraulic controller. This is a three-stage controller in a parallel structure, a **P**roportional-**I**ntegral-**D**erivative controller (PID for short). This is considered a standard tool for process control and has become established in many industrial applications. (Naik, K. Anil et al. 2012)

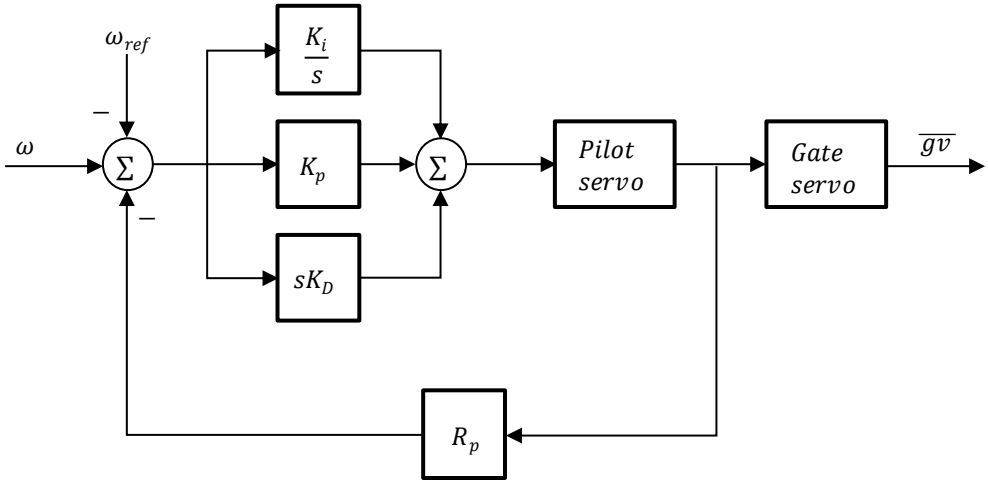

Figure 55: Electric-hydraulic PID controller (Kundur 1994).

The improved reaction speed of the PID controllers – compared to the mechanical-hydraulic controller – resulted from the fact that both an increase and a reduction of the amplification can be provided depending on the situation. The PID controller can be used polytropically due to its adaptability: The simple control design is sufficient for frequency control and can even represent reactions to small changes in the system frequency. A PID structure is therefore often used in practice. As can be seen, the mechanical-hydraulic controllers also have two servo motors for the supply valve and the inlet. (IEEE Power & Energy Society 2013)

A comparison of Figure 54 and Figure 55 shows that the feedback and thus the transient static R_T and the time constant T_R of the mechanical-hydraulic controller are substituted by the PID controller. The D-element must be considered separately: If a control deviation develops, the

differential triggers a strong, short change in the control output variable proportional to the control deviation. The D-element acts in the derivative action and thus enables - if the parameters are correctly set - a faster elimination of the control difference which occurs (Plassmann and Schulz 2013). Consequently, the derivative term is useful if individual plants have to be controlled in isolated operation, but in practice the D-element is sometimes completely omitted in some cases because it is difficult to handle and can lead to instabilities. Therefore, the PI-controller shown in Figure 56 will be discussed first.

The block diagram shown corresponds to the PID controller in Figure 55, but the derivative term $K_D = 0$ has been chosen. A comparison of the frequency characteristics of the PI controller with the mechanical-hydraulic controller confirms that both controllers achieve an increase in transient statics and even show identical control behaviour in the following parameterisation (cf. formula (3.20)) (Kundur 1994):

$$K_P = \frac{1}{R_T} \; ; \; T_R = \frac{K_p}{K_I} \tag{3.20}$$

Controllers often have other control objectives besides frequency control, such as the response to load changes. This leads to a multitude of different, individual control loops.

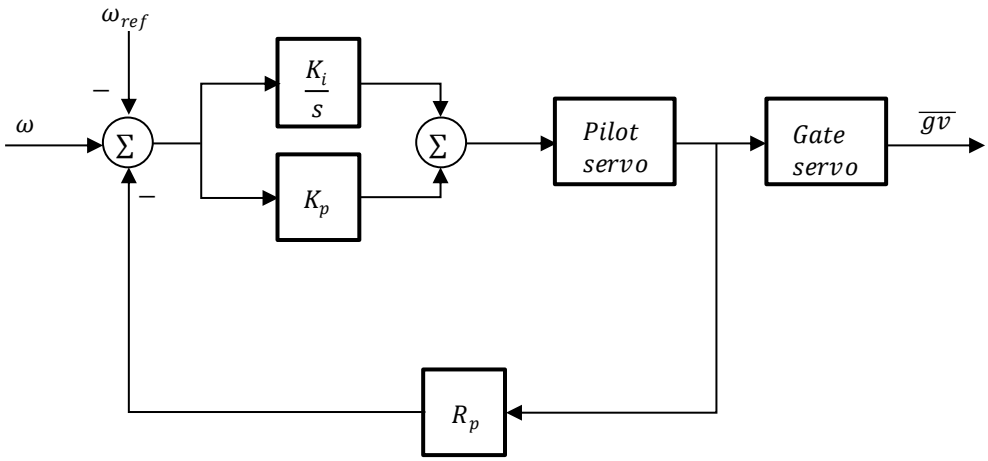

Figure 56: Electric-hydraulic PI controller (Kundur 1994).

Figure 57 shows the block diagram of a PI+D controller that is frequently used in Nordic hydropower plants. This model has a virtual switch that can be used to vary the input of the generic PI+D controller. This allows on the one hand a feedback of the output signal of the parallel connection of proportional and integral element and on the other hand a feedback of the electrical power. If the electrical power is chosen as a reference value, in theory a more precise control between the decrease in turbine speed and the power deficit can be achieved. However, in practice this often leads to a strong oscillation around the reference value of the controlled variable.

For this reason, a feedback of the above mentioned parallel structure is often used. This approximation of the electrical power prevents oscillations.

As shown in Figure 57, the power reference value can be included via a ramp function as an additional input variable of the servo element, consisting of the servo motor of the pilot valve and the main gate servo motor. Thus, in the case of a jump-like specification, the reference signal can be increased continuously in order to slowly vary the flow rate limited by the valve position (Lunze 2016). The grey-shaded block is representative for one of the turbine models presented in section 3.4.2.1. While in the previous models the controlled variable turbine speed is present as an external, implicit input variable, the speed is explicitly calculated in this model. By comparing the output variable of the water turbine P_{mech} and the electrical power P_{el} fed into the grid by the synchronous generator, a power difference is first calculated and then the speed is determined by an integral controller. The speed is fed back via a lead-lag element. The lead-lag element has a low overshoot and, depending on the ratio of the time constants, a predominantly differentiating or delaying behavior (Unbehauen and Ley 2014).

The model shown in Figure 57 will be used for the reference sites and the model shown in Figure 54 will be used for the remaining hydropower plants in the investigations on flexibility needs in grid operation in terms of maintaining frequency stability in Chapter 5.

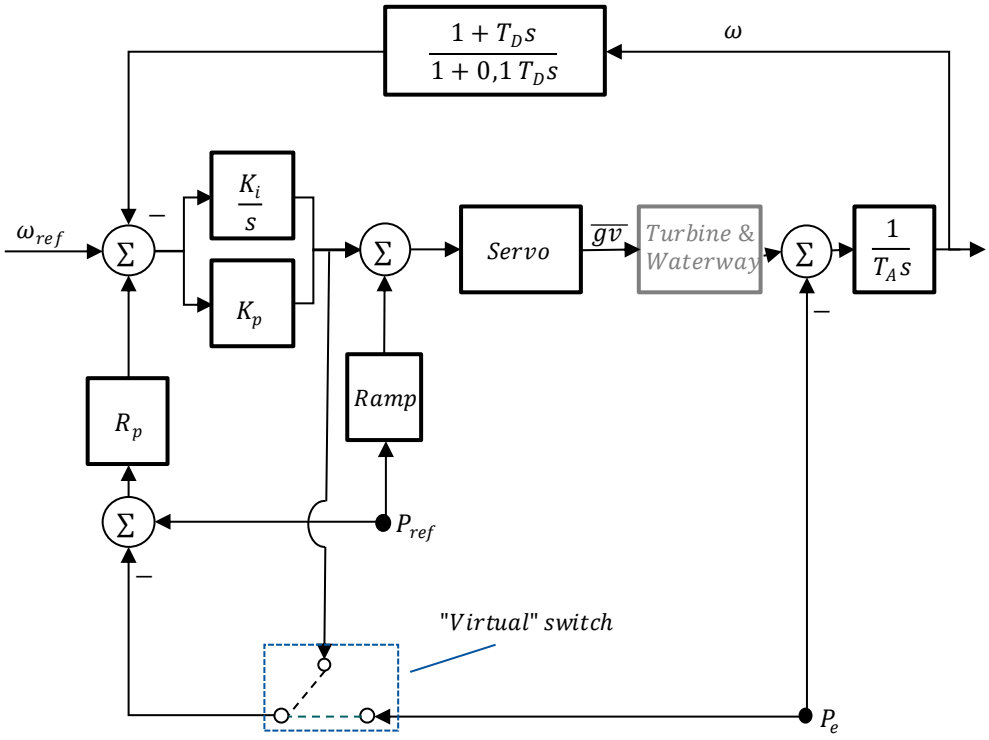

Figure 57: Generic PI+D controller for hydraulic power plants.

3.4.3 Thermal power plants

From a global perspective, thermal power plants make a fundamental contribution to the generation of electrical energy. At this point, the special feature of the Nordic power system should be pointed out. Thermal power plants play a subordinate role compared to hydropower plants. Nevertheless, an adequate representation of thermal power plants, which contribute significantly to security of supply, is important for the accurate modelling of the Nordic generation system (Oeding 2016). Thermal power plants carry out an energy conversion process which starts with the internal fuel energy (combustion of fossil primary energy sources) or the internal binding energy (nuclear fission of fissile atoms) of a primary energy source, converts it into mechanical energy and finally converts it into electrical energy with losses (Zimmer 2017). Regardless of the primary energy source used, different turbine and controller models are to be presented for the thermal power plant types, subdivided according to gas and steam power plants.

3.4.4 Gas turbine power plants

Gas turbine power plants generate electric energy from gas as primary energy source by passing through the Joule-Brayton cycle. Ambient air is compressed to approx. 30 bar by a compressor. The compressed air, which has already been heated by the compression process, is fed into the combustion chamber where it is interspersed with gas. This gas-air mixture is ignited and fed into the gas turbine with a combustion chamber outlet temperature between 1000°C and 2000°C. There the expansion process takes place, the kinetic power generated is transferred via a turbine shaft to the synchronous generator where it is converted into electrical power. (Lechner and Seume 2010)

Gas turbines are characterised by low specific construction costs and high fuel costs. In addition, gas turbine power plants have short start-up times and high performance gradients. These characteristics mean that gas turbines are often used to cover load fluctuations, to provide primary control reserve or as peak load power plants (Hundt). The IEEE recommends the GGOV1 model developed by General Electric for both transient and post-transient studies (IEEE Power & Energy Society 2013; Cabbel 2004). The GGOV1 model is a universal model that can be used for a large number of turbine controls, provided that the turbines are controlled by a PID controller. The high model complexity of the GGOV1 model can be explained by the fact that it consists of three largely independent control loops:

- PID speed control
- PI temperature/load control
- Acceleration control

The PID speed control receives as input signals the speed deviation as well as the actual deviation of the active power output. The current deviation of the active power output is determined from the difference of the electrical active power output P_{el}, taking into account the constant R and the reference value of the electrical active power output P_{ref}. The PI temperature/load control represents a relationship between the maximum possible turbine power and the existing

ambient temperature, while the ambient temperature is assumed to be constant during an iteration step. Temperature changes resulting from a new operating point with respect to the firing system are taken into account via feedback. The acceleration control ensures that the maximum turbine acceleration a_{set} is not exceeded. This is done by comparing the maximum turbine acceleration and the speed change via a differential and a lag element with the time constant T_A (Zimmer 2017). The output variables of the control blocks are the input to a so-called *Low-Value-Select-Block*, which selects the smallest size and passes it on to the subsequent turbine model. Looking at the output parameter P_{mech} of the GGOV1 model in steady state, the mechanical turbine power is given by formula (3.21).

$$\mathrm{P}_{mech} = \mathrm{K}_{turb} * \left(\mathrm{W}_f - \mathrm{W}_{fnl}\right) \tag{3.21}$$

The parameter W_f describes the fuel flow at full speed and zero load. Thus, the fuel consumption of the axial compressor can be modelled. Via the lead-lag element with the time constants T_b and T_c the deceleration of the gas turbine as a consequence of a change in fuel flow is represented (IEEE Power & Energy Society 2013). Since the GGOV1 model can be used to model all thermal power plants with the exception of those with nuclear firing, an additional optional time constant T_{eng} can be used to model a delay of the fuel flow depending on whether the fuel is liquid or gaseous. (International Middle East Power Systems Conference 2010)

In summary, it can be stated that the explicit modelling of all control mechanisms of a gas turbine system is not necessary for investigations of system stability: data acquisition is too costly. In addition, internal, turbine-specific variables have only a minor influence on system stability. The GGOV1 model provides an accurate description of the expected behaviour, provided that a correct parameterisation has been chosen. Accordingly, the GGOV1 model is particularly suitable if the generator unit or the entire power plant is connected to a larger power system and investigations are to be carried out regarding the reaction to load fluctuations. (IEEE Power & Energy Society 2013; Semerow et al. 2015)

3.4.5 Steam turbine power plants

In contrast to gas power plants, steam turbine power plants require an additional steam cycle for electrical energy generation. The simplified energy conversion process is called the Clausius-Rankine cycle, whose working medium alternates between liquid water and gaseous steam (Crastan 2017). Figure 58 shows the standardised TGOV1 model. This is the simplest combination of turbine and speed controller model of a controlled steam process, which is used for dynamic investigations. The TGOV1 model is universally applicable for nuclear, coal, oil and biomass power plants with steam turbines. ENTSO-E recommends its use for power system studies. (Kundur 1994; Semerow et al. 2015)

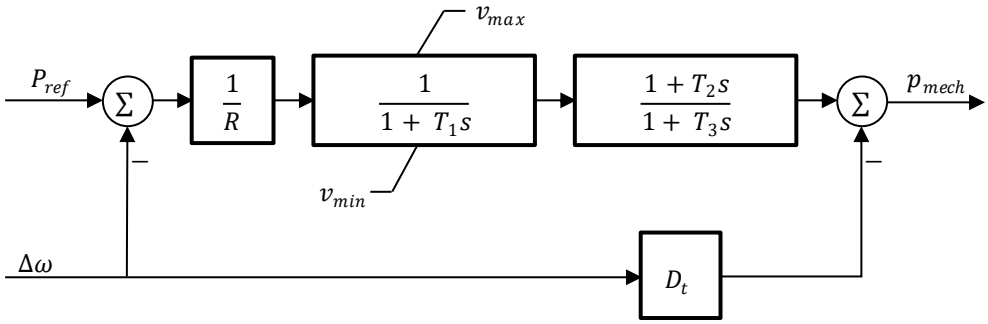

Figure 58: TGOV1 model (IEEE Power & Energy Society 2013).

Input variables of the standardised model are on the one hand the mechanical power reference value P_{ref} and on the other hand the deviation of the turbine speed from the reference speed. Taking into account the minimum and maximum valve position (v_{min} and v_{max}), the PT1 delay element represents the linearised behaviour of live steam valves. Assuming a fixed pressure operation, the steam flow can be assumed to be proportional to the valve opening. The time constant T_1 is used to model the time delay of the valve (Semerow 2018). The third block of the model is a compact representation of a lead-lag element, which depicts the dynamic behaviour of the steam in the turbine stages and the reheater. T_3 is to be understood as the time constant of the reheater. The ratio of T_1/T_2 corresponds to the percentage of the turbine power developed by the high-pressure turbine. The output of the model is the total mechanical power of the power plant. Via the lower path, the product of the speed deviation $\Delta\omega$ and the damping constant D_T is subtracted beforehand, whereby $D_T > 0$ always applies. This can be explained as follows. The speed-dependent friction losses have a negative effect on the available mechanical turbine power (IEEE Power & Energy Society 2013). The constant R represents the statics of the steam turbine and is therefore often referred to the mechanical power reference value(Semerow 2018). The statics is defined as the proportional change of the valve position - and thus also indirectly of the turbine output - to a change in frequency. The continuous curve represents the turbine statics while neglecting the speed-dependent friction losses. If the friction losses described are also taken into account, the dotted line represents the actual mechanical power output. In order to represent the statics of the TGOV1 model correctly, the limits of the valve position and thus also of the mechanical power must also be included. (Semerow 2018)

The IEEEG1 model is another model commonly used in the literature to represent a steam turbine and the associated control system but is not used in practice because of the high data requirement (Attikas 2014). Table 13 summarises the subcomponents represented by the TGOV1 and the necessary neglections and simplifications. The neglections and simplifications show that the TGOV1 is a good starting point for studies on power system stability in general, allows a sufficient representation of reality for frequency studies. Therefore, the TGOV1 model represents the dynamic behaviour of the steam power plants within this work. The parameters of this model used for the investigations are based on parameters given by the general speed turbine governor model developed by (Anderson 2002) and the TGOV1 model of ENTSO-E.

Table 13: Characteristics of TGOV1 model (Semerow et al. 2015)

Modeled subcomponents	Neglections and simplifications
- Integrated proportional speed control - Consideration of a valve delay with limitation of the valve position with anti-windup - Simplified mapping of steam movement by reheater and turbine stages as lead-lag element - Possibility to image a turbine damping	- Neglecting the dynamics of steam boilers - Vapour pressure - Neglect of separate reheater and turbine stages - Neglect of the non-linear deadband

3.4.6 Loads

Besides the generation units presented, consumers also have a major influence on the power system stability. A detailed modelling of all consumers is difficult, since there is a large number of different loads with individual characteristics in a power system, which vary strongly both regionally and seasonally. The specific characteristics to model the voltage and frequency dependencies via parameter sets are often not known. Looking at the cross-section of the loads connected to the power system, they can be described as ohmic-inductive dominated and can be substituted as a combined load model. For an exact representation it is important that both the capacitive, inductive and ohmic properties of the consumers and the resulting voltage dependence of the active and reactive power consumption, as well as the frequency dependence can be modeled. (Heuck 2013; Kleinkorte 2016; Semerow et al. 2015)

The frequency dependence of loads provides a fundamental important contribution to system stability and should therefore be considered in particular in studies investigating generation shortfalls or load shedding. The more the active power consumption of the load decreases with decreasing frequency, the more stable is the overall system (Concordia and Ihara 1982). The literature differentiates between static and dynamic models and within the static models between the exponential model and the ZIP model. The power consumption of a load in static models is modelled as a function of the node voltage V and the frequency deviation via two algebraic equations – for the active power P and the reactive power Q, respectively. The parameters V_0, P_0 and Q_0 correspond to the initial load flow (Merkle 2002). The so-called ZIP model (also polynomial model) superimposes the load impedance Z, current consumption I and active power consumption P, each of which is assumed to be constant (Merkle 2002). Formulae (3.22) and (3.23) describe the ZIP model (Kundur 1994):

$$\mathrm{P} = \mathrm{P}_0 \left[\mathrm{p}_1 \frac{V^2}{\mathrm{V}_0} + \mathrm{p}_2 \frac{V}{\mathrm{V}_0} + \mathrm{p}_3 \right] \cdot \left(1 + \mathrm{K}_{pf} \Delta f\right) \tag{3.22}$$

$$\mathrm{Q} = \mathrm{Q}_0 \left[q_1 \frac{V^2}{\mathrm{V}_0} + q_2 \frac{V}{\mathrm{V}_0} + q_3 \right] \cdot \left(1 + \mathrm{K}_{qf} \Delta f\right) \tag{3.23}$$

The individual components of the ZIP model are weighted by the coefficients p_i for active power and q_i for reactive power. The voltage dependence of the active and reactive power is composed of a quadratic and a linear dependence on the one hand and a constant component on the other. The terms $\left(1 + \mathrm{K}_{if}\Delta f\right)$ model the frequency dependence while Δf is the frequency deviation. (Kundur 1994)

Formulae (3.24) and (3.25) describe another static model, the exponential model (Oswald 2009):

$$\mathrm{P} = \mathrm{P}_0 \left(\frac{V}{\mathrm{V}_0}\right)^{a} \left(\frac{f}{f_0}\right)^{p} \tag{3.24}$$

$$\mathrm{Q} = \mathrm{Q}_0 \left(\frac{V}{\mathrm{V}_0}\right)^{\beta} \left(\frac{f}{f_0}\right)^{q} \tag{3.25}$$

Analogous to the ZIP model, different consumer compositions can be modeled using the weighting coefficients (here a, β) of the exponential model (Merkle 2002). The coefficients p and q describe the frequency dependence of the load. (Heuck 2013)

In case of very large voltage and frequency deviations from the setpoint, the static models do not allow a sufficiently accurate representation of the load. The literature recommends the use of dynamic load models for the investigation of inter-area oscillations and voltage stability (especially large signal voltage stability) or similar (major) events. However, if a consumer model is considered for a conglomerate of different loads, it reacts – analogous to reality – quickly to voltage and frequency changes and reaches a steady state in a short time. The use of a static model for frequency investigations within a synchronous network is therefore justified and used within this work. (Kundur 1994; Heuck 2013; Merkle 2002; Cutsem and Vournas 1998)

4 Investigation of scheduled flexibility provision by hydropower plants

In this chapter, exemplary investigations regarding the flexibility provision of hydropower plants from the Nordics for the European region and the Nordics themselves are carried out on the basis of future scenarios. Therefore, the methods presented in Chapter 3 are used. The considered areas of the market simulation and the hydraulic unit commitment simulation are shown in Figure 59. Due to their highly complex structure, the hydropower plant parks of Sweden and Norway are initially considered in aggregated form in the market simulation. In the hydraulic unit commitment simulation, the previously aggregated hydropower plant parks are considered in detail. Thus, a detailed area-wide simulation of highly complex hydropower plant parks is possible.

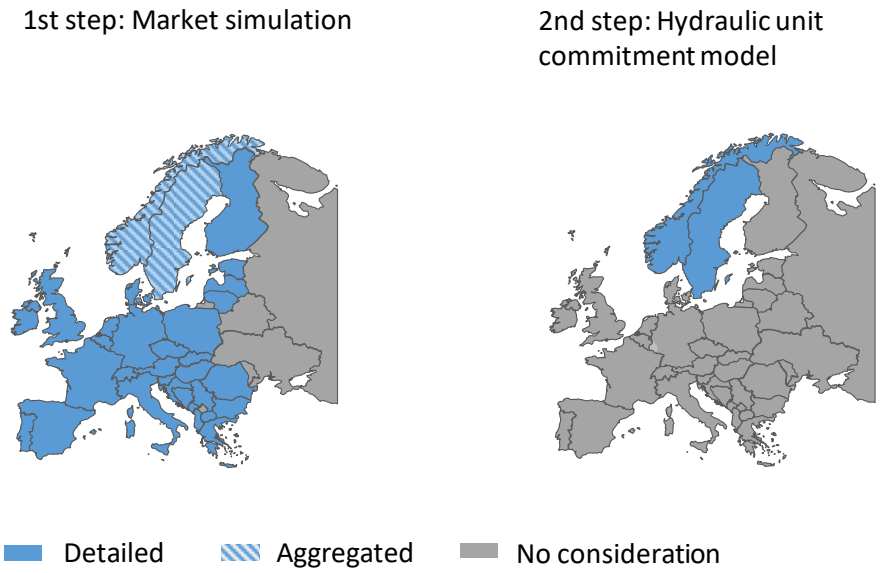

Figure 59: Considered areas of the individual process steps.

In the market simulation as well as in the hydraulic unit commitment simulation the countries Norway and Sweden are divided into several bidding zones. The Nordic bidding zones described in section 2.3 are partly summarized in the exemplary investigation. When defining the bidding zones, the areas with comparatively high exchange capacities are combined into one bidding zone.The new bidding zone boundaries are shown in Figure 60. The bidding zone NOs comprises the bidding zones NO1, NO2, and NO5 (c.f. Figure 14). The remaining Norwegian bidding zones NO3 and NO4 are described in the following as NO. In Sweden, only the bidding zones SE1, SE2 and SE3 are grouped together in SE. SE4 remains unchanged. Since SE4 has almost no hydropower plants, this bidding zone will not be considered further in the context of the investigations.

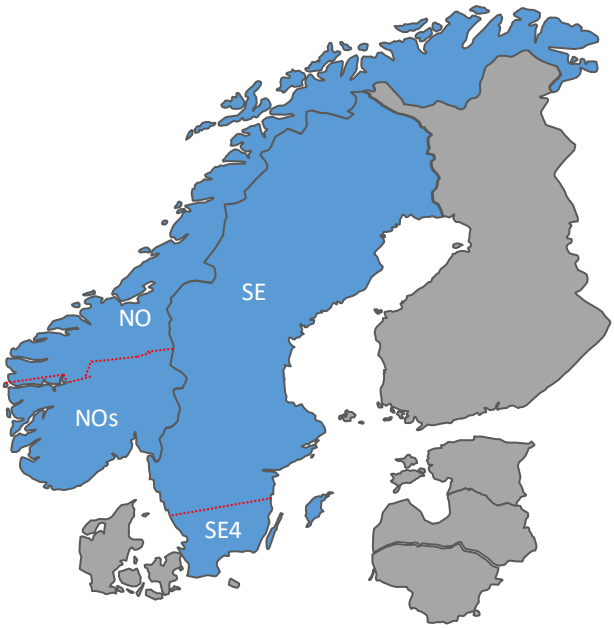

Figure 60: Bidding zone boundaries of the area under consideration in the context of the exemplary studies.

In the following, exemplary investigations are carried out in which the market-based methodology described in Chapter 3 is applied. First, different future scenarios are presented in section 4.1, which correspond to the input data of the market simulation. Then, the investigation program of the chapter is described in section 4.2. Subsequently, in section 4.3 the vertical factor, which is needed to run the hydraulic unit commitment simulation with a quarter-hourly time resolution, is parameterized and plausibilized. Section 4.4 presents and compares the results of the different scenarios according to the first step of the procedure, the market simulation. The exemplary examinations of the overall results according to the second step of the procedure are described in section 4.5. In this section, due to the diversity of the input parameters of the hydropower plant deployment simulation, the following investigations are performed:

- Comparison of the different flexibilization criteria (e.g. flexibilization of the largest hydropower plants or the oldest or the ones with the best or worst power-flow ratio (c.f. section 3.3.2)

- View of different flexibilization rates (10 to 50% flexibilization of the viewed portfolio)

- Comparison of the presented future scenarios (c.f. section 4.1)

- Investigation of a partial flexibilization of the power plant parks with non-flexibilized power plant parks

- Sensitivity analysis with higher shares of wind turbines in the Nordics

4.1 Definition of three European energy scenarios

The demand for and provision of flexibility in the future is only possible to forecast with a high degree of uncertainty. To cope with the uncertainty, the definition of several scenarios helps to systematically map many future eventualities. The simulations allow more precise statements to be made about the future on the basis of the scenarios. For this reason, hydraulic unit commitment simulations for different future scenarios are carried out within the scope of this work package of the project. The scenarios of the European power system considered in this study are already defined in (Siemonsmeier et al. 2018). A distinction is made between a Reference scenario, Green Hydro scenario and Prosumer scenario. An overview of the considered scenarios for different time points is shown in Figure 61.

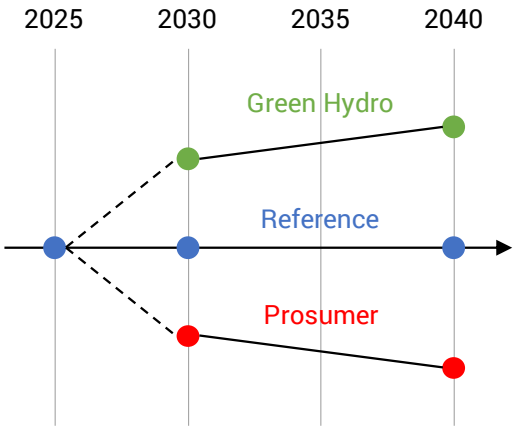

Figure 61: Schematic representation of the scenarios considered at different points in time.

For the year 2025 only the Reference scenario is examined, since the uncertainties in the near future are not significantly high and the Reference scenario represents the most probable scenario. In addition to the Reference scenario, the Green Hydro scenario and the Prosumer scenario are also examined for the years 2030 and 2040. All scenarios are derived from the TYNDP scenarios of ENTSO-E.

4.1.1 Reference scenario

The Reference scenario is characterized by conservative developments and is designed as best guess scenario. Figure 62 shows the characteristics of this scenario, classified by their extent in the essential factors in a radar chart. This essential factors are defined in (Siemonsmeier et al. 2018) and describe the key factors that will affect the possibilities of hydropower for future scenarios. The defined essential factors are: net transfer capacity, extent of grid expansion, relation of hydropower to other sources of flexibility as well as of electrical power generation, the total intermittent RES (IRES) share – which includes the volatile renewable plants such as PV systems and wind turbines – and the distribution ratio. As can be seen, all factors are in balance in the Reference scenario. Neither kind of power plant technology dominates the composition of power plant units but contains base load and peak load power plants in equal proportion. Intermittent RES are integrated into power systems to an extent which is manageable by base

and peak load power plants. Putting this categorisation into perspective, gas is gradually replacing coal and lignite in electrical energy production. The reduction of greenhouse gas emissions is an important goal of European countries, but is pursued sustainably. Grids are expanded when reasonable and needed based on economic advantages. As large-scale power plants are only gradually being replaced by intermittent RES, the need for further interconnections of power systems is only moderately evolving. Without high levels of interconnection within Europe, flexibility provisions from the Nordic countries can be distributed across Continental Europe to a moderate extent. Consequently, the rise of NTCs is not an urgent matter and not developed to a significant degree.

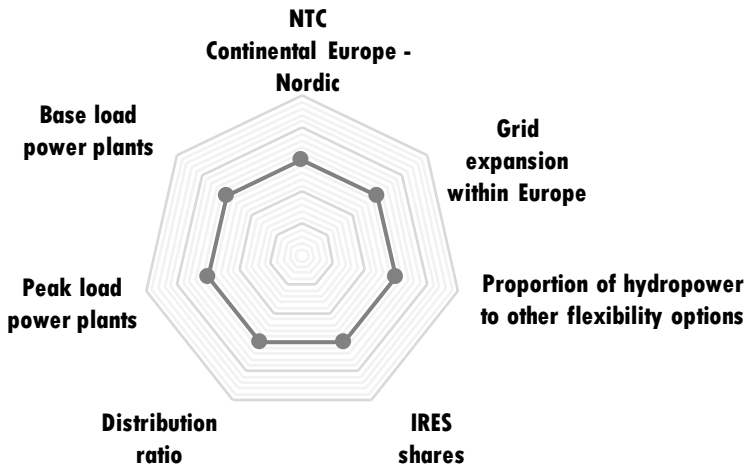

Figure 62: Essential factors of the Reference scenario.

4.1.2 Green Hydro scenario

The Green Hydro offers more possibilities of relevance for Nordic hydropower in comparison to the Reference and Prosumer scenario. In order to limit global warming, rapid global collaboration at an early stage characterises the Green Hydro scenario. These results in higher intermittent RES shares already by the year 2030. Consequently, the amount of coal and lignite power plants is reduced at an early stage. Therefore, a need for flexibility options arises at an earlier point in time and to a higher extent. Figure 63 shows the aspects of this Green Hydro scenario, using the essential factors. While intermittent RES shares are high in this Green Hydro Scenario, peak load power plants are not numerous. However, there is a number of competitors regarding flexibility, large opportunities for hydropower to cover peak load are available. Figure 63 also depicts that base load power plants are higher in their characteristic than peak load power plants. Therefore, there are chances for hydropower to function as base load power plants and provide Frequency Containment Reserves.

The distribution ratio is low, describing a system of large-scale electrical power generation units. The Green Hydro scenario includes only little decentral generation units and flexibility options,

e.g. roof-top solar panels and home battery systems. The large-scale electrical power generation contains power plants as well as large-scale wind parks, off-shore wind parks, and PV units on free spaces. This constellation leaves high demand in balancing demand and generation.

The extent of NTCs and grid expansion are both higher than in the Reference scenario. NTCs between the Nordic countries and Continental Europe are well-developed in the Green Hydro scenario. The Green Hydro scenario assumes more grid expansion projects realised between the Nordic countries and Central Europe than the Reference or Prosumer scenario. With a high amount of NTCs and low extent of grid expansion within Europe, flexibility provision by Nordic hydropower is a likely future development.

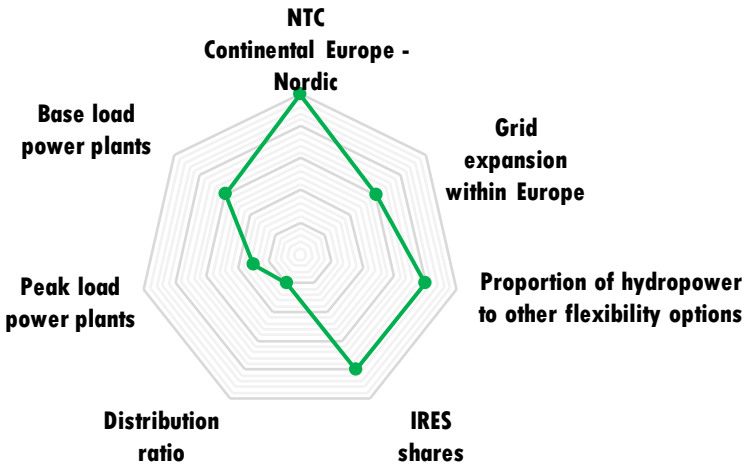

Figure 63: Essential factors of the Green Hydro scenario.

4.1.3 Prosumer scenario

The Prosumer scenario is designed in order to evaluate chances of hydropower in unfavourable circumstances. It captures developments with respect to hydropower not being the flexibility option and thus presents the pessimistic scenario in this study.

A high amount of small-scale solar panels combined with batteries as storage systems characterizes this scenario. The batteries are an advanced technology, causing them to achieve high profitability and thus be widely used in this scenario. At the centre of this scenario are prosumers, actively taking part in a decentralised electrical power generation system. These prosumers are owners of high amounts of solar panels acting as both consumers and producers of electricity. Prosumers are balancing their own electricity demand with small-scale solar panels and batteries and, thus, provide flexibility themselves. Due to the technological improvement of batteries in general, the electromobility sector has thrived and led to high numbers of electric vehicles as well. These technologies offer a high number of additional options to provide flexibility. This development might decrease the need for Nordic hydropower.

As technological developments are assumed to have evolved rapidly in this scenario, digitalisation, intelligent networking of technologies and communication systems are common in households and industries. Smart home appliances are widely used and connected with power systems. These technologies can often regulate demand automatically, offering numerous options of Demand Side Management. The high availability of these technologies causes more flexibility needs to be met on a local level. This high demand side flexibility might hinder opportunities of hydropower. High numbers of peak load power plants cover flexibility needs not provided for by these technologies. This competition might reduce the need for flexibility by Nordic hydropower further.

In this environment of high demand side flexibility and solar power storage by batteries, the overall need for additional flexibility provided for example by hydropower is rather low. High numbers of peak load power plants provide regulatory control, not covered by these options on the demand side. Figure 64 shows the extent of peak load power plants in relation to the other essential factors of this Prosumer scenario.

Numerous measures of Demand Side Management balance the fluctuating electricity generated by a high amount of intermittent RES on a local level. As a result, the proportion of hydropower to other flexibility options is low and thus opportunities are few. The involvement of high numbers of prosumers lessens the need for the provision of flexibility and thus the opportunities of hydropower plants. The NTCs between Continental Europe and the Nordic countries will not be significantly expanded in the Prosumer scenario. This complicates the opportunities of Nordic hydropower plants. Due to the high amount of other flexibility options available in this scenario, opportunities for Nordic hydropower providing flexibility might be low.

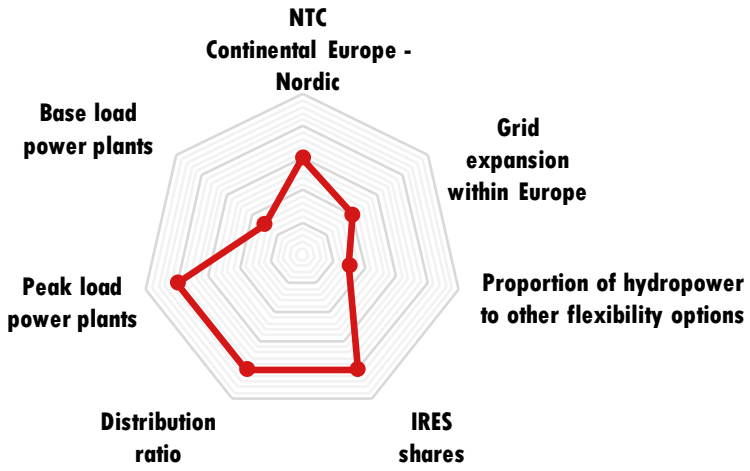

Figure 64: Essential factors of the Prosumer scenario.

As electricity supply and demand are balanced locally to a great extent, grid expansion within Europe is not of high importance. There is no significant need to expand the power grids as electricity is primarily transferred on local levels. Following the same reasoning, NTC levels between the Nordic countries and Central Europe show similar characteristic value. However, the distribution grid will be well expanded due to the highly decentralised electrical power generation and flexibility. As European countries are able to balance their power systems using decentralised small-scale technologies, there might be low demand for exchanging electricity between the Nordic countries and Central Europe. Without suitable amounts of NTC between the Nordic and Central European countries, flexibility is not easily provided by Nordic hydropower. The lack of transfer capacities could cause hydropower to be difficult to be obtained.

4.1.4 Comparison of intermittent RES shares for the different scenarios

Since the Nordic countries are in the focus of the investigations carried out within the scope of this study, the developments of the scenarios for the considered bidding zones (c.f. Figure 60) are briefly descussed below. Since intermittent RES development in particular could have an enormous impact on the use of hydropower in the Nordics, this will be focused on. As electricity generation from PV units plays a minor role in Nordic due to its low expansion, only the development of wind turbines will be discussed (c.f. Figure 65).

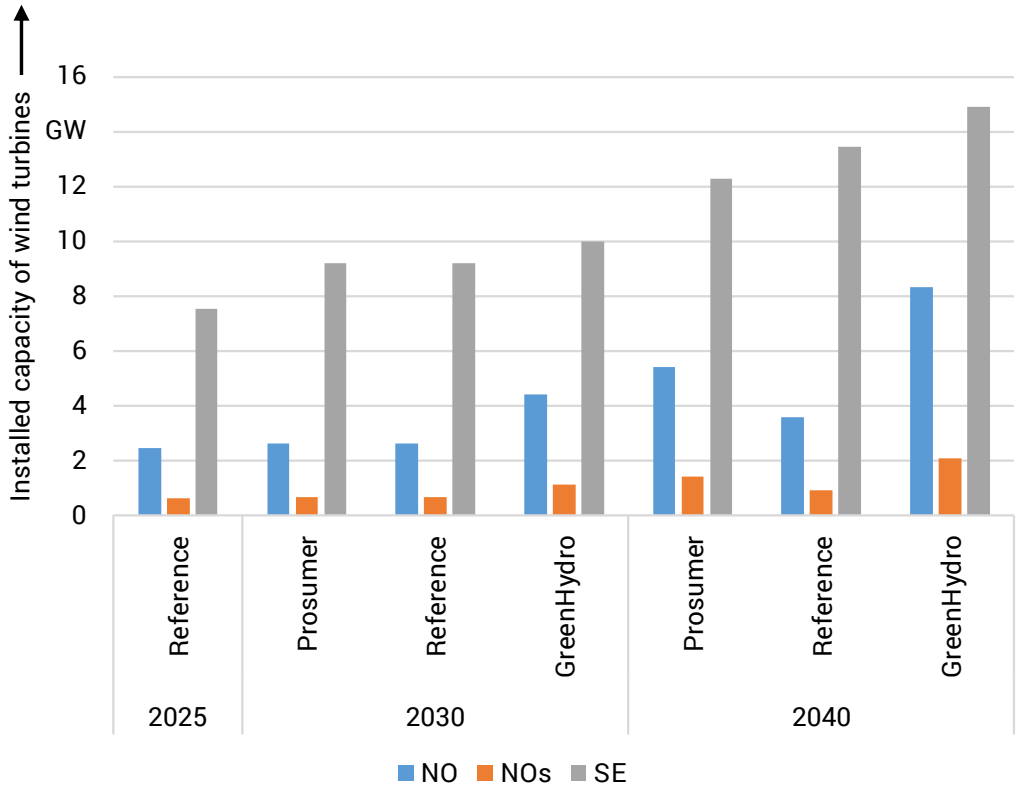

Figure 65: Installed capacity of wind turbines in the scenarios and bidding zones under consideration.

Figure 65 shows the installed capacity of wind turbines of the Nordic bidding zones in the described scenarios. It is noticeable that the installed capacity of the wind turbines in the SE bidding zone is the highest over all the years and scenarios under consideration compared to the bidding zones NO and NOs. In NOs, the installed capacity of the wind turbines is lowest in all scenarios at approx. 1 GW to 2 GW. In NO, the installed capacity of the wind turbines is between approx. 2 GW and just under 9 GW, depending on the scenario and year under consideration. A more exact view and comparison of the individual scenarios is given in the scenario report (Siemonsmeier et al. 2018).

4.2 Investigation program

In the investigations on detailed hydraulic unit commitment simulation carried out in the context of this study, the power plant parks of Norway and Sweden analyzed in Section 2.3.2 are considered. Only the hydro storage power plants above 10 MW are considered. Thus, the installed capacity of the hydropower plants in the bidding zone NO is about 9 GW, in NOs about 20 GW and in SE about 12.4 GW (see Section 2.3.2). Since the hydropower plants below 10 MW installed capacity that are not considered in detail here mostly represent run-of-river power plants, which are treated as must-run power plants and accordingly considered in the simulations.

Within the HydroFlex project five hydropower plants are used as reference sites for the research and innovation activities. The geographic location and size of the reference sites are shown in Figure 66. The Bratsberg power plant with 124 MW installed capacity is located in the bidding zone NO, the Kvilldal power plants with 1240 MW and Lysetbotn 2 with 370 MW installed capacity in NOs, and the Stornorrfors power plants with 599 MW and Porjus with 465 MW installed capacity in SE (Hydroflex 2019). The percentage of reference sites in relation to installed capacity is approximately 1.4 % in NOs, 8 % in NOs and 8.6 % in SE.

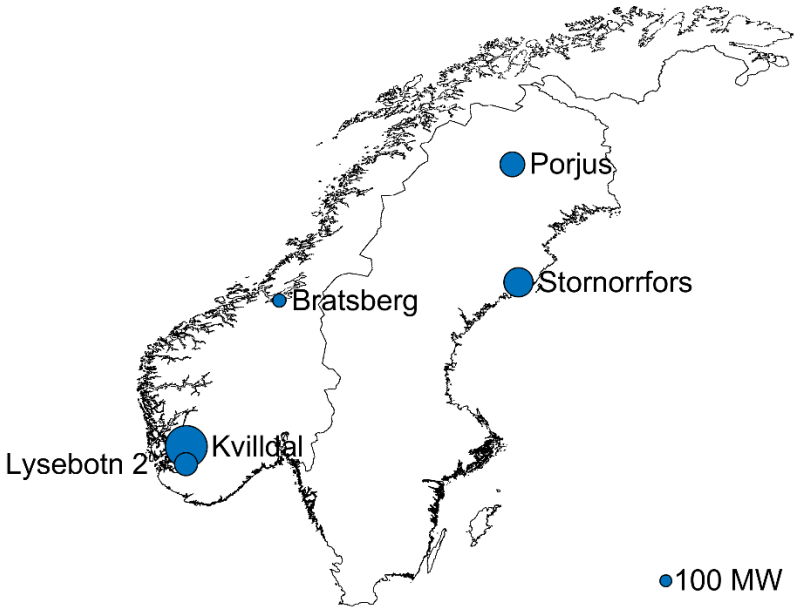

Figure 66: Geographic location and size of reference sites used in the HydroFlex project (Hydroflex 2019).

4.3 Parameterization of the vertical factor for the interpolation of volatile time series

Since the market simulation is carried out in hourly temporal resolution due to the complexity and high computational time, the results have to be extended to a quarter-hourly resolution, which corresponds to the temporal resolution of the intraday market, in order to ensure a representative evaluation of flexibility. For this purpose, a method for the interpolation of volatile time series has already been described in the model building in section 3.3. In the following, the vertical factor, which corresponds to the degree of freedom of the interpolation method, is parameterized and plausibilised for the interpolation of the market simulation results.

The analysis of the volatility of wind time series in section 2.5 shows that most of the power changes of wind time series are in the single-digit percentage range of the nominal power and that the share of larger power changes decreases with increasing size of the power change. Since the vertical factor is a measure for the magnitude of the power changes (c.f. section 3.3.1), the distribution of the vertical factor over the considered period of time should correspond approximately to the same distribution of the power changes of the wind time series in section 2.5. Due to the bell-shaped distribution of the power changes analyzed in section 2.5, the choice of a Gaussian distribution of the vertical factor is obvious. The density function of a Gaussian distribution is defined by the following formula (Kamps):

$$f(x) = \frac{1}{\sqrt{2\pi} \cdot \sigma} \exp\left(-\frac{(x-\mu)^2}{2\sigma^2}\right);\ for -\infty < x < \infty, \mu > 0, \sigma^2 > 0 \tag{4.1}$$

The parameter μ describes the expected value and σ^2 the variance. In order to ensure that the energy balance of the time series remains unchanged, the expected value μ is set to zero. With the variance σ^2 the bell-shaped distribution can be stretched or compressed. Since the vertical factor must be selected in the interval [-1; 1], the variance must be determined accordingly. For the normal distribution, 99.73 % of the values lie in the interval [-3σ; 3σ] (Kamps). Thus the variance σ^2 results:

$$1 = 3\sigma \Leftrightarrow \sigma = \frac{1}{3} \tag{4.2}$$

$$\sigma^2 = \left(\frac{1}{3}\right)^2 = \frac{1}{9} \tag{4.3}$$

The values greater than one or less than minus one are set to zero. Finally, the proportions of the size of the power changes are checked and adjusted. The analysis in section 2.5 shows that 75 % of the power changes of the quarter-hourly time series correspond to less than 5 % of the nominal power. With a normally distributed vertical factor, a quantile calculation would show

that 75 % of the values have an amount smaller than approx. 43 % of the maximum vertical factor of one. The vertical factors are therefore chosen too high and must be adjusted in such a way that the proportion of smaller power changes increases. To ensure the bell-shaped distribution, the previously determined normal distribution is cubed. The 75 % quantile of the amount of power changes is now calculated at approx. 5.7 %. This corresponds approximately to the distribution of the power changes from the quarter-hourly time series in section 2.5. The distribution of the vertical factor α for a year under consideration with 8760 entries is shown in Figure 67 as a histogram.

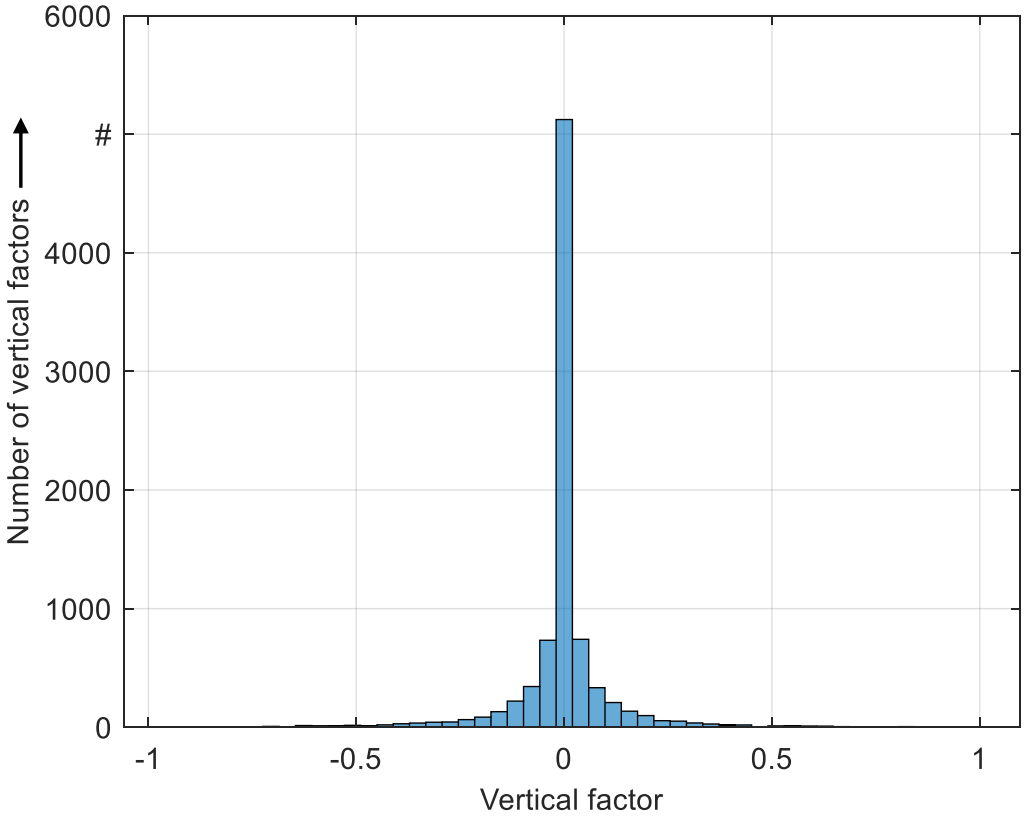

Figure 67: Distribution of the vertical factor α for the calculation of the volatile interpolation of time series.

The interpolation procedure presented in Section 3.3.1 can now be applied with the calculated vertical factor to the results of the market simulation. To check the plausibility of the determination of the vertical factor and the interpolation method, the method for volatility determination of time series from Section 2.5.1is applied to the volatile interpolated time series of the aggregated Germany time series from Section 2.5.2. Figure 68 shows the number of power changes of the aggregated hourly Germany time series and its quarter-hourly interpolation.

It becomes clear that the number of power changes in the single-digit percentage range of the nominal power has increased in the quarter-hourly time series. The overall ratio of the volatility

of both time series corresponds approximately to that of the analysis results of the comparison of hourly and quarter-hourly time series in Section 2.5. The plausibility of the parameterization is accordingly validated. However, the total number of power changes is smaller than the number of power changes of the individual wind turbines. Thus, the total number of power changes of the interpolated time series is always proportional to the number of power changes of the corresponding hourly time series.

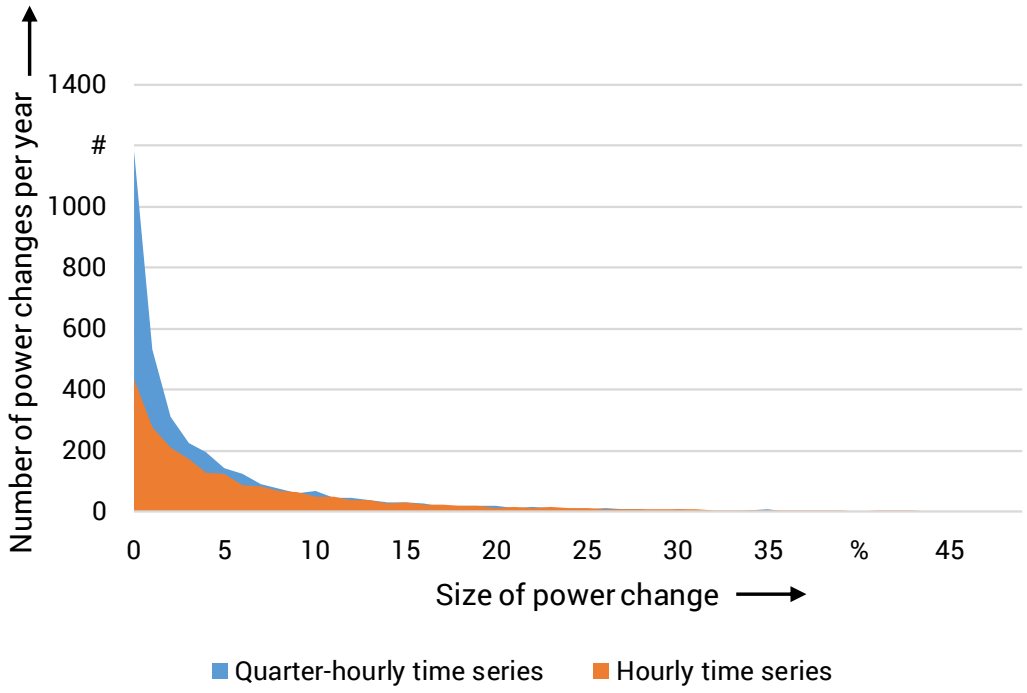

Figure 68: Number and size of power changes in the aggregated hourly Germany time series and its quarter-hourly resolved volatile interpolation.

4.4 Investigating the market simulation results

In this section the exemplary results of the market simulation are examined and evaluated. In particular, it is investigated what effects uncertain different developments, which are represented by the different scenarios, have on the demand for flexibility in Central Europe and the Nordics. Besides the aggregated hydraulic generation time series of the Nordics, also exemplary exchanges between Norway and Central Europe are considered in the following.

4.4.1 Evaluating hydraulic generation time series of different scenarios

The focus of the investigation is the operation of hydropower plants in Norway and Sweden. In order to provide an initial indication of the maximum demand for flexibility provision by hydropower in the defined scenarios, the following analyzes the results of the aggregated hydropower operation first. The aggregated hydropower plants are assumed to have maximum flexibility in order to not underestimate the flexibility required, as described in the methodology in Section 3.1.

For this purpose, the volatility is compared on the basis of the number of power changes, which is chosen as a measure of the demand for flexibility, in the aggregated hydropower time series by use of the method presented in Section 2.5.1. Those power changes are measured as the minimum distance from a high point to the nearest low points. Figure 69 shows the number of power changes above 100 MW per year of the aggregated hydropower generation time series, which is the result of the market simulation, for all considered scenarios and bidding zones. Smaller power changes are not considered, as minor impact on the flexible use of hydropower plants is assumed.

The number of power changes above 100 MW varies between almost 700 and approx. 1100 in each bidding zone of the scenarios. This corresponds on average to two to three power changes per day. The total sum of the power changes of all bidding zones in the respective scenarios increases slightly the further the simulation year is in the future. For example, the number of power changes in the Reference Scenario from 2310 in 2025 increases by about 5 % in 2030 and by about 15 % in 2040. This trend is also noticeable in the Prosumer and Green Hydro scenario. Overall, the number of power changes in the Prosumer Scenario is lowest in both 2030 and 2040 compared to the other scenarios. At the same time, the number of power changes is highest in the Green Hydro Scenario.

One reason for the increase in power changes the further the simulation year is in the future is the increasing share of RES, in particular wind turbines. The number of new wind turbines is lowest in the Prosumer Scenario and highest in the Green Hydro Scenario. Furthermore, this dependency is also noticeable when considering the individual bidding zones. In the bidding zone SE, the number of power changes and the associated need for flexibility is highest, followed by NO and lastly NOs. The increasing share of wind turbines in the Nordic bidding zones could, thus, be a driver for the need for this new type of turbine technology.

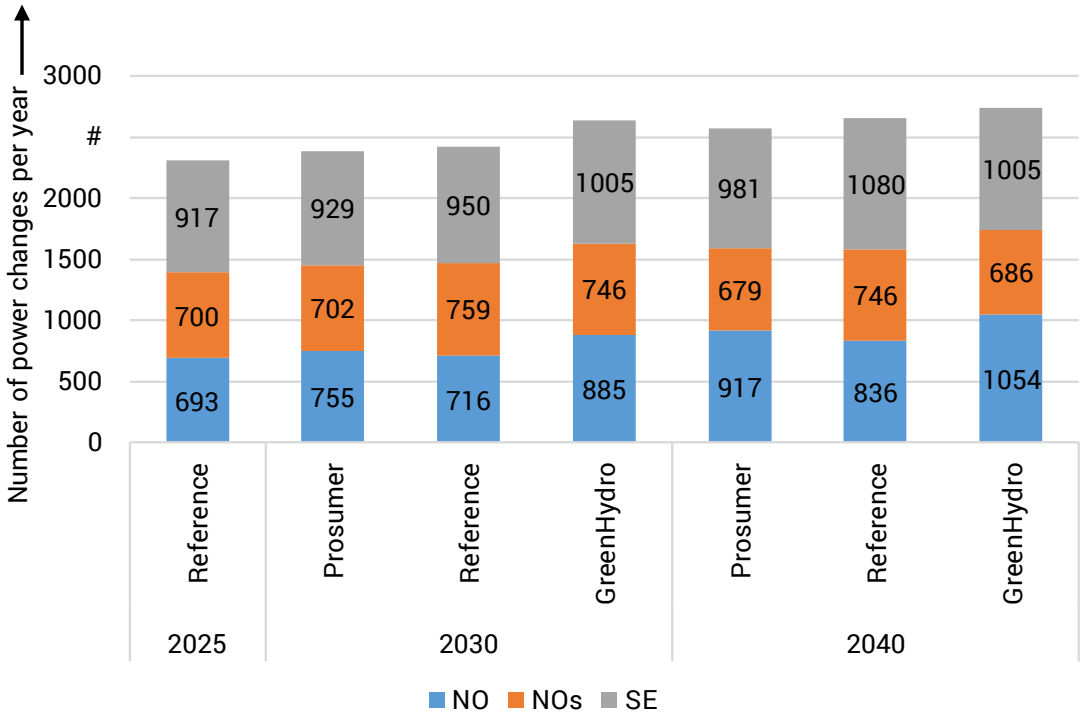

Figure 69: Number of power changes above 100 MW of the considered scenarios and bidding zones per year.

4.4.2 Investigating the exchanges between the Nordics and Central Europe

The results of the study above raise the question why the need for flexibility increases only slightly while a significant increase in flexibility demand is expected in the European area due to the expected high expansion of volatile RES plants. Furthermore, the question arises why the number of power changes in NOs does not change greatly despite the very diverse scenarios. As the changes in the Central European power system are most significant compared to the Nordics, the following focuses on interdependencies between those regions. Because the Prosumer scenario has faces the lowest demand for flexibility (c.f. Figure 69), the exchanges in this scenario for the viewing year 2040 is considered more in detail in the following. Figure 70 shows the aggregated hydraulic feed-in time series of NO and NOs of the Prosumer scenario for 2040 for a period of about ten days in the summer of the year. Additionally, the aggregated PV time series of Germany (DE) is illustrated. The lower graph presents the net exchange from NOs to DE.

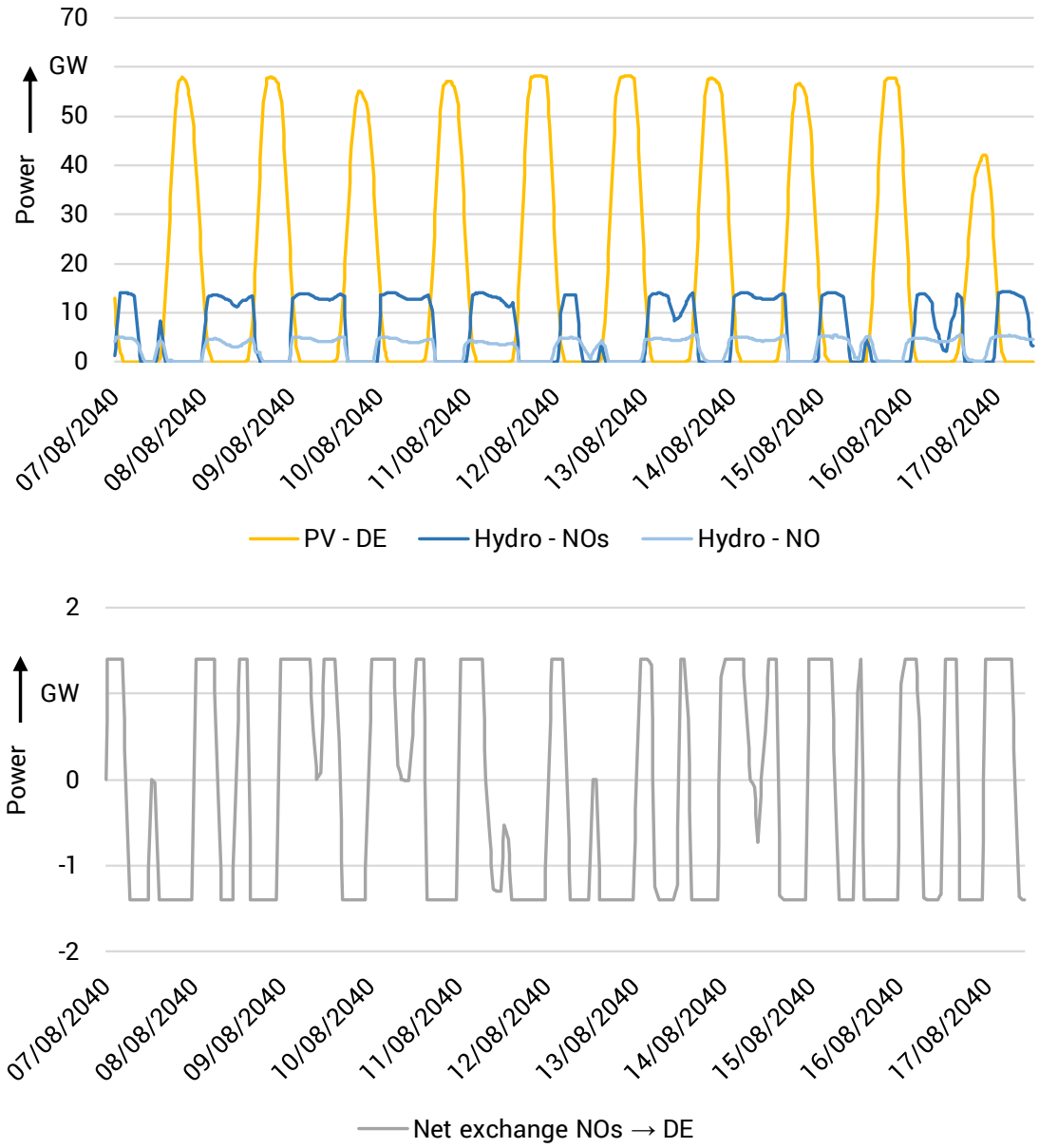

Figure 70: Section of the hydraulic generation time series of Norway and the generation from PV units in Germany of the Prosumer Scenario 2040 (upper graph) and the net exchanges from NOs to DE (lower graph).

The time series show that the generation of Norwegian hydropower plants in 2040 is highly dependent on generation from German PV units. When the generation from PV units in Germany is high, the Norwegian hydropower plants operate hardly. Conversely, when the generation from PV units in Germany is low, Norway's hydropower plants are operating at high capacity. The net exchanges of the considered bidding zones in the lower chart confirm the dependency, as the exchange capacity is usually operating at full capacity and mostly switching direction two times per day. Either Norway exports to maximum when German PV generation is low, or vice versa.

The net exchange is usually fully utilized and is very little subject to fluctuations. In the future, however, this behavior will require hydropower plants to run at least one cycle per day.

This behavior of the net exchanges indicates no significantly increasing need for flexibility provision by Norwegian hydropower through the future expansion of RES plants in Germany with respect to the variables investigated here, such as the power exchanges. To apply these results to the overall picture of the flexibility provision by Nordic hydropower to the neighboring countries, Figure 71 shows the annual duration curves of the net exchanges to the neighboring bidding zones of the NOs market. The annual duration curve represents the values of the net exchanges over one year in descending order.

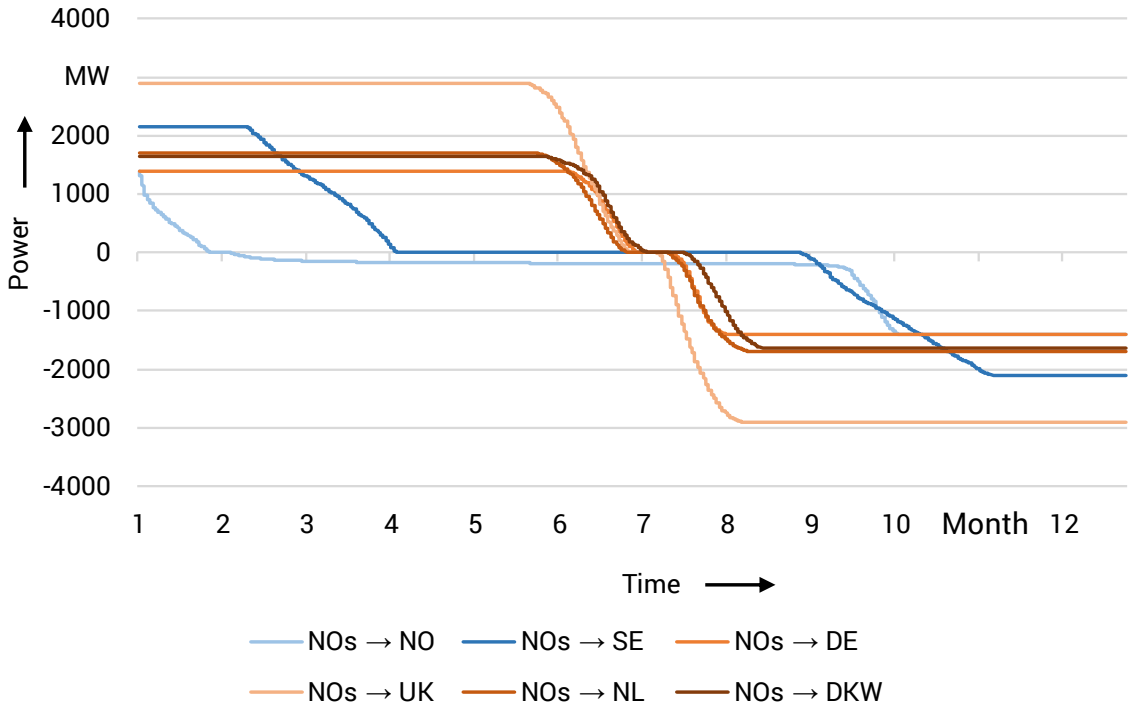

Figure 71: Annual duration curves of net exchanges of NOs to all neighbouring bidding zones.

The annual duration curve of the net exchange from NOs to DE shows the mostly complete operating capacity utilization described above, as the net exchanges corresponds to the maximum of the transmission capacity in about ten out of twelve months. The net exchanges of NOs to the United Kingdom (UK), the Netherlands (NL) and the bidding zone Denmark West (DKW) show a similar trend. Accordingly, a similar behavior of electricity prices and exchanges is expected in these bidding zones.

However, the annual duration curves of the net exchanges from the bidding zone NOs to SE and NO differ from the others. The exchange capacity of these is much less frequently fully utilized and often no net exchanges take place between these bidding zones.

The reason for this behavior lies in the different power plant parks. While the Nordics primarily generate electricity with hydropower, Central Europe has a significant share of thermal generation capacity in addition to many RES units. This leads to similar electricity prices within Central Europe and within the Nordics but wider price spreads between them.

Another reason is the difference in net generation capacity (NGC) between Central Europe and the Nordic countries. Germany itself has about seven times more NGC than Norway (ENTSO-E 2018). Therefore, even with higher exchange capacities, possible net exchanges to the Nordics may have only little impact on price spreads. Thus, the mostly maximum utilization of exchange capacities remains and does not lead to a significant increase in the demand for flexibility provision by Nordic hydropower assuming full utilization of the capacity for power exchanges.

4.4.3 Interim summary of results of the market simulation

In this study, the results of the market simulation have been analyzed with respect to the flexibility needs of the Nordics and Central Europe for different future scenarios. Furthermore, the power changes of the aggregated hydraulic time series of the Nordics have been used to evaluate the flexibility supply of the hydropower plants for the different scenarios. It was determined that due to the increase in the share of PV systems in Central Europe and the Great Britain, the generation from these PV systems influences the hydropower plant operation of the Nordics. This means that during the day, electricity in the Nordics is mainly imported to meet the demand in the Nordics itself, especially in the summer months, while at night the Nordics acts as an exporter by means of generation from hydropower plants. The number of power changes of the hydropower plants in the Nordics is therefore in most cases not more than two per day. Thus, the aggregated generation time series of the bidding zone NOs, which has the strongest connection to the Central European countries and Great Britain, behaves similarly in all considered scenarios. This is also the case because the capacity of the PV system in every scenario is so enormous in comparison to the capacity of hydropower in the Nordics that these are dominating the correlated behavior of the hydropower of the Nordics. As a result, the flexibility demand in the Nordics is only slightly higher due to this described behavior in comparison to the present operation. Because of the enormous capacity of the PV systems of Central Europe and hydropower of the Nordics compared to the exchange capacities, the exchange capacities are mostly fully utilized either in the one and the other direction. This results in a flat demand curve with less flexibility demand, since the power change of the curve corresponds to the demand of flexibility.

4.5 Investigating the results of the hydraulic unit commitment model

In the following, further exemplary selected investigations are carried out on the basis of hydropower plant operation simulation. The investigations provide clarity on the flexibility demand of the Nordics considering different scenarios, as well as on the provision of flexibility from haudraulic power plants of the Nordics. In addition, the flexibly drivable turbine developed in the project will be used in some plants to analyze its utilization and benefits and to study the impact on the Nordic power plant park. A suitable selection of the plants to be flexibilized is part of the investigations and is carried out on the basis of certain criteria, which are already described in Section 3.3.2, and evaluation variables such as the degree of utilization and the total water consumption. Then, it is examined how the different parameterizations of the scenarios affects the operation of the flexible and inflexible hydropower plants. In addition, it is analyzed which further effects and advantages a partial flexibilization of the hydropower plant fleet has. For this purpose, the results of two simulations are compared, one with partial flexibilization and one without flexibilization. Finally, the suspected dependency between the generation from wind turbines and the flexibility demand in a bidding zone is further analyzed within a sensitity analysis.

For the investigations a minimum operating time respectively minimum downtime of all non-flexible plants of two hours is assumed. Accordingly, due to the model, only two classes are distinguished, more flexible plants without minimum operating time respectively minimum downtime and less flexible plants with a minimum operating time respectively minimum downtime of two hours.

First, in section 4.5.1, different flexibilization rates and flexibilization criteria are compared with each other regarding the total water consumption and the more flexible use of the more flexible plants. Subsequently, in Section 4.5.2 the results of the whole method of the pre-defined scenarios are evaluated. Furthermore, the advantages of a flexibilization of hydropower plants are highlighted in Section 4.5.3. Finally, a sensitivity analysis is carried out in Section 4.5.4, in which the Green Hydro Scenario for the year 2040 is supplemented by a further expansion of wind turbines in Norway.

4.5.1 Consideration of different flexibilization rates and flexibilization criteria

After it has already been found out that in the bidding zones of the Nordics partly different flexibility demands emerge, the question arises, which and how many hydropower plants are most likely to be flexibilized and to receive the new turbine technology. For this purpose, different flexibilization criteria, which are already presented in Section 3.3.2, and flexibilization rates are investigated in the following. The objective of this study is to find a suitable selection of the plants to be flexibilized, which guarantees the most efficient use of the available water while at the same time optimizing the use of the flexibilized plants. A reasonable strategy of flexibilization is thus obtained for a high average number of start/stop cycles of the more flexible plants with a simultaneous reduction of water consumption. For this study, the rule-based algorithm for the reference scenario of the year 2030 is applied for all flexibilization criteria defined in Section 3.3.2 at flexibilization rates between 10 % and 50 %. Additionally, in one case only the

reference sites are made more flexible. The flexibilization rates for a flexibilization of the Reference Sites are approx. 1.4 % in the NO bidding zone, approx. 8 % in NOs and approx. 8.6 % in SE (see Section 4.2). Figure 72 shows the total water consumption over the average total number of start/stop cycles of the more flexible sites per year for all 31 cases considered.

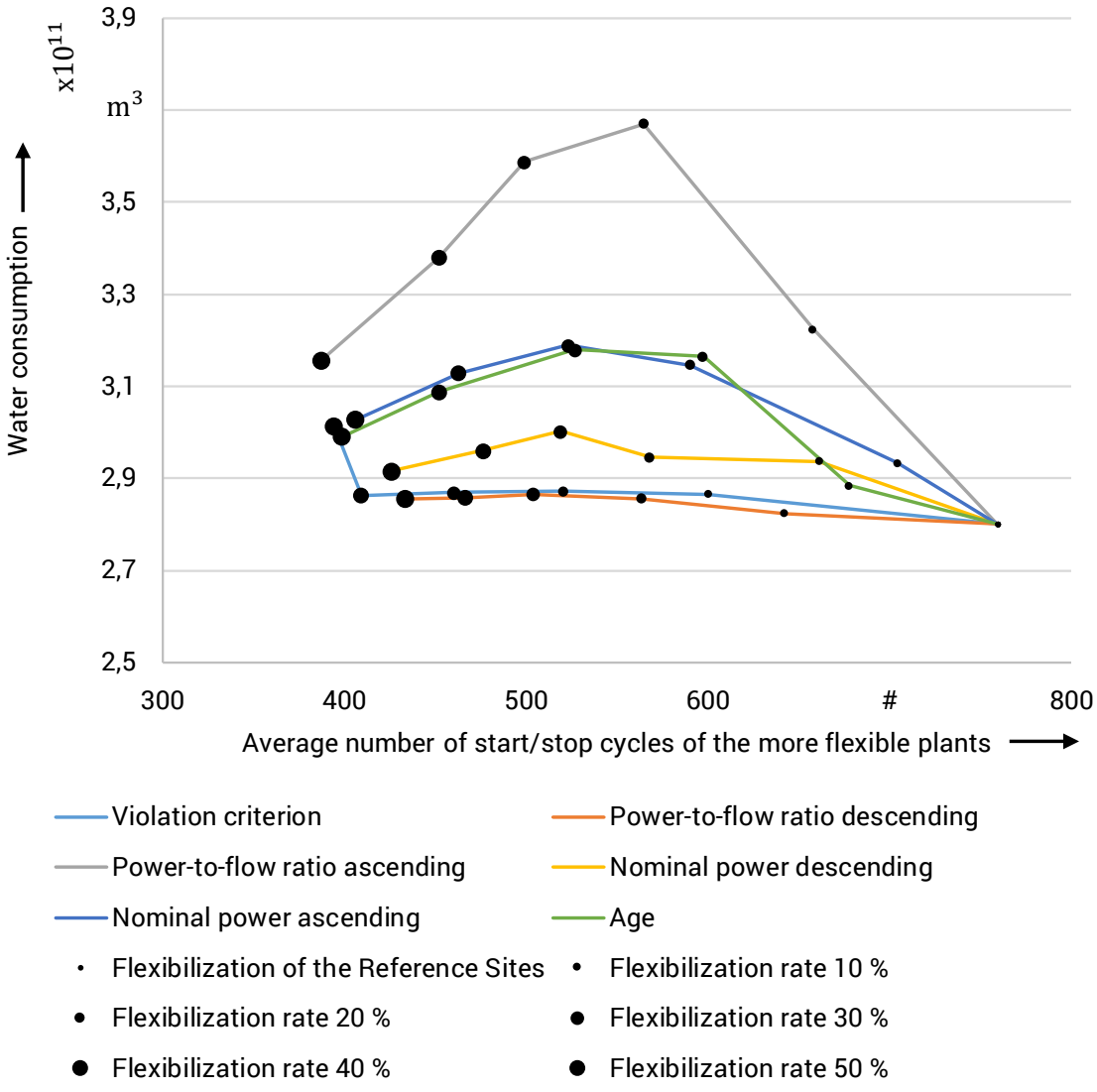

Figure 72: Water consumption and average number of total cycles of the more flexible plants per year for different flexibilization criteria and flexibilization rates.

The figure shows that a lower rate of flexibilization leads to a higher utilization of the more flexible plants. The higher the rate of flexibilization is chosen, the more plants are used to cover the base load at low load fluctuations. This leads to a lower utilization of the more flexible plants and reduces the average number of start/stop cycles of the more flexible plants. The highest utilization of the more flexible plants with simultaneously low water consumption is thus achieved with the sole flexibilization of the reference sites. However, an increase in the rate of flexibilization could reduce the number of operating violations and the less flexible plants could

be used to a large extent only to cover the base load, which could contribute to a slower technical aging of the less flexible plants. When looking at the water consumption, it becomes apparent that it is highest for almost all flexibilization criteria at a flexibilization rate between 20 % and 40 %. Only in the criterion where the most efficient plants are made more flexible (P-/Q˙ ratio - descending), the water consumption is almost constant for all flexibilization rates. Since not only efficient plants are made more flexible in the other criteria, but these are very frequently used in the case of high load fluctuations at a flexibilization rate of up to 40 %, water consumption increases by up to 20 % at flexibilization rates between 20 % and 40 %. At a flexibilization rate below 20 %, the share of inefficient flexibilized plants is comparatively low, so the selection of the plants to be flexibilized does not have a strong impact on water consumption. At a flexibilization rate of more than 40 %, the water consumption and the number of total cycles of the more flexible plants are reduced again and are equalized for the different flexibility criteria, as the same plants are increasingly flexibilized and the inefficient flexibilized plants are only used in case of excessive load fluctuations or full load.

4.5.2 Comparison of the results of the pre-defined scenarios

This section examines how the scenario framework affects the operation of flexible and inflexible hydropower plants. In addition, the influence of the simulation year is checked. The comparison of the scenarios is carried out exemplarily for a minimum operating time or minimum downtime of the more inflexible plants of two hours and a flexibilization of the Reference Sites, since this flexibilization offers an optimal utilization of the technology advantages by an efficient use of the available water, as investigated in the previous section. Since the number of start/stop cycles of the more flexible and inflexible plants is a measure of the utilization of the technology advantages of the flexibilized plants in the individual scenarios, the evaluation and comparison of the scenarios is carried out below on the basis of the number of start/stop cycles. First, the results of the Reference scenarios are compared for the considered years 2025, 2030 and 2040. Then, the results of the different scenarios are presented for the years 2030 and 2040.

Figure 73 shows the average number of start/stop cycles of the more flexible and less flexible plants of the individual bidding zones for the Reference Scenario for the observation years 2025, 2030 and 2040 as a box diagram. The box corresponds to the area where the middle 50% of the power changes are located. The line in the middle of the box describes the median of the data. The antennas are a measure of the outliers of the distribution. When considering the scenario over several future points in time, it is noticeable that the average number of start/stop cycles of the more flexible plants increases over the years in all bidding zones. This could be related to the increasing installed capacity of wind turbines in the individual bidding zones (c.f. Figure 65) as well as to the number of power changes described in section 4.4 (c.f. Figure 69), which are used as a measure for the flexibility demand.

Since there is only one flexibilized turbine in the bidding zone NO and the entire flexibility demand has to be covered by this turbine, the largest utilization of the flexibilization benefits results for this turbine with more than 1300 start/stop cycles in all years under consideration. The

spread of the number of start/stop cycles is indicated by the height of the respective boxes. This is lower for the flexibilized plants in the bidding zone NOs than in the bidding zone SE. Since the load fluctuations in NOs are mostly relatively high due to the exchanges to Central Europe and Great Britain described in section 4.4.2, the more flexible plants are often used at the same time, which could explain the lower dispersion. Furthermore, it is noticeable that the average number of start/stop cycles of the more flexible plants is lowest in the NOs bidding zone. On the one hand, this could be explained by the exchanges to Central Europe and Great Britain. However, the lower installed capacity of wind turbines compared to the bidding zone SE could also influence the number of start/stop cycles.

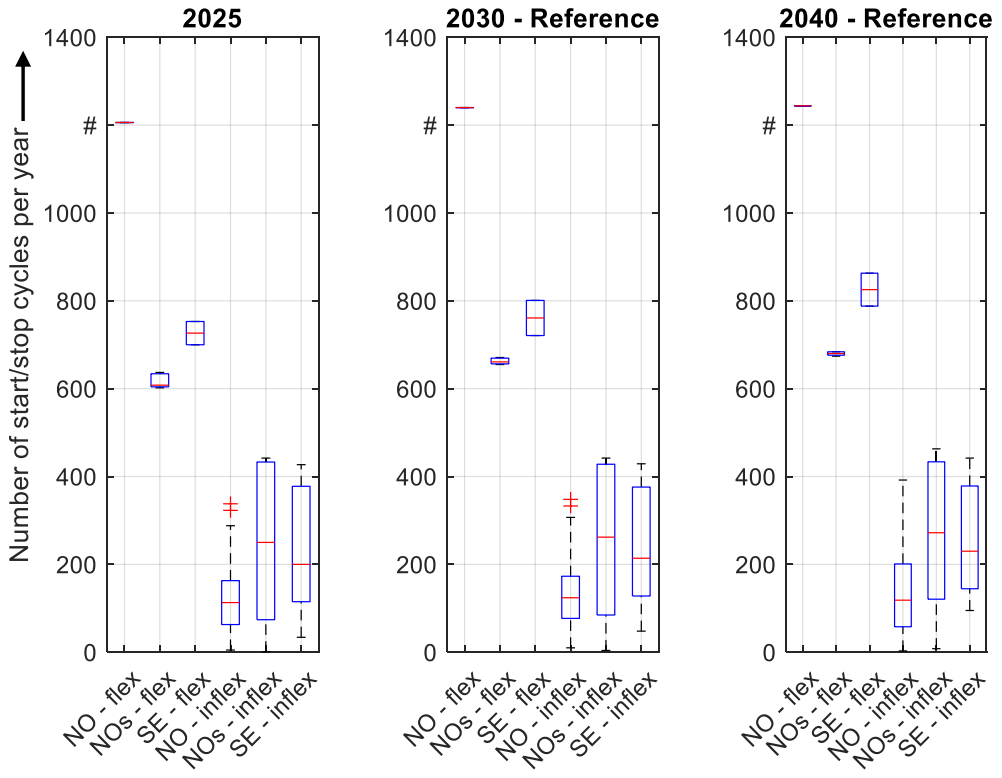

Figure 73: Number of start/stop cycles of the more flexible and less flexible plants in the Reference Scenario for different years of observation and bidding zones.

Regarding the more inflexible turbines, an increase of the average number of start/stop cycles from 2025 to 2040 can also be observed. However, the average number of start/stop cycles for these plants, with a median of around 200 cycles in all bidding zones considered, is many times lower than the number of start/stop cycles for the more flexible plants. However, it becomes apparent that in the future even the less flexible plants will not be used continuously to cover the base load, but will run one to two cycles per day in the summer months, mainly due to generation from PV plants in Central Europe and Great Britain.

In order to investigate the influence of different future potential parameters, the results of the predefined scenarios are compared in the following. When considering the Prosumer, Reference

and Green Hydro scenarios for the year 2030, only minor differences can be identified (c.f. Figure 74). The differences in the parameterization of the scenarios only have a minor impact on the hydropower plant utilization and the resulting number of start/stop cycles of the more flexible and less flexible plants for this year of observation. Only a more flexible use of the reference site in the bidding zone NO can be observed in the Green Hydro scenario compared to the other scenarios. Since the share of wind turbines is highest in this scenario, a connection between the share of wind turbines and the flexibility requirement can also be suspected.

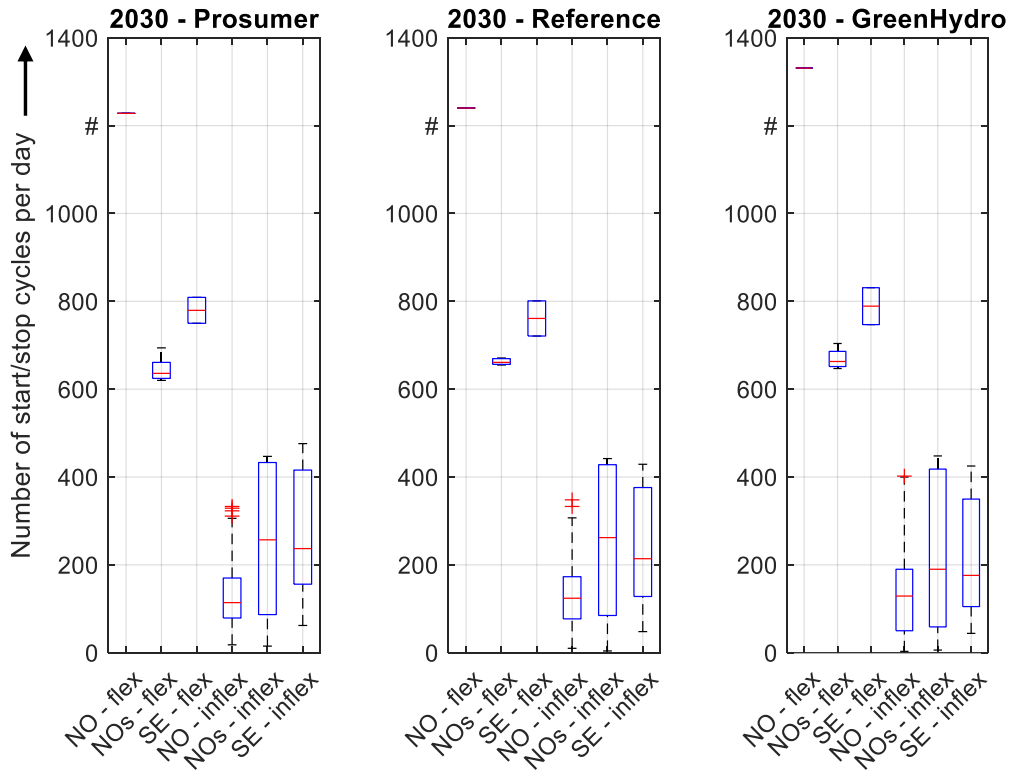

Figure 74: Number of start/stop cycles of the more flexible and less flexible plants of different scenarios and bidding zones for the observation year 2030.

Also, by comparing the results of the individual scenarios for the observation year 2040, no significant differences between the scenarios can be detected, analogous to the observation year 2030 (c.f. Figure 75). For both the more flexible and the less flexible plants, the average number of start/stop cycles only varies by about 100 between the scenarios.

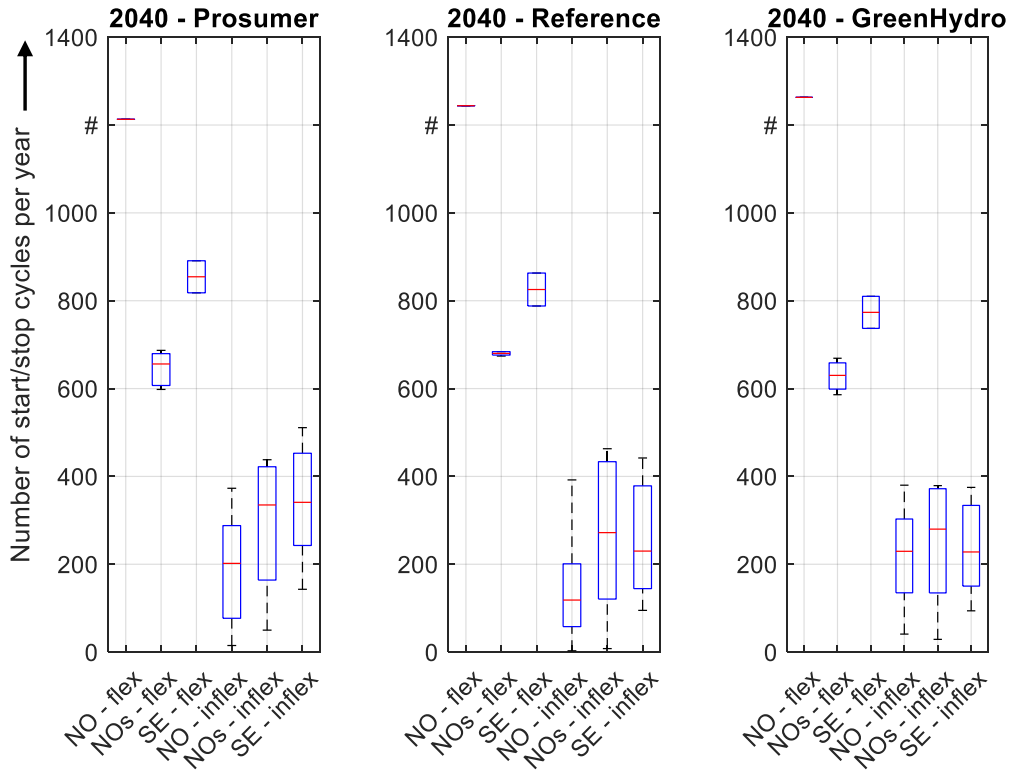

Figure 75: Number of start/stop cycles of the more flexible and less flexible plants of different scenarios and bidding zones for the observation year 2040.

The results of the hydropower plant deployment simulation in the Nordics show that the different characteristics and conditions of the individual scenarios have only a minor effect on the number of start/stop cycles of the plants. A flexibilization of hydropower plants, however, increases the number of start/stop cycles by a significant factor in all scenarios considered.

4.5.3 Flexibilization vs. no flexibilization

This section examines the extent to which flexibilization changes hydropower plant operations of both the flexibilized and not flexibilized plants as well as the advantages and disadvantages of flexibilization. For this purpose, the number of operational violations, the number of start/stop cycles of the less flexible plants and the water consumption are investigated. In the case with a partly flexibilization of the power plant park, only the Reference Sites are assumed to be flexibilized. For the more inflexible plants, a minimum operating time respectively a minimum downtime of two hours is assumed. For the parameterization, the Reference Scenario for the year of observation 2040 is chosen as an example. The total number of all operational violations for the respective bidding zones is compared in Figure 76 for the partially flexibilized and non-flexibilized power plant park.

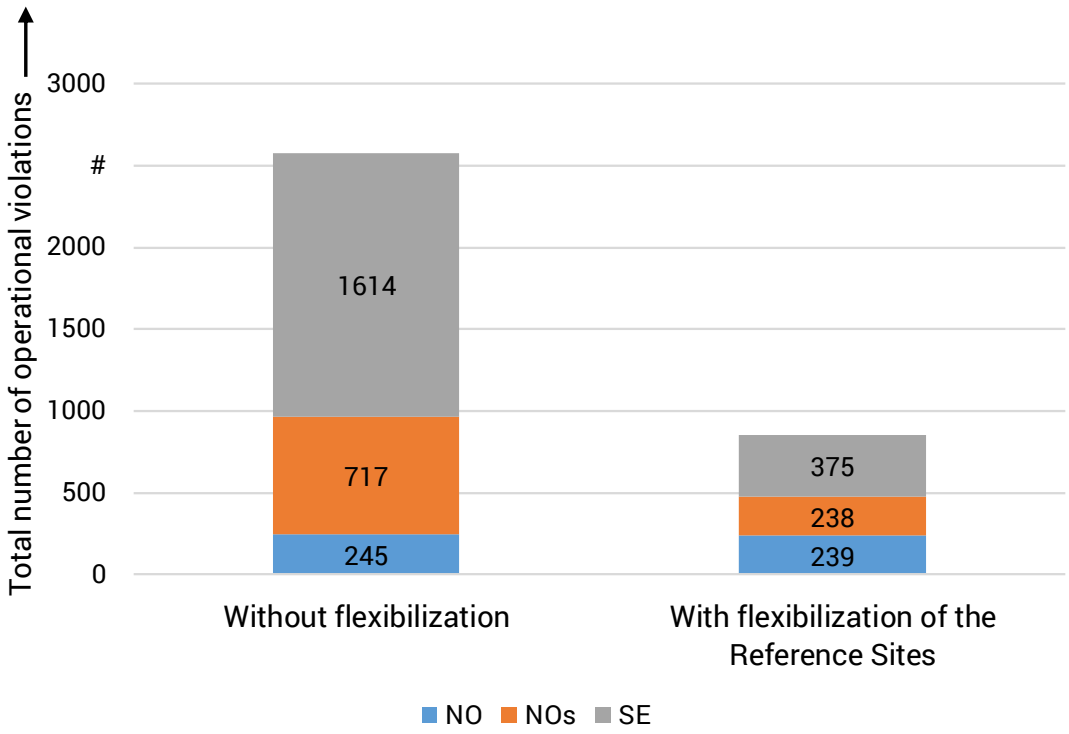

Figure 76: Total number of operational violations in the respective bidding zone for flexibilization of reference sites and no flexibilization.

The total number of all operational violations of the hydropower plants of the considered bidding zones in the case of no flexibilization with 2576 corresponds to about three times the total number of operational violations in the case of flexibilization of the reference sites with 852. The reduction of the operational violations becomes particularly clear in the bidding zones NOs and SE. Since the share of flexibilized plants is higher in these bidding zones than in NO (see Section 4.2), it can be derived that a higher flexibilization rate results in a lower number of operational violations, which is correlated to a slower aging of the plant.

In addition, Figure 77 shows the number of start/stop cycles of the less flexible plants per year for the case with flexibilization of the reference sites and the case without flexibilization as a box diagram. The graph shows that the number of start/stop cycles for inflexible plants is higher in the case without flexibilization than in the case with flexibilization in all bidding zones considered. In the bidding zone NO, the median number of start/stop cycles drops from 127 to 118.5, in NOs from 288.5 to 272 and in SE from 250 to 230. By flexibilizing the reference sites, the number of start/stop cycles of the less flexible plants can thus be reduced by more than 5 % on average in each bidding zone.

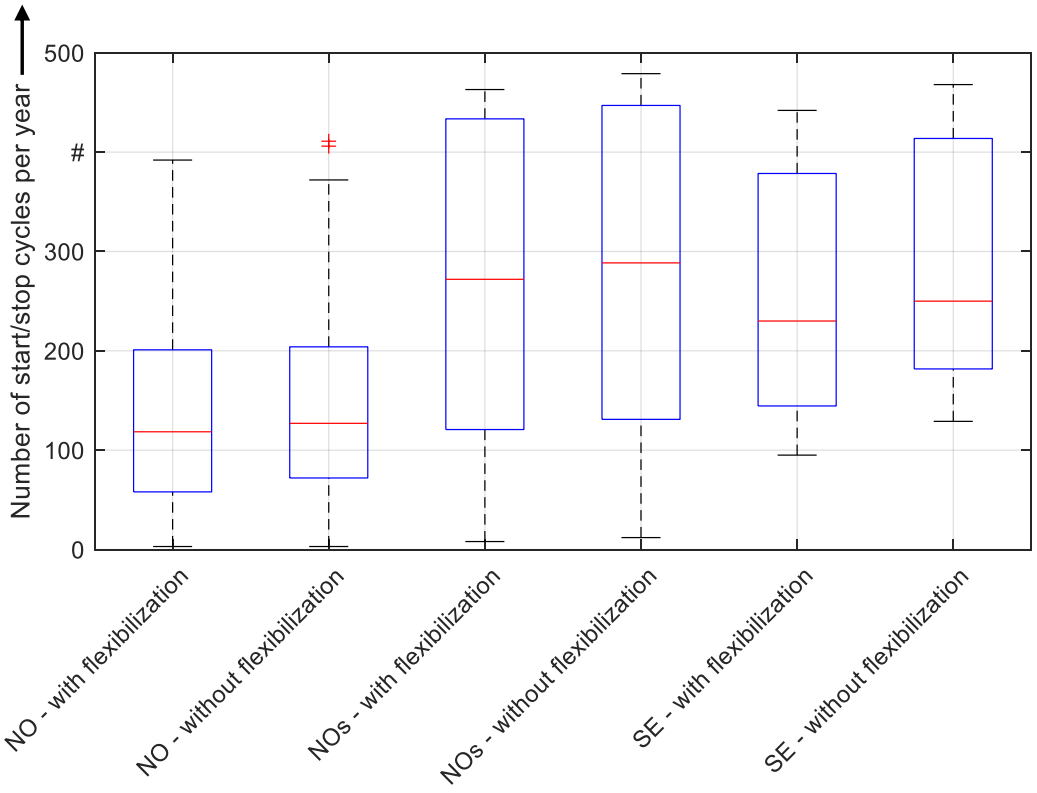

Figure 77: Comparison of the number of start/stop cycles of the less flexible plants with flexibilization of the reference sites and no flexibilization.

Since an increased number of start/stop cycles as well as the violation of minimum operating time and minimum downtime leads to a faster aging of the inflexible plants, the lifetime of the power plant park can be extended by flexibilization of a part of the considered hydropower plant park. However, under certain conditions, such flexibilization may lead to additional consumption of available water with identical efficiency of the plant, unless the flexibilized plants also represent the most efficient plants in the hydropower plant park. The total water consumption of all bidding zones over one year for the investigated cases in this section is illustrated in Figure 78. The additional consumption of available water when the Reference Sites are flexibilized is about 4 % compared to the case without flexibilization.

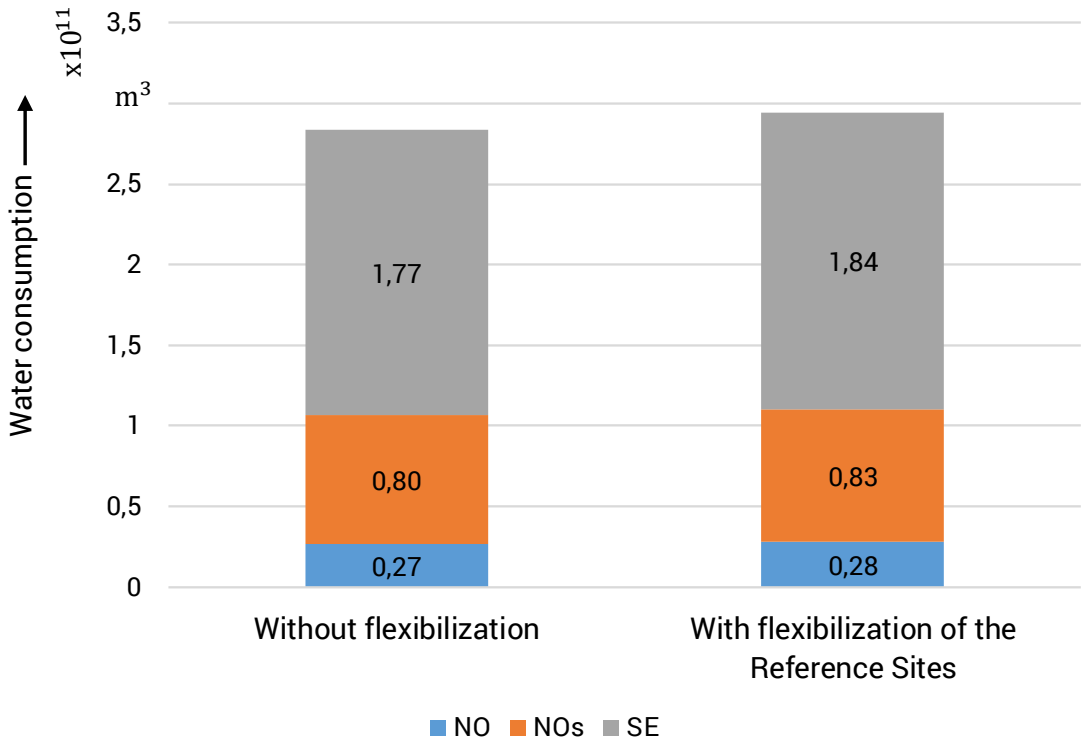

Figure 78: Water consumption of all bidding zones over one year with no flexibilization and with flexibilization of Reference Sites.

4.5.4 Sensitivity analysis

In section 4.4.1, a dependency between the generation from wind turbines and the flexibility demand in a bidding zone has already been suspected. This sensitivity analysis therefore examines the effect of a further expansion of wind turbines in Norway on the hydropower plant operation in the Nordics.For this purpose, the method developed in this study is applied to the Green Hydro scenario for the observation year 2040. An accelerated expansion of wind turbines in Norway is assumed according to a scenario in (Skar and et al.). The generation capacity of wind turbines in Norway in this sensitivity analysis is 28 GW instead of 10.44 GW (c.f. Figure 65, Green Hydro Scenario 2040 NO plus NOs) (Skar and et al.). A comparison of the resulting number of start/stop cycles of the more flexible and less flexible plants of the Green Hydro scenario and the sensitivity analysis for the year 2040 is shown as a box diagram in Figure 79.

Due to the further expansion of wind turbines in Norway, the number of start/stop cycles of the Reference Site in NO increases from approx. 1300 to approx. 2200. The average number of cycles of the less flexible turbines in NO also increases. However, the number of start /stop cycles of the more flexible plants in NOs remains almost unchanged. In the bidding zone SE, there are also no significant differences in the number of start/stop cycles for both the more flexible and the less flexible plants.

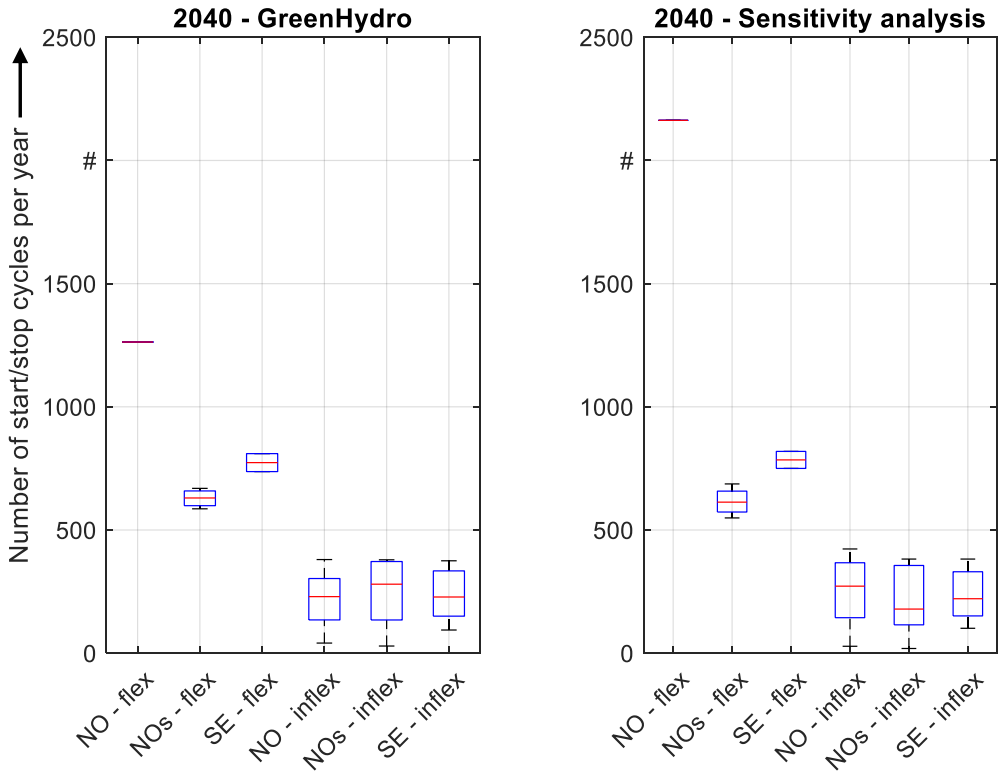

Figure 79: Number of start/stop cycles of the more flexible and less flexible plants of different bidding zones for the Green Hydro scenario and the sensitivity analysis for the observation year 2040.

To summarize, it becomes clear that the number of start/stop cycles of the more flexible plants and thus the need for flexibility increases in bidding zones with a high share of wind turbines. This effect is lower when the generation from PV plants of neighboring bidding zones influence the generation from hydropower plants of one's own bidding zone and the associated number of start/stop cycles of the more flexible plants is not too great, as is the case, for example, in the NOs bidding zone. Furthermore, it is noticeable that an expansion of wind power plants has hardly any effect on the number of start/stop cycles of the more flexible plants and the associated flexibility demand of a neighboring bidding zone.

4.6 Interim summary of results of the hydraulic unit commitment model

Due to the diversity of selectable input parameters and future scenarios, several investigations have been carried out regarding the overall method. First, various flexibilization criteria and flexibilization rates have been used to investigate which and how many hydropower plants need to be flexibilized in order to make optimal use of the technology advantages of the plants while minimizing overall water consumption. As a result, a flexibilization of the Reference Sites suits best and is therefore assumed for further investigations.

Then, it was analyzed how the scenario framework of the different predefined scenarios affects the operation of the flexible and inflexible hydropower plants. The comparison of the scenarios is carried out exemplary for a minimum operating time or minimum downtime of two hours and a flexibilization of the Reference Sites. Due to the described influence of the generation from PV plants of Central Europe and Great Britain on the generation from hydropower plants of the Nordics, the results of the market simulation, the first process step of th market based methodology, are relatively similar, which analogously results in a similar operation of the power plants in the hydraulic unit commitment model. Nevertheless, it is noticeable that the more flexible plants have a multiple of start/stop cycles compared to the less flexible plants. However, even the less flexible plants run one to two start/stop cycles per day in the summer months due to the influence of generation from PV plants in Central Europe and the UK.

In order to examine the extent to which a partly flexibilization of the hydropower plant park changes hydropower plant operations of both the flexibilized and not flexiblized plants, the simulation results for an assumed partial flexibilization of the Nordic power plant parks, in which the Reference Sites were flexibilized, are compared to the results of a simulation with no assumed flexibilization. The comparison has shown that a partly flexibilization of the hydropower plant park can reduce the operational violations of the less flexible plants by more than 60 %. In addition, the number of start/stop cycles of the less flexible plants is lower in the case of partial flexibilization. However, the water consumption in the case of partial flexibilization is about 4 % higher than in the case considered without flexibilization. With regard to slowing down the aging process of a power plant fleet, both the reduction in operational violations and the reduction in the start/stop cycles of the less flexible plants have a positive effect.

Finally, a sensitivity analysis was carried out in which the method was applied to a scenario with an increased expansion of wind turbines in Norway, as indicators for a dependency of the flexibility demand with the installed capacity of wind turbines in the respective bidding zones under consideration were identified in previous studies. In this analysis, a relation between an increased flexibility demand and an expansion of wind turbines in the same bidding zone could be found. However, the expansion of wind turbines has only a minor impact on the flexibility demand of neighboring bidding zones.

5 Investigation of frequency stability

This chapter contains the frequency stability investigation, which is performed by a time domain simulation to derive possible future flexibility needs in the Nordic power system. It is mainly divided into two parts: A validation of the models developed in this work and a frequency stability investigation carried out to the Nordic power system. In Section 5.1 the validation of the models established in Section 3.4, a standard parameterization of the water turbine model (cf. Figure 57) is first applied to the IEEE 39 bus system. Subsequently, Section 5.2 carries out a simulation of the Nordic power system.

As shortly explained in Section 3.1 a time domain simulation is only practicable for a short time period because of its high requirements of computional resources. Therefore, it is necessary to identify critical situations in grid operations, which may lead to frequency instabilities. These situations are given in grid operation with few operating rotating mass as synchronous generators and much electrical energy production by RES which are connected to the grid via converters. After identifying these situations different faults are applied to the power system and the resulting frequency series are analyzed.

5.1 Validation of investigation method

The dynamic response of the developed model firstly will be demonstrated using the "IEEE 39 bus system", which is often referred to in the literature as the "10-machine New-England Power System". For the validation, two different fault cases are considered. On the one hand, a generation deficit is modeled by a sudden load increase. On the other hand, a line failure is considered. The line failure represents the consequence of a short circuit on a line and the subsequent disconnection. Figure 80 illustrates the IEEE 39 bus system.

Hydropower plants with the basic configuration presented in Section 3.4.2 are connected to the grid via the ten synchronous generators. There are also 18 frequency-dependent loads on the grid, which are mapped using the exponential model, cf. Section 3.4.6. The nominal frequency is 60 Hz – in contrast to the nominal frequency of 50 Hz in the Nordic power system. However, this is not relevant for the following validation of the controller concept, as the display and evaluation of the results is carried out in the per unit system. Thus, the value 1 represents the nominal frequency. The sampling rate for the time domain simulation is 10 ms which is sufficient (Plassmann and Schulz 2013). Table 16 presents the parameters of the loads and generation units of the power system. The power flow calculation is based on the Newton-Raphson method (Schwab 2017).

Within the reference grid, a distinction is made between three different node types. Nodes 1 to 29 are defined as load or PQ nodes. Their active and reactive power is predefined. Nodes 30 to 39 are regulated or PV nodes. As can be seen from the name, the active power and the voltage are predefined at these nodes. In contrast, the phase angle and voltage are initially unknown. Generator 2 and the associated node 31 are defined as slack. For the reference node, the magnitude ($U = 1.0\,p.u.$) and phase angle of the voltage ($\theta = 0°$) are assumed to be known. The

power fed into the grid by generator 2 corresponds to the deficit still to be covered between generation and consumption, taking into account any losses. (Schwab 2017)

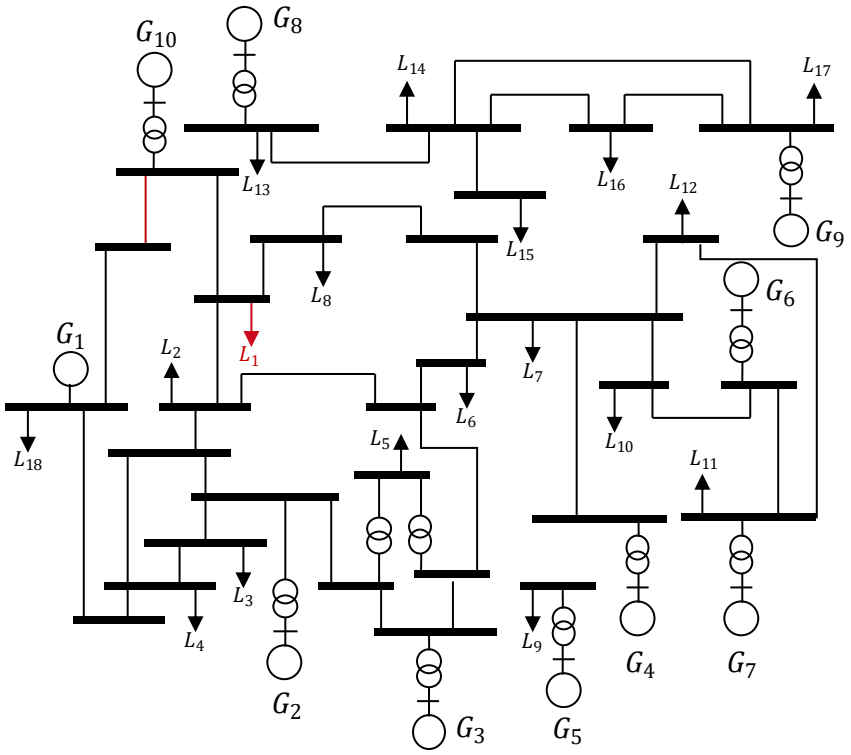

Figure 80: IEEE 39 bus system (IEEE Transactions on Automatic Control 2014).

5.1.1 Deficit in production

After completion of the power flow calculation, a dynamic simulation of the power system starts at time t = 0 s. Due to the selected initial states of the differential-algebraic equation system, no transient processes result. At time t = 1 s, there is a load increase at load 1, shown in red in Figure 80, by 400 % to 1610 MW. In the following, there is a generation deficit in the entire synchronous grid system.

Figure 81 shows the angular frequency in the power system at the 18 loads. The relationship between the angular frequency of the synchronous generators and the grid frequency can be seen via the connection described in Section 3.4.1.1. On average, the grid frequency corresponds to the rotor angular speed of the synchronous machines connected to the respective node. The frequency decreases within the first seconds and recovers to a steady state at the end of the simulation. As an example, the frequency curve of the loads is examined in more detail at this point: The local angular frequency at load 1 drops particularly sharply. At this node, there is the highest generation deficit, which cannot be covered instantaneously by the generation units.

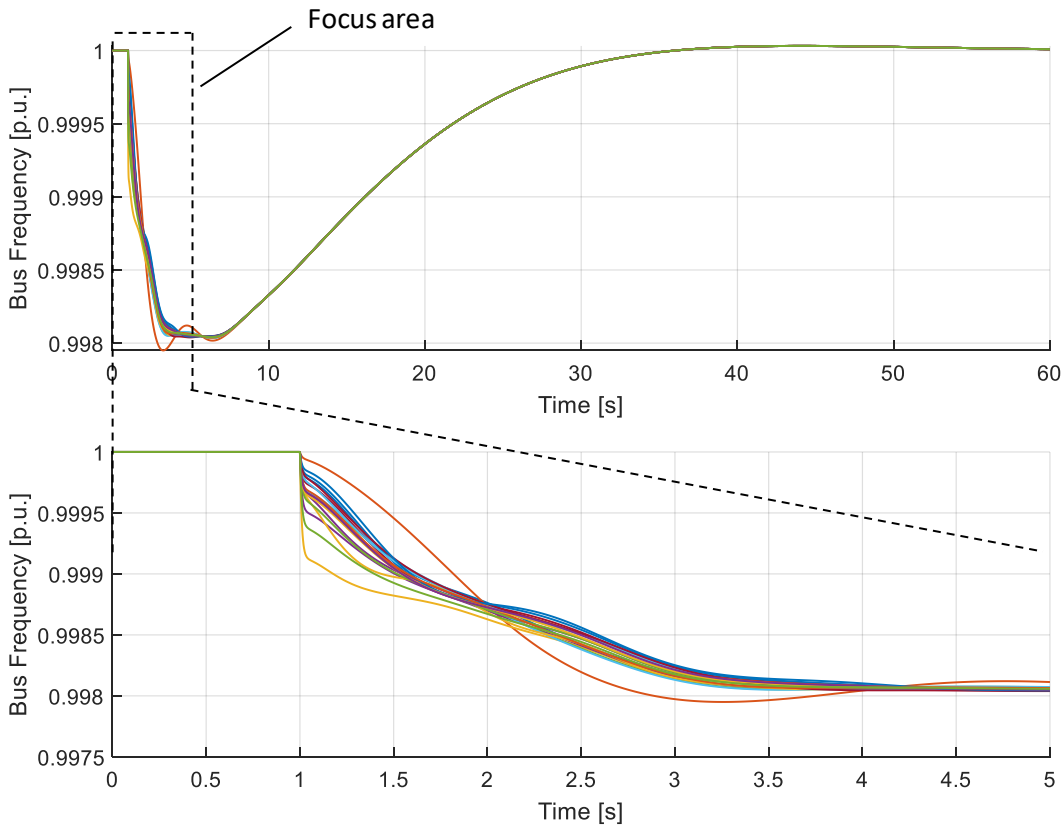

Figure 81: Frequency response after load increase.

5.1.2 Line Outage

In the following, a line failure marked in red in Figure 80 after one second is considered. Similarly, Figure 82 shows the course of the angular frequency over time.

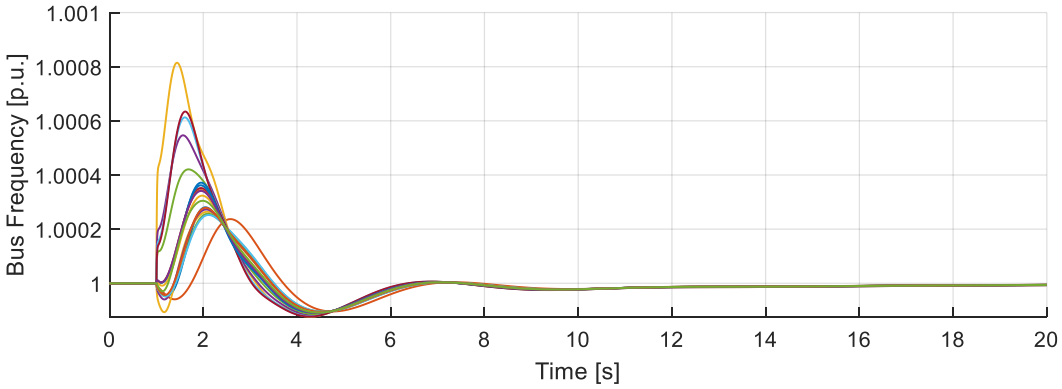

Figure 82: Frequency response after line outage.

An ambivalent frequency curve can be seen. While the local frequency at a few loads initially increases at the time of the line failure, the frequency at other loads decreases. An explanation for this is that the line failure changes the network topology, which leads to a shift in the load flow. At the load nodes, which have a close galvanic coupling to the generation units, there is a generation surplus shortly after the line failure. The mechanical (turbine) power exceeds the electrical power consumed by the loads. Meanwhile, a generation deficit results immediately at poorly coupled load nodes. Due to the relatively weak meshing, the supply to the loads is no longer guaranteed. At the time of the line failure, the active power demand exceeds the active power supply at these nodes. Overall, frequency oscillations can be seen over the course of time. The speed control regulates continuously and tracks the feed-in of the frequency change. In summary, the frequency curve can be validated by considering the transients resulting from a generation deficit or line failure.

Finally, Figure 83 compares the quasi-stationary behaviour for both fault cases. The observation period is 60 seconds. The mean value of the local frequencies of the load buses is plotted. In accordance with the previous explanations, a load increase of 400 % at load 1 and a line failure are considered at the time of the fault at t = 1 s. The load increase is then compared with the line failure.

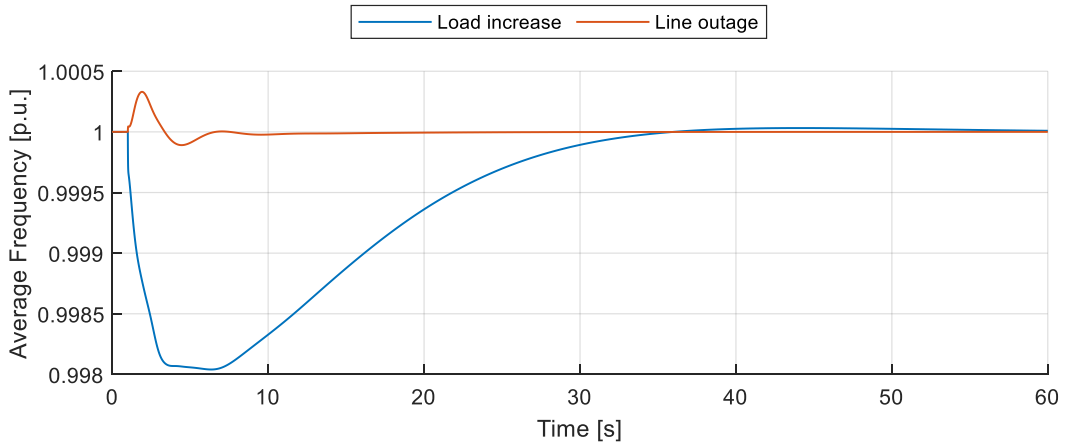

Figure 83: Quasi-stationary behaviour after load increase or line failure.

A comparison of the frequency curves shows that there is an underfrequency from the load increase in the period between 1 and approx. 36 seconds. The maximum frequency deviation is present at approx. 8 seconds. This can be explained by the existing generation deficit and the resulting loss of kinetic energy of the synchronous generators. In the further course, the controller increases the mechanical power input to the generator and accelerates the rotor so that the frequency increases. At approx. 36 seconds the frequency is at nominal frequency for the first time, but overshoots it in the further course until it reaches and stays at the nominal frequency. In contrast, the frequency oscillates in the event of a line failure in the period between

one and approx. twelve seconds, whereby the local maxima of the oscillation at t = 2 s represent an overfrequency. After twelve seconds a quasi-stationary state is reached.

5.1.3 Comparison of the power plant configurations

A typical problem of field measurements is the identification of a representative object of investigation - in this case a representative hydropower plant (Saarinen 2015). Different parameterizations strongly influence the change of the valve position and thus the mechanical power in response to frequency deviations. The gain factors of the integrative link (K_i) and the proportional link (K_p), as well as the time constant of the inlet servo motor (T_G) and the static (R_p), which have been explained in detail in Section 3.4.2.2.

In the following, three simulations are performed to consider the effects on the frequency response, when the electrical feed-in power and the mechanical power plant output if the generation units of the IEEE 39 bus system only consist of hydropower plants of only one configuration listed below for each simulation to validate their behavior according to their parametrization. Table 14 shows the different configurations.

Table 14: Parameter configurations of the different power plants

Parameters	Configuration 1	Configuration 2	Configuration 3
K_I	0.417	0.2	0.24
K_P	2.0	3.0	1.2
T_G	0.3	0.15	0.3
R_P	0.04	0.06	0.06

At time t = 1 s, there is a load increase at load 1 by 400 % to 1610 MW and the average frequency in the grid is considered. Figure 84 first shows the grid frequency over time. The local frequencies have been normalized to their mean value in order to represent the average frequency prevailing in the network. For all power plant configurations, the frequency is decreasing for the first seconds after the fault. The power supply is dominated by the instantaneous reserve during this period. The characteristic time behaviour of the individual power plant configurations modelled can be observed after this period: As time progresses, three different frequency characteristics emerge. A comparison of the extremes shows that the global minimum frequency of power plant 1 is above that of power plant 2 and power plant 3. This can be explained by the lower time constant of the gate. The frequency deviation of configuration 1 is lower than of configuration 3 because of the higher proportional and integral gain. After about 100 seconds, a new stable operating point at a frequency of 1 p.u. is reached. Comparing the three power plant configurations shown, the second has the fastest step response and the lowest global minimum but takes longer to reach a state near the nominal frequecy.

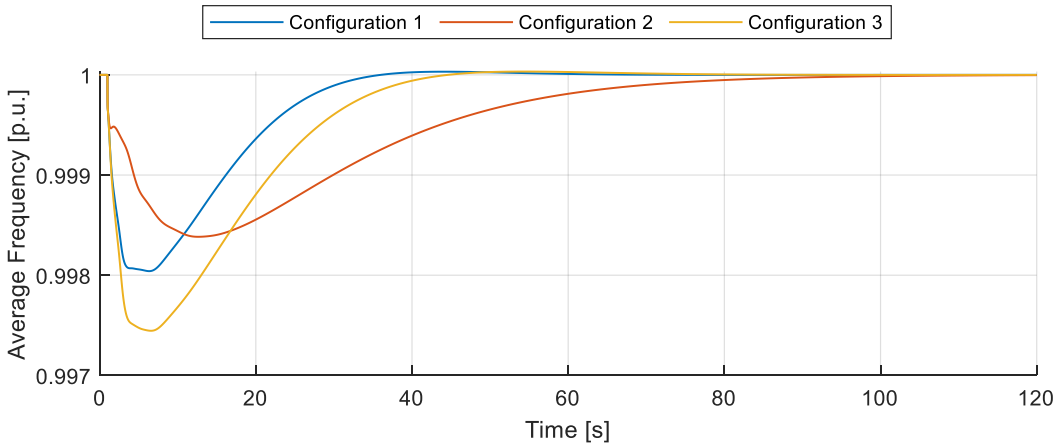

Figure 84: Frequency of power plant configurations 1-3.

For a more detailed understanding of the connection between the generation deficit and the frequency curve, the mechanical power and the electrical power are shown in Figure 85. Both quantities are normalized to the base power of 100 MVA and summarized over the 10 power plants.

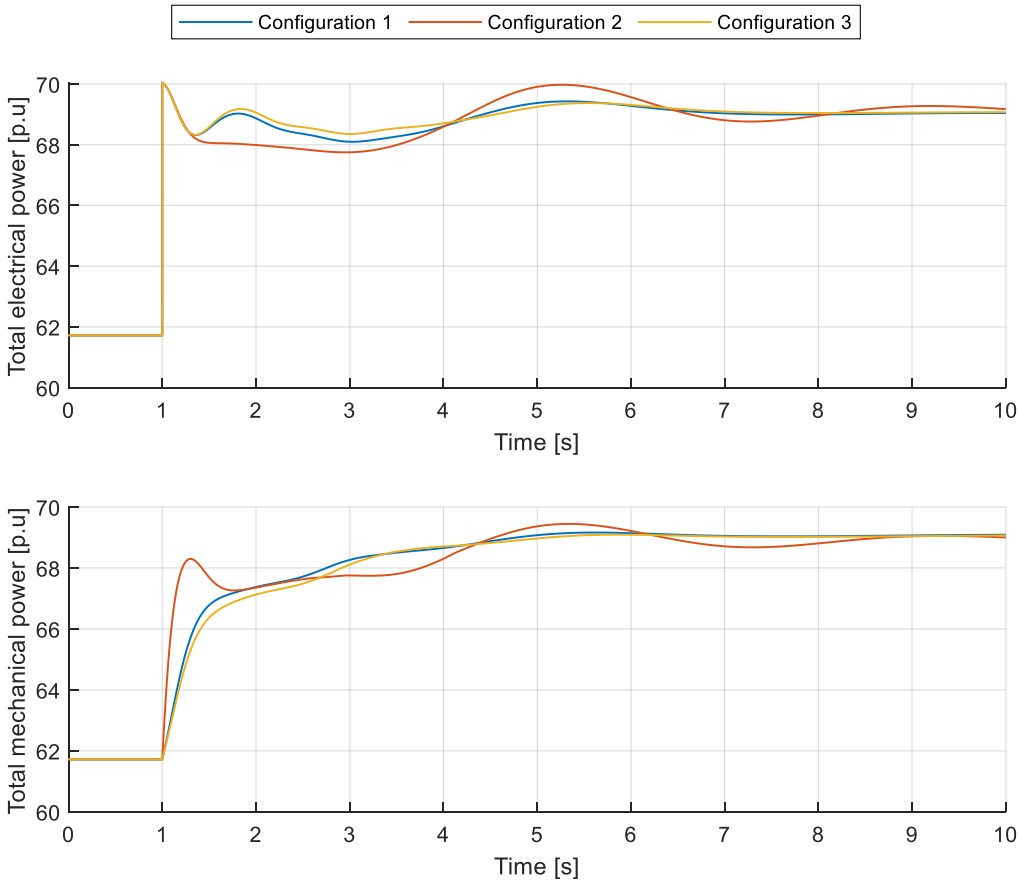

Figure 85: Mechanical and electrical output of power plant configurations 1-3.

At the time of the fault, the electrical power jumps instantaneously to 113.5 % of the initial state. In the further course, the electrical power oscillates and decreases, which can be explained by the frequency dependence of the load hence the load power decreases with falling frequency. The mechanical turbine power rises not as much as the electrical power which explaines the decreasing rotor speed: the electrical energy is drawn from the kinetic energy of the rotor. In the further course of time, the mechanical power is successively increased, but remains below the electrical power during the time range considered in Figure 85. Depending on their time constants, the power plants can increase their turbine output at different rates.

If the previously analyzed frequency curve is taken into account, this picture can be verified. Figure 86 shows the ratio of mechanical to electrical power. If the electrical power exceeds the generated mechanical power, the frequency drops (cf. Section 2.2.2). In the steady state, the ratio is 1, as the efficiency is not taken into account. There is no change in the frequency.

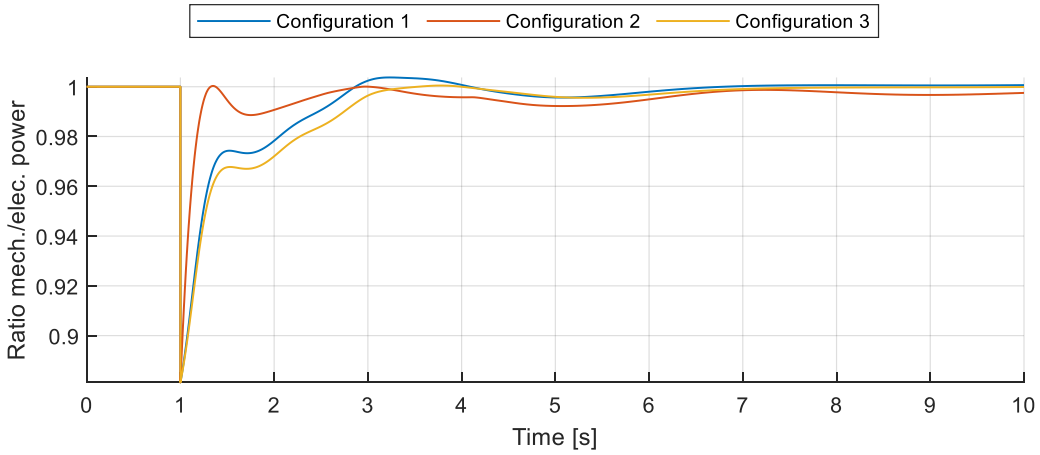

Figure 86: Ratio of mechanical power to electrical power.

Up to approx. three seconds, the frequency at at configurations 1 and 3 is at or below the frequency curve resulting from power plant configuration 2. In the further course, the mechanical power provided at configuration 1 in the period under consideration exceeds that of the other two power plant configurations. For all power plant configurations, the ratio is approx. 1 from a certain point in time. It is valid that power plant configuration 2 leads to a faster mechanical power increase than the other two power plants because of its lower gate time constant and that power plant configuration 1 leads to the highest ratio at a point after three seconds because of its higher integrative gain compared to power plant 1 and 2.

You can draw the conclusion that the models presented in Section 3.4 show a plausible behavior for different types of faults (generation deficit by load increase and power flow shift by line outage) and for different parametrizations. The next section carries out the simulations from the IEEE 39 bus system to the Nordic transmission grid.

5.2 Frequency stability investigation in NORDEL grid

In the following section, different fault scenarios and their effects on frequency stability and possible flexibility needs in the Nordic transmission grid are analysed. Since HVDC transmission capacities today are available only for scheduled energy transmission, the investigations do not include power systems which are connected to the Nordic transmission system via HVDC.

To derive possible flexibility needs in the future, to different relevant scenarios from view of the frequency stability are investigated: First, a model of the power plant park of the Nordic power system is chosen to represent power system as it is today. Second, the nuclear power plants are phased out and replaced by wind power plants.

Figure 87 shows the geographical locations of the reference sites in the Nordic transmission grid. The voltage levels of the transmission grid are highlighted in colour: Red colour symbolises 380 kV, blue colour 330 kV and green 220 kV. In addition, the fault locations investigated in the further course are drawn in. Five hydropower plants with specific parametrizations provided by the plant operators, have been chosen as reference sites within this project: Bratsberg, Kvilldal, Lysebotn 2, Porjus and Stornorrfors.

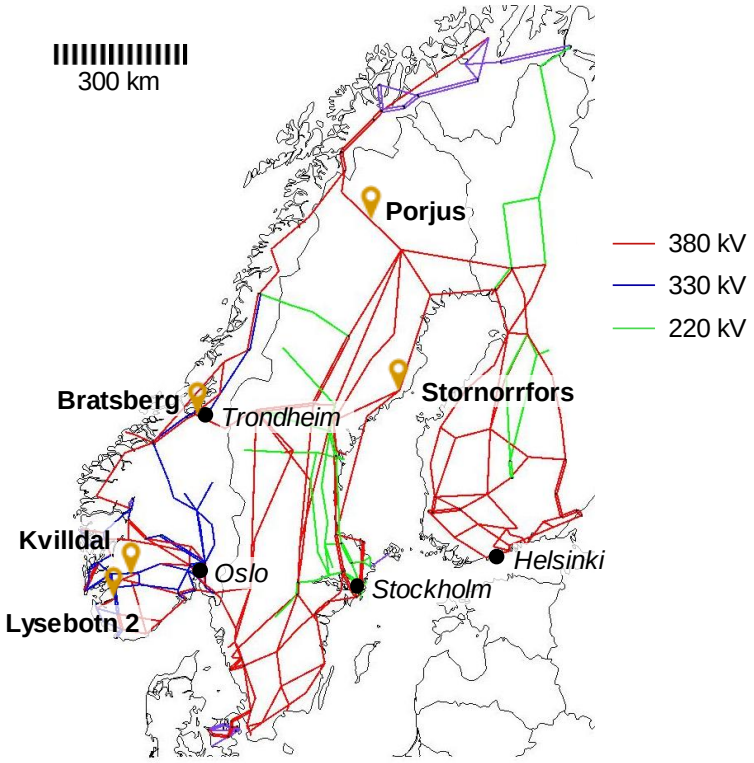

Figure 87: Geographical location of the reference sites.

In total, there are 1105 power plants in the IAEW grid model that is based on the TYNDP for the year 2030. 819 of these powerplants are generators coupled synchronously to the grid and 286 powerplants are based on RES. The associated synchronous generators are each equipped with an excitation system, a turbine and a governor and – except the reference sites – parametrized

corresponding to their nominal electrical power output as described in (Anderson 2002). Within the power plants with a power output of more than 20 MW, a division is made according to the generation technology, so that a distinction is made between 5 nuclear power plants, 6 coal power plants, 24 gas power plants, 12 oil power plants, 528 hydropower plants and 5 non-RES power plants without further classification. The feed-in of the power plants was taken from the results of the market simulation performed in Chapter 4. RES units as well as hydropower plants that are in pumping mode and consequently have a negative output from a grid perspective are modeled as constant power loads that do not provide any ancillary services in case of disturbances in the power to create worst-case scenarios from the point of frequency stability. Additionally, there are 244 real loads that are modeled as frequency-dependent loads. There are also 16 HVDC lines connected to the Nordic transmission system.

For the starting solution, the hour with the least synchronously coupled power plants from a night at the end of November was chosen. The total electrical energy production is 45.1 GW and the load is 44.2 GW. Therefore, the power loss of the electrical grid is approx. 0.9 GW. The is no infeed of PV power plants and the infeed of wind power plants is approx. 11.5 GW while the infeed of power plants with synchronous coupling to the grid is approx. 23.8 GW. The power output of the hydraulic power plants is 15.2 GW and the power output from thermal power plants is 8.6 GW. Table 15 shows the power import (in total: 9.8 GW) and export (in total: 3.1 GW) to the Nordic power system via HVDC. Positive values describe a power import to the Nordic power system while negative values describe a power export.

Table 15: Power import to the Nordic power system via HVDC

HVDC transmission line	Power import [MW]
DK-NO	1700
GB-NO 1	1400
GB-NO 2	1400
DE-NO	1400
NL-NO	700
DK-SE	740
LT-SE	-700
PL-SE	-600
DE-SE 1	615
DE-SE 2	700
EE-FI 1	-221
EE-FI 2	-393
Dannebo FS II	-800
Finnboele FS I	-400
Rauma FS 1	374
Rauma FS 2	771

The fault types investigated within this work are:

- Load increases
- Power plant outages
- Line outages
- Wind gusts

The location of the faults is chosen to cause the maximum amount of stress to the system and differs between the investigations. The objective is to evaluate the flexibility potentials of the reference power plants for different fault cases. First, three load increases within the Nordic power system are investigated. Stockholm for Sweden, Helsinki for Finland and Oslo for Norway, each as the most populous city, were chosen as representative locations (City Population). Afterwards power plant outages, line outages and wind gusts are applied to the grid as fault situations.

Each investigation is also carried out to a future Nordic power system where nuclear power plants are replaced by wind power plants. To investigate worst-case scenarios, the wind power plants are modeled as negative constant power loads without any ancillary services in case of disturbances in the power system.

Since the present work is dedicated to the investigation of frequency stability in the Nordic power system, primarily the frequency curves resulting from the faults that cause an imbalance between electrical energy production and consumption are analyzed. The objective is to enable a qualitative evaluation of the existing interactions in the grid and to derive possible flexibility needs in the future Nordic power system.

5.2.1 Load increase in load centers

Firstly, different load increases in load centers are investigate in the city of Stockholm, Oslo and Helsinki (only one load increase per simulation). After the simulation time of one second, the active power consumption in one of the load centers increases abruptly by 2050 MW which is equal to the dimensioning of the FCR-N and FCR-D in the Nordic power system. Figure 88 exemplary shows the frequency curves of the nodes to which the reference power plants are connected for a load increase in Stockholm until a steady state is reached. The solid line represents the status quo and the dashed line the future Nordic power system.

The frequency at the nodes of the reference power plants shows a similar curve with a few deviations depending on the electrical distance to the fault location for each scenario. The minimal frequency is approx. 49.53 Hz for the status quo and 49.52 Hz for the future scenario, respectively and the steady state frequency is approx. 49.98 Hz for both scenarios. The frequency is more oscillating in case of the future scenario because of the lower damping and has a lower nadir because of the lower rotating mass after the phase out of the nuclear power plants. But in the given situation the (mostly) hydraulic power plants operating are able to stabilize the power system in a similar manner. The comparison between the status quo and the future scenario

shows that there is no need for additional flexibility to maintain the frequency stable in case of disturbances in the Nordic power system caused by a generation deficit of 2050 MW.

The frequency series of the reference sites for load increases in Oslo and Helsinki are not displayed here because of their very similar curves and can be found in Figure 92 and Figure 93 in Appendix 1.

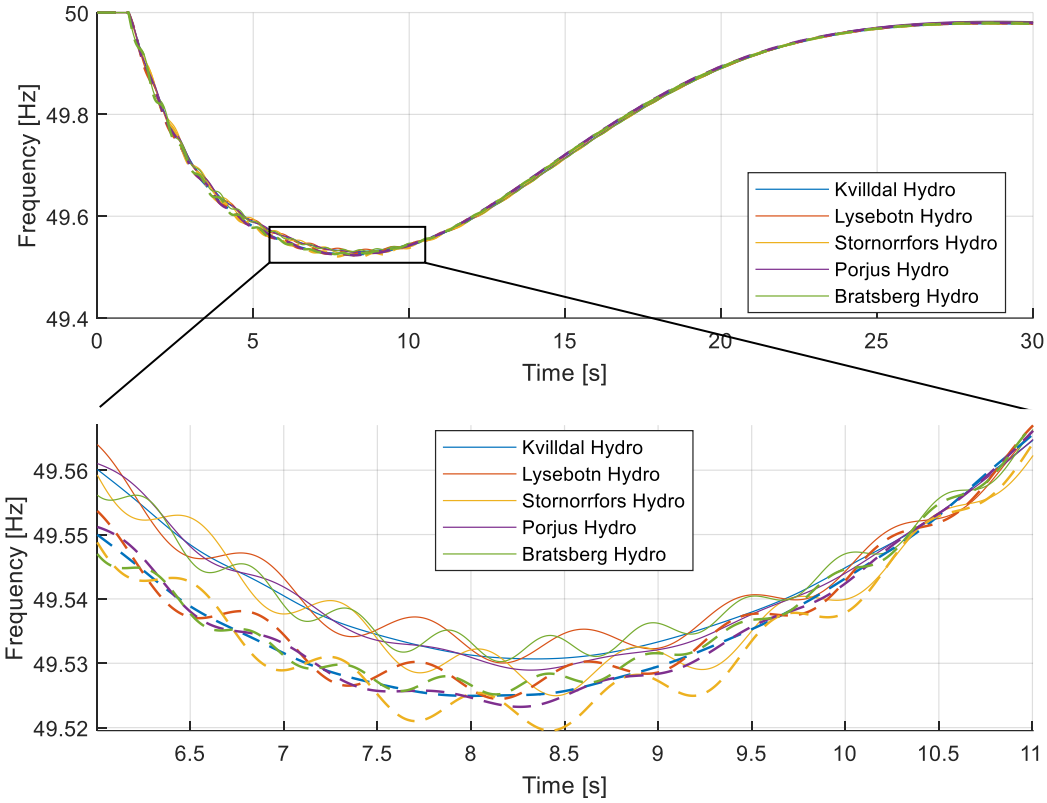

Figure 88: Frequency response after load increase in Stockholm.

5.2.2 Power plant outage

Besides a generation deficit by increasing loads, a generation deficit can be caused by power plant outages. The following investigation considers a multiple hydropower plant outage within the Nordic power system at the power plants of Värme power plant, Naturkraft CCPP gas power plant and Harsprånget hydropower plant for both the status quo and the future scenario. Their total power infeed in the given starting solution is approx. 1500 MW. After one second, the outages occur. Figure 89 shows the local frequencies of the reference sites.

The frequency nadir is reached at 49.65 Hz after approx. 8.5 seconds for the status quo (solid line) and in the future scenario (dashed line). The frequency reaches steady state after 40 seconds with a value of 49.98 Hz. This investigation shows that even a multiple power plant outage of Norwegian hydropower plants does not endanger frequency stability in the Nordic power system for both scenarios under the given situation and modelling assumptions.

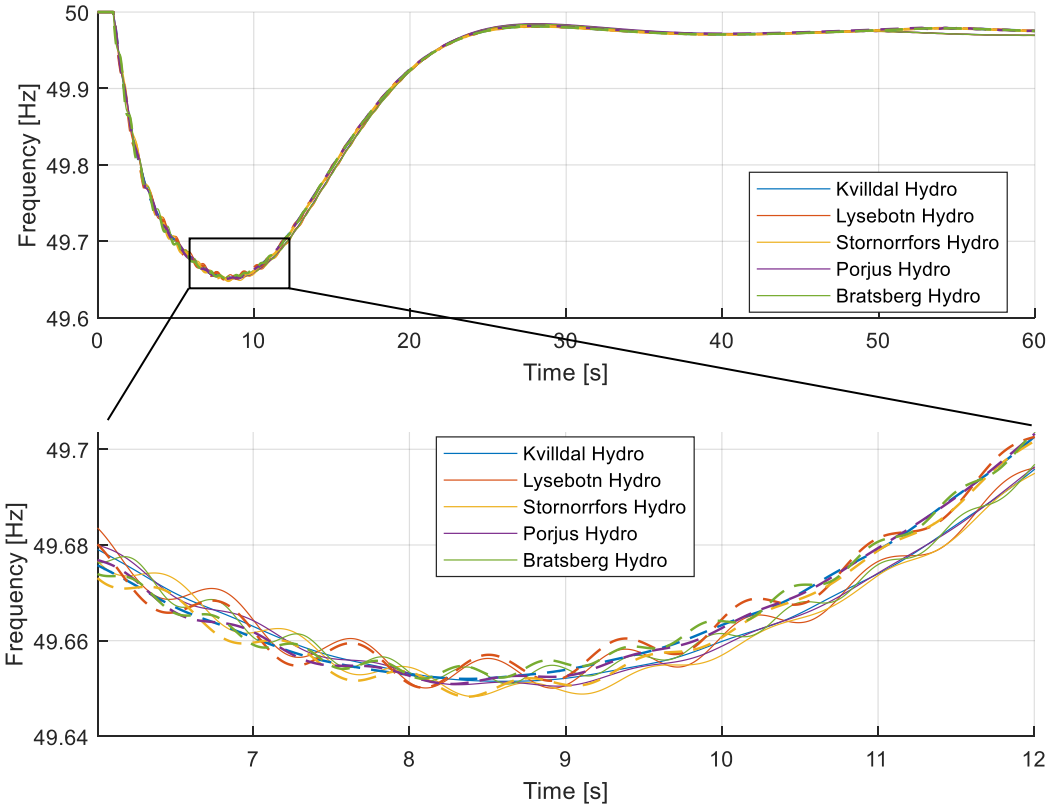

Figure 89: Frequency response after multiple power plant outage.

5.2.3 Wind gusts

In the following, an imbalance with a generation surplus caused by windgusts is investigated. On the south coast of Sweden (cf. Figure 87), there is a sudden increase in feed-in from wind turbines by 3000 MW. As a result, there is a generation surplus in the Nordic power system, the consequence of which is an overfrequency.

Figure 90 shows the frequency response for both scenarios, the status quo (solid lines) and the future scenario (dashed lines). The average grid frequency first increases after the wind gusts are applied after one second. This is plausible because the generation surplus resulting from the increased feed-in of the wind turbines is stored in the synchronous machines in the form of kinetic energy: Based on the results, it is clear that the average speed of the synchronous machines subsequently increases uniformly. After approx. 9 seconds the maximum frequency of approx. 50.83 Hz and 50.85 Hz is reached, respectively. This can be explained by the less rotating masses of the synchronous generators of nuclear power plants, which have been replaced by wind power plants. After 30 seconds a steady state is reached. At that point the average grid frequency is 50.00 Hz for both scenarios.

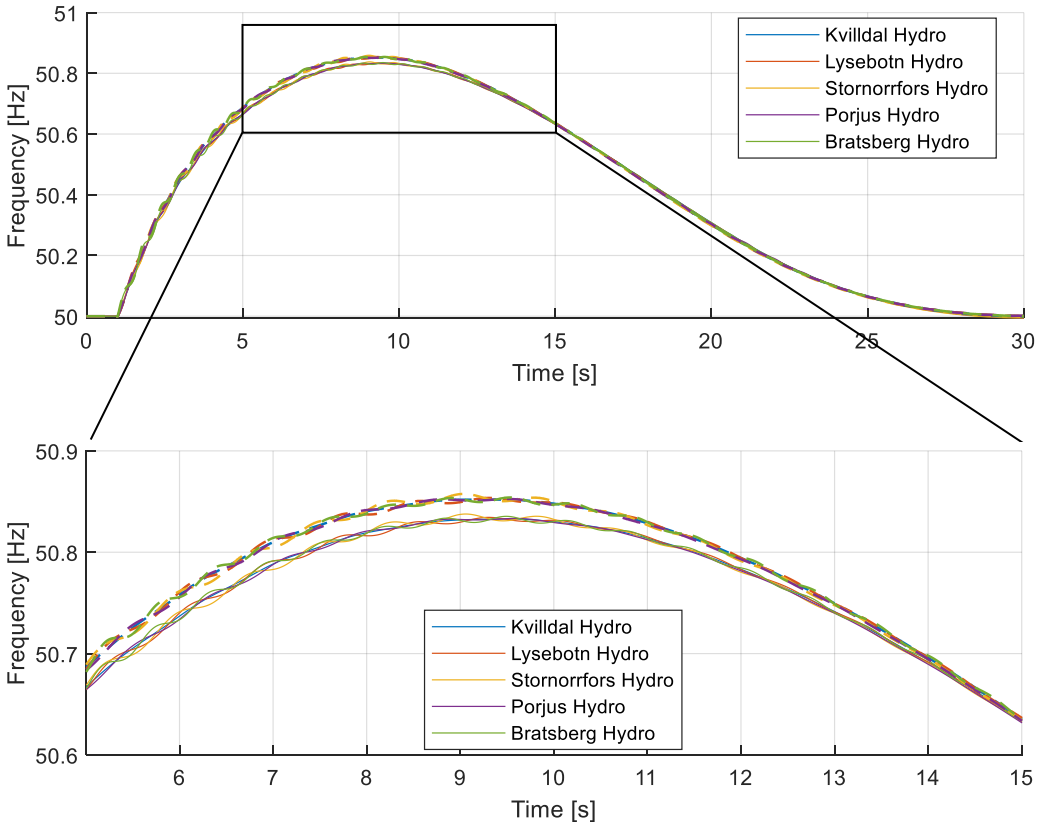

Figure 90: Frequency response during wind gusts.

The results of the time series for wind gusts as one possible type of disturbance, which causes a generating surplus in the power system, show that they can be handled in today's and the future scenario of the Nordic power system.

5.2.4 Line outage

Finally, a line failure in Norway is considered for both the status quo and the future scenario. The 380 kV line spanning between Trondheim and the connection node of the Nea hydropower has a length of 98.7 km and a rated line current of 2720 A. Several generation units are directly connected to the node of hydropower plant Nea. The changed network topology causes a new power flow and its consequences are investigated by the dynamic behavior of the reference sites. The line outage occurs after one second and is set back to operation after two seconds.

Figure 91 shows the local frequencies of the reference sites. The small oscillatory deviations from the nominal frequency can be explained by the spinning reserves going through a balancing process that is caused by the new power flow. After approx. five seconds the oscillations decay and the frequency at the nodes of the reference sites is set back to 50 Hz. In line of this line outage the frequency deviations for the future scenario are higher than for the status quo because of the less damping of wind power plants compared to nuclear power plants.

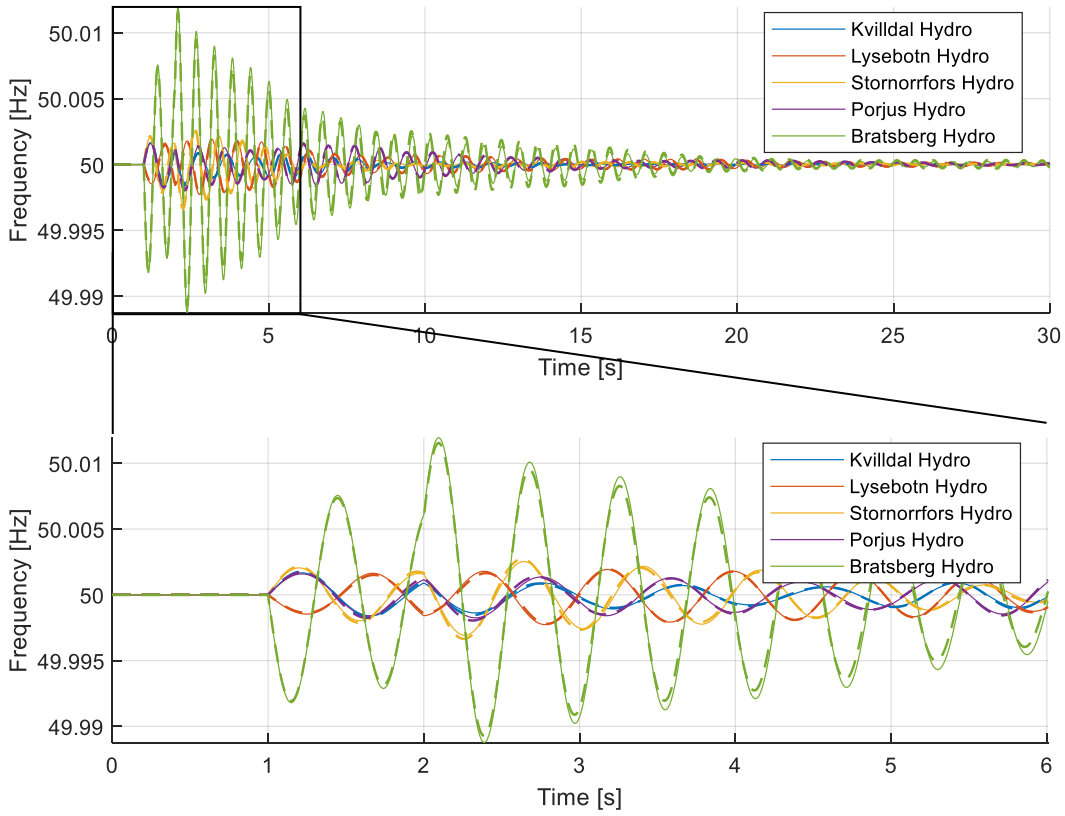

Figure 91: Frequency response after line outage.

You can draw the conclusion that this line outage is no threat to the frequency stability at all and therefore no additional flexibility in the Nordic power system for both the status quo and the future scenario.

5.3 Interim Summary

This chapter investigates the flexibility needs of the Nordic power system. At first, the governor model provided by the operators of the reference sites are tested with exemplary parametrizations and validated on the IEEE 39 bus system. The validation shows that the governor model and its parametrization are plausible. Within a second step the investigations were carried out to the Nordic power system for two different scenarios: for one scenario today's power plant park is considered and for the second scenario the nuclear power plants are substituted by RES. To create worst-case scenarios all RES power plants are connected to the grid as negative constant power loads that do not provide any ancillary services in case of disturbances in the power. Different types and locations of faults were applied to the power system and the scenarios are compared to each other. The investigations show that the deviation of the frequency from the nominal frequency is slightly higher and reached earlier which can be explained by the less spinning reserve because of the phase out of the nuclear power plants. Frequency stability within the Nordic power system is guaranteed for all load and fault situations in both scenarios considered and there is no need for additional flexibility for grid operation under the given assumptions and for the models used. To represent the dynamic behavior in a more detailed way it is necessary to use more detailed models of all power plants in the Nordic power system and speed governing systems of more than just the five reference sites that have been chosen for the HydroFlex project. Also, the impact of RES that are connected to the grid via converters and their dynamic behavior are neglected within this work.

6 Conclusion

In the context of climate change and the climate policy goals of the European Union (EU), the European power system is undergoing a structural transformation to a CO_2-neutral system. At the EU summit in December 2020 it was decided to reduce greenhouse gas emissions internally by at least 55 % net by 2030 compared to 1990 (European Council 2020). Accordingly, generation plants based on RES are increasingly replacing conventional thermal generation plants such as lignite and coal-fired power plants. The high volatility and difficult predictability of renewable energies – especially wind turbines and PV systems – pose a challenge for the design of the power system. In addition, some European countries such as Germany and Belgium are planning to phase out nuclear power by 2022 and 2025 respectively and replace the resulting loss of electricity generation with generation from RES. It is expected that this expansion will lead to an increased need for flexibility within the European power system due to the supply dependence of these generation plants. Furthermore, the increasing power feed-in via converters and the lack of synchronous coupling on the one hand, as well as the reduction of rotating masses in the grid on the other hand, change the dynamic behaviour of the grid. The stabilizing influence of the rotating masses on the grid frequency as a momentary reserve is lost, as RES that are connected to the grid via converters do not intrinsically contribute to power system stability (Forschungsverbund erneuerbare Energien 2014). Therefore, the objective of this guide is to identify and describe the demands hydropower plants will be confronted within future power systems. The focus is on identifying dynamic loads such as those resulting from providing high ramping rates and frequent start-stop cycles. In order to achieve this main objective, market simulations to analyse the time interval before physical fulfilment and stability simulations to analyse real-time operations are conducted.

To provide the necessary flexibility, different options are available, which provide flexibility in different ways. Hydro storage power plants, such as those in operation in the Nordic and the Alpine region, can provide flexibility both by adjusting generation and by shifting generation over time. In the case of pumped storage power plants, flexibility can also be provided on the consumer side for the power system. Another form of flexibility, as inertia and primary control reserve, is needed in case of disturbances in grid operation to keep the grid frequency near to its nominal frequency. Since the flexibility requirement is strongly dependent on the volatility of electricity generation from supply-dependent generation plants, the volatility of the generation time series from wind turbines and PV plants has been quantified using a method developed as part of the analysis. In order to ensure that the described flexibility represents a systemic added value for the entire European power system, it needs to be transferred from the Nordics to continental Europe via the existing HVDC links.

The used toolchain contains three parts in order to identify the demand for flexibility both before physical fulfillment and in real-time operations: A European power market simulation, grid operation simulations and time domain simulations to investigate frequency stability. The market-based method for simulating hydropower plant operations of highly complex hydropower plant

parks is divided into two steps in order to cope with the complexity and the amount of constraints which come with the simulation of interconnected hydropower plant parks. In the first step of the method, a market simulation is carried out with the objective of minimizing the power generation costs. In this market simulation, hydropower plants are aggregated in bidding zones with strongly interconnected hydropower plant parks. Furthermore, the market simulation is carried out in hourly temporal resolution to reduce the computing time. In the second step, a detailed quarter-hourly hydropower plant schedule is calculated based on the hydropower plant schedules from the market simulation, which were previously optimized in an aggregated manner due to the complexity. The hydropower plant park is disaggregated in this process step. The objective of this algorithm is the optimal operation of the plants with regard to their technical restrictions. In the third step, dynamic models follow to adequately represent the balancing processes that take place after a disturbance occured. Conventional generation units are modeled as coherent models of synchronous generator, excitation system, turbine and speed controller. The frequency dependence of the load is also taken into account.

In this study, the results of the market simulation have been analyzed with respect to the flexibility needs of the Nordics and Central Europe for different future scenarios. In this context, the power changes of the aggregated hydraulic time series of the Nordics have been used to evaluate the flexibility provision of the hydropower plants for the different scenarios. It was determined that the generation from PV systems in Central Europe and Great Britain, which capacity increases enourmous in the future scenarios, influences the hydropower plant operation in the Nordics. During the day, electricity in the Nordics is mainly imported to meet the demand in the Nordics itself, especially in the summer months, while at night the Nordics acts as an exporter. The number of power changes of the hydropower plants in the Nordics is therefore in most cases not more than two per day. Thus, the aggregated generation time series of the bidding zone NOs in the south of Norway, which has the strongest connection to the Central European countries and Great Britain, behaves similarly in all considered scenarios. As a result, the flexibility demand in the Nordics is only slightly higher due to this described behavior in comparison to the present operation from the spot market perspective.

Due to the diversity of selectable input parameters and future scenarios, several investigations have been carried out regarding the overall method. First, various flexibilization criteria and flexibilization rates have been used to investigate which and how many hydropower plants need to be flexibilized in order to make optimal use of the technology advantages of the plants while minimizing overall water consumption. As a result, a flexibilization of the Reference Sites suits best and is therefore assumed for further investigations.

Then, it was analyzed how the scenario framework of the different predefined scenarios affects the operation of the flexible and inflexible hydropower plants. First, the results of the hydraulic unit commitment model were relatively similar between the scenarios as already with the aggregated results. Due to the same reasons according to PV generation, the unit commitment of

individual hydropower plants did not differ much between scenarios. Nevertheless, it is noticeable that the more flexible plants have a multiple of start/stop cycles compared to the less flexible plants. However, even the less flexible plants run one to two start/stop cycles per day in the summer months.

Upon that, we investigated a partly flexibilization of the hydropower plant park. In this case, we assumed only the Reference Sites to be flexibilized. The comparison between another simulation run without any flexibilization showed that a partly flexibilization of the hydropower plant park can reduce the operational violations of the less flexible plants by more than 60 %. In addition, the number of start/stop cycles of the less flexible plants is lower in the case of partial flexibilization. With regard to slowing down the aging process of a power plant fleet, both the reduction in operational violations and the reduction in the start/stop cycles of the less flexible plants have a positive effect.

Finally, a sensitivity analysis by simulating another scenario with an increased expansion of wind turbines in Norway followed. Following previous studies, this analysis should investigate a possible relation between flexibility demand and wind turbines in the respective bidding zones. In this analysis, a relation between an increased flexibility demand and an expansion of wind turbines in the same bidding zone could be found. However, the expansion of wind turbines has only a minor impact on the flexibility demand of neighboring bidding zones.

To investigate the flexibility needs in the Nordic power system, time domain simulations were carried out. At first, the governor model provided by the operators of the reference sites are tested with exemplary parametrizations and validated on the IEEE 39 bus system. The validation shows that the governor model and its parametrization are valid. Within a second step the investigations were carried out to the Nordic power system for two different scenarios: For one scenario today's power plant park is considered and for the second scenario the nuclear power plants are substituted by RES. To create worst case scenarios all RES power plants are connected to the grid as negative constant power loads that do not provide any ancillary services in case of disturbances in the power system. Different types and locations of faults were applied to the power system and the scenarios are compared to each other. The investigations show that the deviation of the frequency from the nominal frequency is slightly higher and reached earlier which can be explained by the less spinning reserve because of the phase out of the nuclear power plants. Frequency stability within the Nordic power system is guaranteed for all load and fault situations in both scenarios considered and there is no need for additional flexibility for grid operation under the given assumptions and for the models used. To represent the dynamic behavior in a more detailed way it is necessary to use more detailed models of all power plants in the Nordic power system and speed governing systems of more than just the five reference sites that have been chosen for the HydroFlex project. Also, the impact of RES that are connected to the grid via converters and their dynamic behavior are neglected within this work.

Table of Figures

List of Tables

References

50 Hertz Transmission GmbH. “Hansa PowerBridge: Gleichstromverbindung Zwischen Deutschland Und Schweden.” Accessed September 01, 2019. https://www.50hertz.com/de/Netz/Netzentwicklung/ProjekteaufSee/HansaPowerBridge.

ABB. “HVDC Light (VSC).” Accessed September 02, 2019. https://new.abb.com/systems/hvdc/hvdc-light.

ABB. “Kontek: Zealand's Second International Interconnection.” Accessed September 01, 2019. https://new.abb.com/systems/hvdc/references/kontek.

ABB. “Konti-Skan: Konti-Skan HVDC Link Was the First Interconnection Between Sweden and the Western Grid in Denmark.” Accessed September 01, 2019. https://new.abb.com/systems/hvdc/references/konti-skan.

ABB. “Skagerrak: An Excellent Example of the Benefits That Can Be Achieved Through Interconnections.” Accessed September 01, 2019. https://new.abb.com/systems/hvdc/references/skagerrak.

Agricola, Annegret-Cl., Hannes Seidl, and Reemt Heuke. 2015. “Regelleistungserbringung Aus Dezentralen Energieanlagen: Analyse Des Weiteren Handlungsbedarfs Der Dena-Plattform Systemdienstleistungen.” Accessed July 14, 2019. https://www.dena.de/fileadmin/dena/Publikationen/PDFs/2018/9216_Regelleistungserbringung_aus_dezentralen_Energieanlagen.pdf.

Amprion GmbH. 2019. “Projektbeschreibung ALEGRO.” Accessed August 30, 2019. https://www.amprion.net/Netzausbau/Aktuelle-Projekte/ALEGrO-Deutschland-Belgien/.

Anderson, P. M. 2002. “Power System Control and Stability.” IEEE Press series on power engineering, Second edition, IEEE Press Wiley-Interscience; IEEE Xplore.

Anwar, Andre. 2016. “Deutschlands Vorbild Schweden Will Atomkraft Zurück.” Accessed August 30, 2019. https://rp-online.de/wirtschaft/unternehmen/deutschlands-vorbild-schweden-will-atomkraft-zurueck_aid-21470867.

Argonne National Laboratory. 2013. “Review of Existing HydroelectricTurbine-Governor Simulation Models.” Accessed April 04, 2021. https://ceeesa.es.anl.gov/projects/psh/ANL_DIS-13_05_Review_of_Existing_Hydro_and_PSH_Models.pdf.

Attikas, R. 2014. “Modelling of Control Systems and Optimal Operation of Power Units in Thermal Power Plants.”.

Barteczko, Agnieszka. 2018a. “Poland Expects First Nuclear Power Plant to Start in 2033.” 2018. Accessed August 30, 2019. https://www.reuters.com/article/us-poland-nuclear-power/poland-expects-first-nuclear-power-plant-to-start-in-2033-idUSKCN1NS1DB.

Barteczko, Agnieszka. 2018b. “Poland Plans New Coal Mine as Climate Talks Loom.” November 29. Accessed November 30, 2019. https://www.reuters.com/article/us-poland-energy-coal/poland-plans-new-coal-mine-as-climate-talks-loom-idUSKCN1NY1MT.

Boldea, Ion. 2016. *Synchronous Generators.* Second edition. Electric Generators Handbook. Boca Raton, Florida, London England, New York: CRC Press. http://search.ebscohost.com/login.aspx?direct=true&scope=site&db=nlebk&AN=1802592.

Bonfert, K. 1962. “Betriebsverhalten Der Synchronmaschine - Bedeutung Der Kenngrößen Für Planung Und Be-Trieb Elektrischer Anlagen Und Antriebe.”.

Bundesamt für Energie. 2015. “Kohle.” Accessed August 30, 2019. https://www.bfe.admin.ch/bfe/de/home/versorgung/fossile-energien/kohle.html.

Bundesamt für Energie. 2017. “Stromversorgung.” Accessed August 30, 2019. https://www.bfe.admin.ch/bfe/de/home/versorgung/stromversorgung.html.

Bundesnetzagentur. 2017. “Flexibilität Im Stromversorgungssystem: Bestandsaufnahme, Hemmnisse Und Ansätze Zur Verbesserten Erschließung Von Flexibilität.” Accessed July 15, 2019. https://www.bundesnetzagentur.de/SharedDocs/Downloads/DE/Sachgebiete/Energie/Unternehmen_Institutionen/NetzentwicklungUndSmartGrid/BNetzA_Flexibilitaetspapier.pdf?__blob=publicationFile&v=1.

Bundesnetzagentur für Elektrizität, Gas, Telekommunikation, Post und Eisenbahnen. 2019. "BBPlG, Vorhaben 33: Schleswig-Holstein – Südnorwegen (NordLink)." Accessed September 01, 2019. https://www.netzausbau.de/leitungsvorhaben/bbplg/33/de.html.

1999. "Bundesverfassungsgesetz Für Ein Atomfreies Österreich." In *Bundesgesetzblatt Für Die Republik Österreich*. Vol. 1999, 1161. https://www.ris.bka.gv.at/Dokumente/BgblPdf/1999_149_1/1999_149_1.pdf. Accessed August 30, 2019.

Cabbel, D. et al.M. 2004. "The New Thermal Governor Model Used in Operating and Planning Studies in WECC." IEEE Power Engineering Society General Meeting ISBN 0-7803-8465-2.

Chrisafis, Angelique. 2019. "France Failing to Tackle Climate Emergency, Report Says: Stark Warning Comes as UK Commits to Net Zero Emissions Target for 2050." Accessed August 22, 2019. https://www.theguardian.com/world/2019/jun/25/france-failing-on-climate-emergency-report.

City Population. "Population Statistics for Countries." http://www.citypopulation.de/.

"Climate Deal Makes Halving Carbon Emissions Feasible and Affordable." 2019. News release. June 28, 2019. Accessed August 28, 2019. https://www.government.nl/topics/climate-change/news/2019/06/28/climate-deal-makes-halving-carbon-emissions-feasible-and-affordable.

Concordia, C., and S. Ihara. 1982. "Load Representation in Power System Stability Studies." Bd. PAS-101, Heft 4. IEEE Transactions on Power Apparatus and Systems Print ISSN: 0018-9510.

Consentec. 2014. "Description of Load-Frequency Control Concept and Market for Control Reserves." https://www.consentec.de/wp-content/uploads/2014/08/Consentec_50Hertz_Regelleistung-smarkt_en__20140227.pdf.

Crastan, V. 2015. *Elektrische Energieversorgung.* 4., bearbeitete Auflage. Heidelberg: Springer Vieweg.

Crastan, V. 2017. *Elektrische Energieversorgung 2.* Berlin, Heidelberg: Springer Berlin Heidelberg,

Crastan, V., and D. Westermann. 2018. *Elektrische Energieversorgung 3.* Berlin, Heidelberg: Springer Berlin Heidelberg.

Cutsem, T., and C. Vournas. 1998. “Voltage Stability of Electric Power Systems.”.

Dena. 2016. “Momentanreserve 2030.” https://shop.dena.de/fileadmin/denashop/media/Downloads_Dateien/esd/9142_Studie_Mo-mentanreserve_2030.pdf.

Detering, M. 2018. “Wasserkraft.”.

Deutsche Botschaft Prag. 2019. “Wirtschaft: Umwelt- Und Energiepolitik.” Accessed August 30, 2019. https://prag.diplo.de/cz-de/themen/willkommen/laenderinfos/wirtschaft#content_2.

Deutsche-Presse-Agentur. 2019. “„Auf Gutem Weg“: Belgischer Außenminister Bekräftigt Atomausstieg Bis 2025.” Accessed August 22, 2019. https://www.aachener-zeitung.de/nrw-region/belgien/belgischer-aussenminister-bekraeftigt-atomausstieg-bis-2025_aid-37532895.

Directive (EU) 2018/2001 of the European Parliament and of the Council of 11 December 2018 on the Promotion of the Use of Energy from Renewable Sources. European Union. Abl. 82. 2018a. Accessed May 10, 2019. https://eur-lex.europa.eu/eli/dir/2018/2001/oj.

Directive (EU) 2018/2002 of the European Parliament and of the Council of 11 December 2018 Amending Directive 2012/27/EU on Energy Efficiency. European Union. Abl. 210. 2018b. Accessed May 10, 2019. https://eur-lex.europa.eu/eli/dir/2018/2002/oj.

Donadio, Rachel. 2011. “Italian Voters Come Out to Overturn Laws and Deliver a Rebuke to Berlusconi.” Accessed August 28, 2019. https://www.nytimes.com/2011/06/14/world/europe/14italy.html.

Drees, Tim. 2015. “Simulation des europäischen Binnenmarktes für Strom und Regelleistung bei hohem Anteil erneuerbarer Energien.” Dissertation, RWTH Aachen; Print Production M. Wolff GmbH.

DutchNews.nl. 2018. “VVD Leader Backs Nuclear Power to Solve Climate Problems.” Accessed August 28, 2019. https://www.dutchnews.nl/news/2018/11/vvd-leader-backs-nuclear-power-to-solve-climate-problems/.

ENTSO-E. 2013. “Network Code on Load-Frequency Control and Reserves.”.

ENTSO-E. 2018. “Statistical Factsheet 2018.” Accessed February 28, 2020. https://doc-store.entsoe.eu/Documents/Publications/Statistics/Factsheet/entsoe_sfs2018_web.pdf.

ENTSO-E. 2019. “ENTSO-E Transparency Platform: Actual Generation Per Generation Unit.” Accessed August 30, 2019. https://transparency.entsoe.eu/generation/r2/actualGenerationPerGenerationUnit/show.

European Commission. “International Action on Climate Change: Paris Agreement.” Accessed July 09, 2019. https://ec.europa.eu/clima/policies/international/negotiations/paris_de.

European Commission. 2014. “Framework for Climate & Energy 2030: Outcome of the October 2014 European Council.” Accessed February 28, 2020. https://ec.europa.eu/clima/sites/clima/files/strategies/2030/docs/2030_euco_conclusions_en.pdf.

European Commission. 2020. “Energy Statistical Datasheets.” Accessed February 19, 2020. https://ec.europa.eu/energy/sites/ener/files/energy_statistical_countrydatasheets.xlsx.

European Council. 2020. “European Council Meeting December 2020.” https://www.consilium.europa.eu/media/47296/1011-12-20-euco-conclusions-en.pdf.

European Network of Transmission System Operators for Electricity. 2013. “Documentation on Controller Tests in Test Grid Configurations.”.

Felix, Bate. 2019. “France Sets 2050 Carbon-Neutral Target with New Law.” 2019. Accessed August 22, 2019. https://www.reuters.com/article/us-france-energy/france-sets-2050-carbon-neutral-target-with-new-law-idUSKCN1TS30B.

Felix, Bate, Simon Carraud, and Benjamin Mallet. 2019. “French Government Sticks to Targets for Closing Coal Power Plants.” 2019. Accessed August 22, 2019. https://www.reuters.com/article/us-france-electricity-coal/french-government-sticks-to-targets-for-closing-coal-power-plants-idUSKCN1RF19N.

Fickel, Norman. 1996. “Visualisierung Der Volatilität Bei Der Interpolation Von Zeitreihen.”.

Finke, Björn. 2019. “Sonne Statt Kohle: Das Britische Stromnetz Kam Über Ostern 90 Stunden Lang Ohne Dreckschleudern Aus, Ein Rekord. Aber Das Königreich Will Auch Bis Zu Sechs

Neue Atomkraftwerke Bauen." Accessed August 09, 2019. https://www.sueddeutsche.de/wirtschaft/grossbritannien-sonne-statt-kohle-1.4418637.

Forschungsverbund erneuerbare Energien. 2014. "Phasen Der Stromwende - Systemstabilität.".

Giancoli, D. C. 2010. "Physik - Lehr- Und Übungsbuch." ph - Physik, 3., aktualisierte Auflage.

Giesecke, Jürgen, and Stephan Heimerl. 2014. *Wasserkraftanlagen.* Berlin, Heidelberg: Springer Berlin Heidelberg.

Göbel, C. 2010. "Modelle Der Synchrongeneratoren Für Die Simulation Der Subsynchronen Resonanzen.".

Heuck, K. et al. 2013. "Elektrische Energieversorgung - Erzeugung, Übertragung Und Verteilung Elektrischer Energie Für Studium Und Praxis." Lehrbuch, 9., aktualisierte und korrigierte Aufl.

"Hochspannungs-Gleichstrom-Übertragung: Grundlagen Und Integration in Die Stromversorgung Der Zukunft." Unpublished manuscript, last modified August 30, 2019. https://library.e.abb.com/public/7c519bd8fe187a62c1257cb4003aca02/K14_017%20DE-ABB%201936%20de%20HGUE.pdf.

Hundt, M. et al. "Verträglichkeit Vonerneuerbaren Energien Und Kernenergie ImErzeugungsportfolio." https://www.ier.uni-stuttgart.de/publikationen/pb_pdf/Hundt_EEKE_Langfassung.pdf.

Hutarew, G. 1969. *Regelungstechnik.* Berlin, Heidelberg: Springer Berlin Heidelberg,

Hydroflex. 2019. "Reference Sites." Accessed August 29, 2019. https://www.h2020hydroflex.eu/about/reference-sites/.

IEEE Power & Energy Society. 1992a. "Hydraulic Turbine and Turbine Control Models for System Dynamic Studies." *IEEE Trans. Power Syst.* 7 (1): 167–79. https://doi.org/10.1109/59.141700.

IEEE Power & Energy Society. 1992b. "Hydraulic Turbine and Turbine Control Models for System Dynamic Studies." Bd. 7, Heft 1. IEEE Transactions on Power Systems.

IEEE Power & Energy Society. 2013. “Dynamic Models for Turbine-Governors in Power System Studies: PES-TR1.”.

IEEE Power & Energy Society. 2014. “IEEE/PES Transmission & Distribution Conference & Exposition (T&D).”.

IEEE Power & Energy Society. 2016. “IEEE Recommended Practice for Excitation System Models for Power System Stability Studies.”.

IEEE Transactions on Automatic Control. 2014. “Optimal Load-Side Control for Frequency Regulation in Smart Grids.” 52nd Annual Allerton Conference on Communication, Control, and Computing.

IEEE/CIGRE Joint Task Force on Stability Terms and Definitions. 2004. “Definition and Classification of Power System Stability.” *IEEE TRANSACTIONS ON POWER SYSTEMS, VOL. 19, NO. 2, MAY 2004*.

“Implementing the End of Unabated Coal by 2025: Government Response to Unabated Coal Closure Consultation.” 2018. Unpublished manuscript, last modified August 09, 2019. https://assets.publishing.service.gov.uk/government/uploads/system/uploads/attachment_data/file/672137/Government_Response_to_unabated_coal_consultation_and_statement_of_policy.pdf.

International Atomic Energy Agency. 2014. “Country Nuclear Power Profiles: Schweden.” Accessed August 30, 2019. https://cnpp.iaea.org/countryprofiles/Sweden/Sweden.htm.

International Middle East Power Systems Conference. 2010. “Comparative Study on Modelling of Gas Turbines in Combined Cycle Power Plants.” Proceedings of the 14th International Middle East Power Systems Conference (MEPCON’10).

Jewkes, Stephen. 2019. “Italy to Block Oil and Gas Exploration Permits.” 2019. Accessed August 28, 2019. https://www.reuters.com/article/us-italy-drilling/italy-to-block-oil-and-gas-exploration-permits-idUSKCN1P31RW.

Jones, Brad. 2017. “Denmark Has Committed to Phasing Coal by 2030.” Accessed August 30, 2019. https://www.weforum.org/agenda/2017/11/denmark-has-committed-to-phasing-coal-by-2030.

Jovcic, Dragan, and Khaled Ahmed. 2015. *High-Voltage Direct-Current Transmission.* Chichester, UK: John Wiley & Sons, Ltd.

Kaltschmitt, M. et al. 2013. *Erneuerbare Energien.* Berlin, Heidelberg: Springer Berlin Heidelberg.

Kamps, U. “Gaußsche Normalverteilung.” Accessed March 10, 2020. https://wirtschaftslexikon.gabler.de/definition/normalverteilung-39769.

Kauranen, Anne, and Lefteris Karagiannopoulos. 2019. “Finland Approves Ban on Coal for Energy Use from 2029.” February 28. Accessed August 30, 2019. https://www.reuters.com/article/finland-energy-coal/finland-approves-ban-on-coal-for-energy-use-from-2029-idUKL5N20N6QV.

Kleinkorte, K. 2016. “Netzbetriebsführung.”.

Kommission „Wachstum, Strukturwandel und Beschäftigung“. 2019. “Abschlussbericht.” Unpublished manuscript, last modified August 30, 2019. https://www.bmwi.de/Redaktion/DE/Downloads/A/abschlussbericht-kommission-wachstum-strukturwandel-und-beschaeftigung.pdf?__blob=publicationFile.

Konstantin, Panos. 2017. *Praxisbuch Energiewirtschaft.* Berlin, Heidelberg: Springer Berlin Heidelberg.

Kou, G. et al. 2014. “Developing Generic Dynamic Models for the 2030 Eastern Interconnection Grid.” 2014 IEEE PES T&D Conference and Exposition.

Kundur, P. 1994. *Power System Stability and Control.* New York.

Lechner, C., and J. Seume. 2010. “Stationäre Gasturbinen.” VDI-Buch, 2., neu bearb. Aufl.

Lehnen, D. 2014. “Simulation Und Analyse Der Dynamischen Wechselwirkung Von Synchronmaschinen Im Axpo-Verteilnetz.”.

Lunze, J. 2016. “Regelungstechnik 1.”.

Machowski, Jan, Janusz W. Bialek, and James R. Bumby. 2012. *Power System Dynamics: Stability and Control.* 2. ed., reprinted with corr. Chichester: Wiley.

Markewitz, P., and M. Robinius. 2017. “Technologiebericht 2.1 Zentrale Großkraftwerke: In: Technologien Für Die Energiewende: Teilbericht 2 an Das Bundesministerium Für Wirtschaft Und Energie (BMWi).” Accessed August 01, 2019. https://epub.wupperinst.org/frontdoor/deliver/index/docId/7048/file/7048_Grosskraftwerke.pdf.

Martin, Lothar. 2019. “Brabec Will Kohlekommission Einsetzen – Aber Grünes Licht Für Grube Bílina.” Accessed August 30, 2019. https://www.radio.cz/de/rubrik/wirtschaftsmagazin/brabec-will-kohlekommission-einsetzen-aber-gruenes-licht-fuer-grube-bilina.

McKinley, S. “Cubic Spline Interpolation.” Accessed March 20, 2020. http://pages.intnet.mu/cueboy/education/notes/numerical/cubicsplineinterpol.pdf.

Merkle, M. 2002. “Dynamische Modellierung Von Verbrauchergruppen Und Statischer Blindleistungskompensa-Toren Zur Untersuchung Der Spannungsstabilität in Netzen.”.

Milano, Federico. 2010. *Power System Modelling and Scripting.* Power Systems 0. Berlin, Heidelberg: Springer-Verlag Berlin Heidelberg.

Mitteldeutscher Rundfunk. 2019. “Kohle-Boom in Polen.” Accessed August 30, 2019. https://www.mdr.de/nachrichten/osteuropa/politik/kohle-polen-tschechien-klima-katowice-100.html.

Morgan, Sam. 2018. “Finland Confirms Coal Exit Ahead of Schedule in 2029.” https://www.euractiv.com/section/energy/news/finland-confirms-coal-exit-ahead-of-schedule-in-2029/.

Morren, J. et al. 2006. “Wind Turbines Emulating Inertia and Supporting Primary Frequency Control.” Bd. 21, Heft 1.

Moser, Albert. 2015. *Elektrizitätsversorgungssysteme- Skriptum Zur Vorlesung.* Aachen.

Moser, Albert. 2018. *Stromerzeugung Und Handel- Skriptum Zur Vorlesung.* Aachen.

Naghizadeh, R. et al. 2014. “Modeling Hydro Power Plants and Tuning Hydro Governors as an Educational Guideline.” Bd. 5, Heft 4.

Naik, K. Anil et al. 2012. “Imc Tuned Pid Governor Controller for Hydro Power Plant with Water Hammer Effect.” Bd. 4. Procedia Technology.

Neplan AG. 2015. “Exciter Models.” Accessed March 14, 2021. https://www.neplan.ch/wp-content/uploads/2015/08/Nep_EXCITERS1.pdf.

Newell, David. Swedish Energy Agency. “Looking Forward: The Swedish Energy System into the 2040s.” Accessed August 28, 2019. http://www.panbalticscope.eu/wp-content/uploads/2019/04/D.-Newel-Energisystemets-utveckling-till-havsm%C3%B6te-.pdf.

Nilsson, O., and D. Sjelvgren. 1997. “Hydro Unit Start-up Costs and Their Impact on the Short Term Scheduling Strategies of Swedish Power Producers.” *IEEE Trans. Power Syst.* 12 (1): 38–44. https://doi.org/10.1109/59.574921.

Nord Pool AS. 2018. “Principles for Determining the Transfer Capacities in the Nordic Power Market.” Accessed September 19, 2019. https://www.nordpoolspot.com/globalassets/download-center/tso/principles-for-determining-the-transfer-capacities.pdf.

Nord Pool AS. 2019a. “Day-Ahead Overview: Nordic/Baltic.” Accessed August 29, 2019. https://www.nordpoolgroup.com/maps/#/nordic.

Nord Pool AS. 2019b. “Historical Market Data: Exchange NO Connections 2019 Hourly.” Accessed September 01, 2019. https://www.nordpoolgroup.com/globalassets/marketdata-excel-files/exchange-no-connections_2019_hourly.xls.

Nord Pool AS. 2019c. “Historical Market Data: Exchange SE Connections 2019 Hourly.” Accessed September 01, 2019. https://www.nordpoolgroup.com/globalassets/marketdata-excel-files/exchange-se-connections_2019_hourly.xls.

Nord Pool AS. 2019d. “Ramping.” Accessed September 24, 2019. https://www.nordpoolgroup.com/trading/Day-ahead-trading/Ramping/.

"Nordic Bidding Zones." 2013. Unpublished manuscript, last modified August 29, 2019. https://www.thema.no/wp-content/uploads/2013/10/THEMA-report-2013-27-Nordic_Bidding_Zones_FINAL.pdf.

Nordic Transmission System Operators: Svenska kraftnät, Statnett, Fingrid and Energinet.dk. 2016. "Challenges and Opportunities for the Nordic Power System.".

"North Seas Ministers Extend and Intensify Cooperation on Offshore Wind." 2016. News release. June 20, 2016. Accessed July 15, 2019. https://windeurope.org/news-room/news/north-sea-ministers-extend-and-intensify-cooperation-on-offshore-wind/.

Oeding, D. 2016. "Elektrische Kraftwerke Und Netze." 8th ed.

Ørsted A/S. "Horns Rev 2: Offshore Wind Farm." Accessed August 28, 2019. https://orstedcdn.azureedge.net/-/media/WWW/Docs/Corp/COM/Our-business/Wind-power/Wind-farm-project-summary/Horns-Rev-2_UK_2018.ashx?la=en&rev=7078128df406404ea7c450c0d8f7ed05&hash=4A6DBD158E73456C07E3598060A0306B.

Oswald, B. R. 2009. "Berechnung Von Drehstromnetzen.".

Pai, M. A. 1989. "Energy Function Analysis for Power System Stability." The Kluwer International Series in Engineering and Computer Science, Power Electronics and Power Systems.

Paris Agreement. United Nations. Abl. 4. 2016. Accessed May 10, 2019. https://eur-lex.europa.eu/legal-content/EN/TXT/?uri=OJ:L:2016:282:TOC.

Pieters, Janene. 2018. "Majority in Dutch Parliament Supports Building More Nuclear Plants." Accessed August 28, 2019. https://nltimes.nl/2018/11/07/majority-dutch-parliament-supports-building-nuclear-plants.

Plassmann, W., and D. Schulz. 2013. "Handbuch Elektrotechnik - Grundlagen Und Anwendungen Für Elektrotechniker." 6., neu bearb. Aufl.

Radio Steiermark. 2019. "Österreich Schließt Letzte Kohlekraftwerke." Accessed August 30, 2019. https://steiermark.orf.at/v2/news/stories/2984926/.

Saarinen, L. et al. 2015. “Field Measurements and System Identification of Three Frequency Controlling Hydropower Plants.” Bd. 30, Heft 3. IEEE Transactions on Energy Conversion.

Sauer, Peter W., and M. A. Pai. 1998. *Power System Dynamics and Stability.* Upper Saddle River, N.J: Prentice Hall.

Sauer, Peter W., M. A. Pai, and Joe H. Chow. 2017. “Power System Dynamics and Stability - with Synchrophasor Measurement and Power System Toolbox.” Second edition.

Schlandt, Jakob. 2019. “AKW-Betreiber Gegen Längere Laufzeiten: „Die Nutzung Der Kernenergie Hat Sich Erledigt“.” Accessed August 30, 2019. https://www.tagesspiegel.de/wirtschaft/akw-betreiber-gegen-laengere-laufzeiten-die-nutzung-der-kernenergie-hat-sich-erledigt/24422262.html.

Schultz, Stefan. 2017. “Langsame Energiewende: Atomausstieg Auf Schweizer Art.” Accessed August 30, 2019. https://www.spiegel.de/wirtschaft/soziales/schweiz-der-langsame-atomausstieg-der-eidgenossen-a-1148756.html.

Schultz, Stefan, and Gerald Traufetter. 2019. “Entwurf Der Kommission: So Soll Deutschlands Kohleausstieg Ablaufen.” Accessed August 30, 2019. https://www.spiegel.de/wirtschaft/soziales/kohleausstieg-so-soll-der-kohleausstieg-ablaufen-a-1249467.html.

Schwab, Adolf J. 2017. “Elektroenergiesysteme.”.

Seiser, Michaela. 2011. “Versuchskraftwerk Zwentendorf: Das Sicherste Atomkraftwerk Der Welt.” Accessed August 30, 2019. https://www.faz.net/aktuell/politik/energiepolitik/versuchskraftwerk-zwentendorf-das-sicherste-atomkraftwerk-der-welt-1610075.html.

Selot, Florian, Daniel Fraile, and Guy Brindley. 2019. “Offshore Wind in Europe: Key Trends and Statistics 2018.” Accessed July 15, 2019. https://windeurope.org/wp-content/uploads/files/about-wind/statistics/WindEurope-Annual-Offshore-Statistics-2018.pdf.

Semerow, A. 2018. “Ein Beitrag Zur Beschreibung Elektromechanischer Ausgleichsvorgänge in Elektrischen Ener-Giesystemen Und Ursachenidentifikation Mittels Weitbereichsmessungen.”.

Semerow et al., A. 2015. “Dynamic Study Model for the Interconnected Power System of Continental Europe in Differ-Ent Simulation Tools.” 2015 IEEE Eindhoven PowerTech Electronic ISBN :978-1-4799-7693-5; USB ISBN:978-1-4799-7692-8.

Shepard, Donald. “A Two-Dimensional Interpolation Function for Irregularly-Spaced Data.” In *The 1968 23rd ACM National Conference*, edited by Richard B. Blue and Arthur M. Rosenberg, 517–24.

Siemens AG. 2017. “SILYZER 200: Mit Hochdruck Effizient Im Megawattbereich.” Unpublished manuscript, last modified August 02, 2019. https://assets.new.siemens.com/siemens/assets/public.1524044774.454108cf8e67964cc7505b8f38c83f4645971833.broschuere-sil200.pdf.

Siemonsmeier, Marius, Philipp Baumanns, Niklas van Bracht, Maik Schönefeld, Schönbauer Andrea, Albert Moser, Ole Gunnar Dahlhaug, and Sara Heidenreich. 2018. “Hydropower Providing Flexibility for a Renewable Energy System: Three European Energy Scenarios: A HydroFlex Report.” Unpublished manuscript, last modified April 18, 2019. https://www.h2020hydroflex.eu/wp-content/uploads/2019/01/HydroFlex-Report_Three-European-Energy-Scenarios.pdf.

Singh, G. 2011. “Simplified Modeling of Hydraulic Governor-Turbine for Stable Operation Under Operating Con-Ditions.” Bd. 39, Heft 2.

Skar, C., and et al. “Norway’s Role as a Flexibility Provider in a Renewable Europe.” Accessed March 23, 2020. https://www.ntnu.no/documents/7414984/1281984692/Norway%E2%80%99s+role+as+a+flexibility+provider+in+a+renewable+Europe.pdf/a055c776-f2a5-468f-bce2-c2cf1943f1fc.

Skolaut, W. 2018. “6., Neu Bearb. Aufl.”.

Statistic Norway. 2017. “Electricity Balance.” Accessed July 15, 2019. https://www.ssb.no/eksport/excel?key=369454.

Statistic Norway. 2019. “Power Stations, by Type: Maximum Output.” Accessed August 29, 2019. https://www.ssb.no/eksport/excel?key=369441.

Statkraft Markets GmbH. 2010. “Statkraft Übernimmt Anteile Der Baltic Cable AB Von E.ON Schweden.” https://www.statkraft.de/presse/Pressemitteilungen/Pressemitteilungen-archiv/2010/statkraft-ubernimmt-anteile-der-baltic/.

Stattnet SF. 2019. “North Sea Link: New Subsea Interconnector Between Norway and England.” Accessed September 01, 2019. https://www.statnett.no/en/our-projects/interconnectors/north-sea-link/.

Stein, T. 1953. “Einfluss Der Selbstregelung Auf Die Stabilität Von Wasserkraft-Anlagen.”.

Sterner, Michael, and Ingo Stadler. 2017. *Energiespeicher - Bedarf, Technologien, Integration.* Berlin, Heidelberg: Springer Berlin Heidelberg.

Strauss, Karl. 2016. *Kraftwerkstechnik.* Berlin, Heidelberg: Springer Berlin Heidelberg.

TenneT TSO GmbH. 2019a. “Hochspannungs-Gleichstrom-Übertragung.” Accessed August 30, 2019. https://www.tennet.eu/de/unser-netz/onshore-projekte-deutschland/suedlink/technik-und-bau/hochspannungs-gleichstrom-uebertragung/.

TenneT TSO GmbH. 2019b. “NorNed.” Accessed September 01, 2019. https://www.tennet.eu/de/unser-netz/internationale-verbindungen/norned/.

The Norwegian Water Resources and Energy Directorate. 2019. “NVE Atlas.” Accessed August 28, 2019. https://temakart.nve.no/link/?link=vannkraft&layer=0,4,5,8&field=vannkraftverkNr&value=273&buffer=3000.

Twidale, Susanna, Mark Potter, and Adrian Croft. 2018. “UPDATE 1-Britain Outlines Plans for 2025 Coal-Power Phase Out.” 2018. Accessed August 09, 2019. https://af.reuters.com/article/africaTech/idAFL8N1P022F.

Unbehauen, H., and F. Ley. 2014. “Das Ingenieurwissen: Regelungs- Und Steuerungstechnik.”.

Union of the Electricity Industry - EURELECTRIC aisbl. 2014. “Flexibility and Aggregation: Requirements for Their Interaction in the Market.” A EURELECTRIC paper. Accessed July 19, 2019.

Vattenfall AB. “Horns Rev 1.” Accessed August 28, 2019. https://powerplants.vattenfall.com/horns-rev.

Vattenfall AB. “Horns Rev 3.” Accessed August 28, 2019. https://powerplants.vattenfall.com/horns-rev-3.

Vattenfall AB. 2019a. “Porjus.” Accessed August 29, 2019. https://powerplants.vattenfall.com/en/porjus.

Vattenfall AB. 2019b. “Stornorrfors.” Accessed August 29, 2019. https://powerplants.vattenfall.com/de/stornorrfors.

Verordnung Zur Festlegung Eines Netzkodex Mit Netzanschlussbestimmungen Für Hochspannungs-Gleichstrom- Übertragungssysteme Und Nichtsynchrone Stromerzeugungsanlagen Mit Gleichstromanbindung. European Commission. August 26, 2016. Accessed September 01, 2019. https://eur-lex.europa.eu/legal-content/DE/TXT/PDF/?uri=CELEX:32016R1447&from=DE.

“Vesterhav Syd and Nord Set to Be Denmark’s Most Efficient Offshore Wind Farms.” 2018. News release. September 14, 2018. Accessed August 28, 2019. https://group.vattenfall.com/press-and-media/news--press-releases/newsroom/2018/vesterhav-syd-and-nord-set-to-be-denmarks-most-efficient-offshore-wind-farms.

Werner, T. 2018. “Geberlose Rotorlagebestimmung in Elektrischen Maschinen.”.

World Nuclear Association. 2018. “Nuclear Power in Italy.” Accessed August 28, 2019. https://www.world-nuclear.org/information-library/country-profiles/countries-g-n/italy.aspx.

World Nuclear Association. 2019a. “Nuclear Energy in Denmark.” Accessed September 30, 2019. https://www.world-nuclear.org/information-library/country-profiles/countries-a-f/denmark.aspx.

World Nuclear Association. 2019b. “Nuclear Power in Czech Republic.” Accessed August 30, 2019. https://www.world-nuclear.org/information-library/country-profiles/countries-a-f/czech-republic.aspx.

World Nuclear Association. 2019c. “Nuclear Power in Finland.” Accessed August 30, 2019. https://www.world-nuclear.org/information-library/country-profiles/countries-a-f/finland.aspx.

Zahoransky, Richard. 2019. *Energietechnik.* Wiesbaden: Springer Fachmedien Wiesbaden.

Zimmer, H. 2017. “Regeldynamik Konventioneller Kraftwerke Im Kontext Veränderter Erzeugungsstrukturen.”.

Appendix 1

Table 16: Power and voltage setpoints in the New England IEEE 39-bus system (Pai 1989)

Bus	Bus Type	Voltage [p. u.]	Load		Generation		
			MW	MVar	MW	MVar	No.
1	PQ		0.0	0.0	0.0	0.0	
2	PQ		0.0	0.0	0.0	0.0	
3	PQ		322.0	2.4	0.0	0.0	
4	PQ		500.0	184.0	0.0	0.0	
5	PQ		0.0	0.0	0.0	0.0	
6	PQ		0.0	0.0	0.0	0.0	
7	PQ		233.8	84.0	0.0	0.0	
8	PQ		522.0	176.0	0.0	0.0	
9	PQ		0.0	0.0	0.0	0.0	
10	PQ		0.0	0.0	0.0	0.0	
11	PQ		0.0	0.0	0.0	0.0	
12	PQ		7.5	88.0	0.0	0.0	
13	PQ		0.0	0.0	0.0	0.0	
14	PQ		0.0	0.0	0.0	0.0	
15	PQ		320.0	153.0	0.0	0.0	
16	PQ		329.0	32.3	0.0	0.0	
17	PQ		0.0	0.0	0.0	0.0	
18	PQ		158.0	30.0	0.0	0.0	
19	PQ		0.0	0.0	0.0	0.0	
20	PQ		628.0	103.0	0.0	0.0	
21	PQ		274.0	115.0	0.0	0.0	
22	PQ		0.0	0.0	0.0	0.0	

23	PQ		247.5	84.6	0.0	0.0	
24	PQ		308.6	-92.0	0.0	0.0	
25	PQ		224.0	47.2	0.0	0.0	
26	PQ		139.0	17.0	0.0	0.0	
27	PQ		281.0	75.5	0.0	0.0	
28	PQ		206.0	27.6	0.0	0.0	
29	PQ		283.5	26.9	0.0	0.0	
30	PV	1.0475	0.0	0.0	250.0		Gen 10
31	PV	0.9820	9.2	4.6			Gen 2
32	PV	0.9831	0.0	0.0	650.0		Gen 3
33	PV	0.9972	0.0	0.0	632.0		Gen 4
34	PV	1.0123	0.0	0.0	508.0		Gen 5
35	PV	1.0493	0.0	0.0	650.0		Gen 6
36	PV	1.0635	0.0	0.0	560.0		Gen 7
37	PV	1.0278	0.0	0.0	540.0		Gen 8
38	PV	1.0265	0.0	0.0	830.0		Gen 9
39	PV	1.0300	1104.0	250.0	1000.0		Gen 1

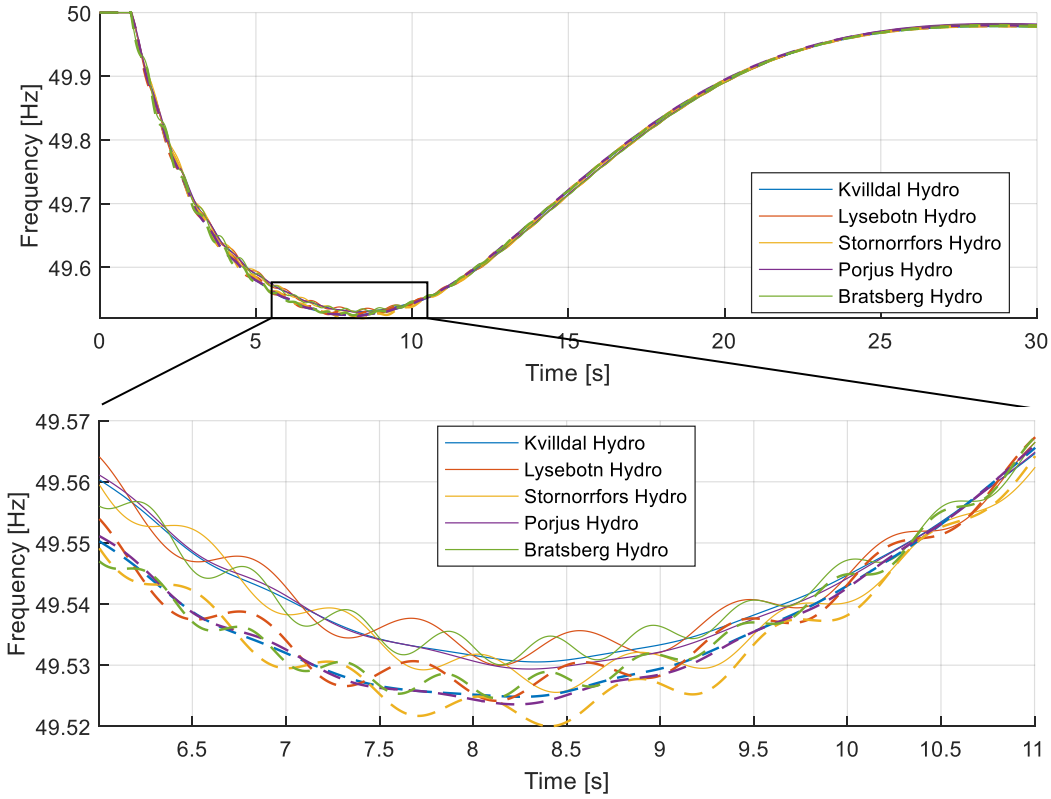

Figure 92: Dynamic behavior of reference sites after load increase in Oslo

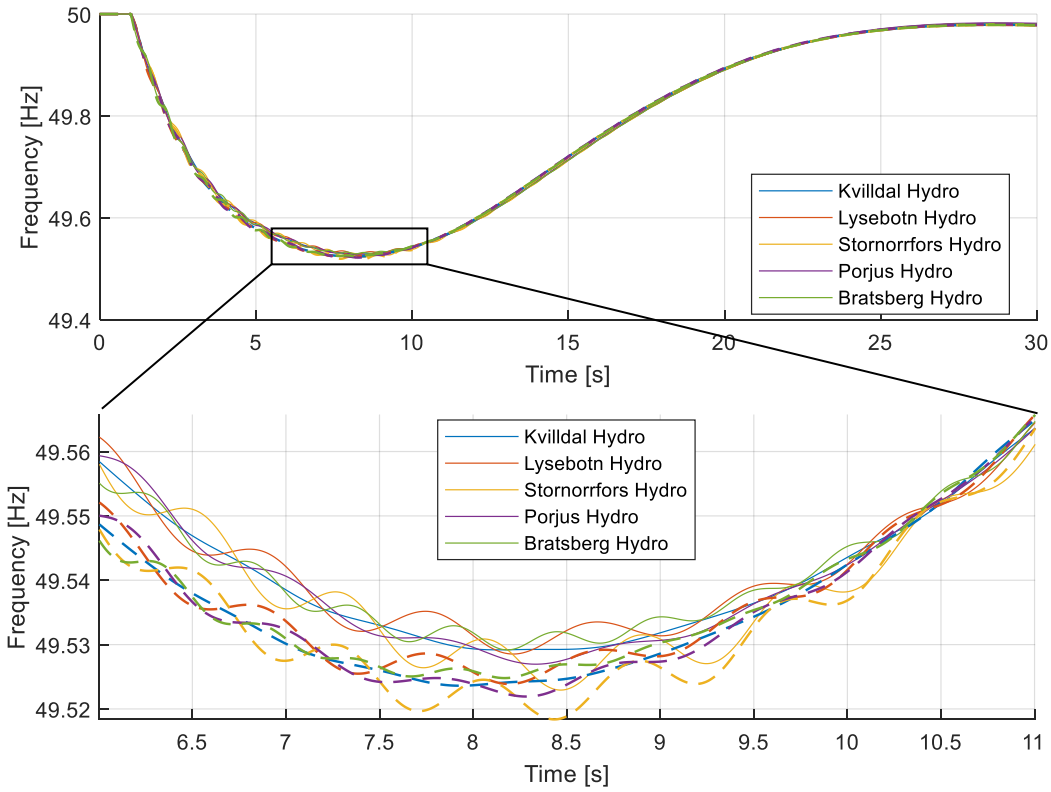

Figure 93: Dynamic behavior of reference sites after load increase in Helsinki